Infectious Prion Strain Directed Conformational Conversion of Recombinant PrP

Von der Fakultät für Lebenswissenschaften

der Technischen Universität Carolo-Wilhelmina

zu Braunschweig

zur Erlangung des Grades einer

Doktorin der Naturwissenschaften

(Dr. rer. nat.)

genehmigte

D i s s e r t a t i o n

von Vandana Gupta

aus Delhi, India

1. Referentin: Prof. Dr. Christiane Ritter
2. Referent: Prof. Dr. Michael Steinert

eingereicht am: 15.05.2013
mündliche Prüfung (Disputation) am: 30.09.2013
Druckjahr 2014

Vorveröffentlichungen der Dissertation

Teilergebnisse aus dieser Arbeit wurden mit Genehmigung der Fakultät für Lebenswissenschaften, vertreten durch die Mentorin der Arbeit, in folgenden Beiträgen vorab veröffentlicht:

Tagungsbeiträge

Gupta V, Deluweit F, Ritter C, Lührs T. Optimal Protein Misfolding Cyclic Amplification of Mammalian Prions (Poster). International Meeting on "Amyloid Fibrils, Prions and Precursors: Molecules for Targeted Intervention". , Halle (Saale), Germany (2011).

Contents

Acknowledgements

First and foremost I wish to express my sincere gratitude to my supervisor Dr. Thorsten Lührs for his constant support and guidance throughout the course of my study. I would like to thank him for giving me intellectual freedom in my work and for critically assessing my performance. I would also like to thank my thesis committee members Prof. Dr. Christiane Ritter and Dr. Andrea Scrima for their interest and valuable suggestions.

My sincere thanks to Dr. Heinrich Lünsdorf for his timely help in Electron Microscopic studies and also to Dr. Manfred Nimtz for helping me out with the mass spectrometric studies. I would like to acknowledge all the members of MOSB for their help and scientific cooperation.

I am grateful to all the present and previous members of the SBIB lab. To Felix, Shyam and Jan for providing a wonderful working atmosphere. Special thanks to Romy for her help in protein purification.

Finally, I would like to acknowledge all my friends in Braunschweig who supported me during my time here. I am indebted to my friends Aruna and Sonam for their constant love and support and for making me feel home in Germany. I greatly value their friendship and I deeply appreciate their belief in me.

Most importantly, none of this would have been possible without the love and patience of my family. I thank my family: my brother, my grandparents and especially my parents, for their great enthusiasm, endless support, and limitless encouragement

Abbreviations

ASA	Amyloid seeding assay
BSE	Bovine spongiform encephalopathy
CD	Circular Dichroism
Cdc-42	cell division cycle 42
CFC	Cell free conversion
CJD	Creutzfeldt–Jakob disease
CLD	Caveolae-like domains
CWD	Chronic wasting disease
Da	Dalton
DRM	Detergent-resistant microdomains
eQuIC	Enhanced QuIC
ER	Endoplasmic Reticulum
ESI-MS	Electrospray Ionisation Mass Spectrometry
et al.	*et alii*
fCJD	Familial Creutzfeldt–Jakob disease
FFI	Fatal familial insomnia
Fig	Figure
FRT	Fischer rat thyroid
FTIR	Fourier transform infrared spectroscopy
GdnHCl	Guanidine Hydrochloride
GPI	Glycosylphosphatidylinisotol
GSS	Gerstmann-Sträussler-Scheinker disease
HFIP	Hexafluoroisopropanol
Hz	Hertz.
kDa	Killo-dalton

LDS	Lithium Dodecyl Sulfate
MW	Molecular weight
MWCO	Molecular weight cutoff
NBH	Normal Brain Homogenate
NMR	Nuclear Magnetic Resonance
O.D	Optical Density
PB	Perfusion Buffer
PBS	Phosphate Buffered Saline
PK	Proteinase K
PMCA	Protein Misfolding Cyclic Amplification
POPG	1-palmitoyl-2-oleoyl-sn-glycero-3-phosphoglycerol
PrP	Prion Protein
PrP^{C}	Cellular for Prion Protein
PrP^{res}	PK resistant form of Prion Protein
PrP^{Sc}	Scrapie isoform of Prion Protein
PTA	Phosphotungstic acid
qPMCA	quantitative PMCA
QuIC	Quaking induced conversion
Rec.	Recombinant
RT-QuIC	Real Time QuIC
sCJD	Sporadic Creutzfeldt–Jakob disease
S-QuIC	Standard QuIC
SAF	Scrapie-associated fibrils
saPMCA	serial automated PMCA
ScBH	Scrapie Brain Homogenate
ScN2a	scrapie-infected N2a

SDS	Sodium dodecyl sulphate
SDS PAGE	SDS polyacrylamide gel electrophoresis
SS	Silver Staining
SSA	Selective Shearing Amplification
TEM	Transmission Electron Microscopy
ThT	Thioflavin T
TSE	Transmissible Spongiform Encephalopathy
vCJD	Variant Creutzfeldt–Jakob disease
Nm	Nanometer
Mg	Milligram
µg	microgram
mL	Microliter
Wt	wild type

Abstract

The term prion was coined by Stanley Prusiner to describe a new biological agent that comprises solely of infectious self-replicating proteins. Prions are capable to cause lethal neurodegenerative conditions that include scrapie in sheep, and Creutzfeldt-Jakob disease (CJD) in humans. They are derived from the conversion of a normal, primarily α-helical, cellular prion protein (PrP^{C}), to an infectious, β-sheet rich conformer (PrP^{Sc}). This proposition was referred to as the protein-only hypothesis where the single protein is responsible for a wide diversity of structures with different pathogenic properties. For decades this hypothesis has motivated the scientific community to decipher the elusive features of this new pathogen. However, many unresolved issues still surround the process of PrP conversion, and the molecular structure of PrP^{Sc} is still missing.

The development of the *in vitro* protein misfolding cyclic amplification (PMCA) assay allows for analysis of PrP^{C} to PrP^{Sc} conversion. An excess of PrP^{C} and repeated cycles of sonication and incubation are used to amplify PrP^{Sc} present in the test sample. However, in many labs, including our own, standard PMCA is rather hard to control. Moreover, for structural elucidation of prions by NMR-Spectroscopy the pre-requisite is to obtain extensive amounts of isotope labeled recombinant (rec.) prions. For this purpose, a novel method had been established in our group called “Selective Shearing Amplification” (SSA), where uniform shear forces were used to optimally balance between prion growth and prion fragmentation. Moreover, SSA allowed to scale-up the reaction volume, which none of the published methods had accomplished so far. It was the key objective of this work to establish SSA for the conformational selection and homogeneous amplification of prion conformations using hamster brain derived prion strains (263K and Sc237) as seed and native recombination prion protein as a substrate for the conversion.

At the start, suitable experimental conditions were established to meet the central goal of this work. During this initial screening of conditions, the formation of recombinant, partially proteinase K resistant PrP (rec. PrP^{res}) was

used to successively improve the reaction efficiency. A total of 800 mg of unlabelled and of isotopically labelled (^{15}N and $^{13}C/^{15}N$) recombinant hamster Sc237 and hamster 263K PrP aggregates were produced by SSA. These products were further characterization by SSA, negative stain electron microscopy, mass spectrometry and solid state NMR spectroscopy.

Using SSA, a wide range of shear forces were scanned, which allowed to amplify prion recombinant conformations. In the Sc237 and 263K seeded reactions substantial formation of rec. PrP^{res} was obtained, while no amplification was observed in non-seeded control reaction run under the same experimental conditions. Moreover, the rec. PrP^{res} generated by SSA could be infinitely propagated *in vitro* without any loss of seeding activity. Some of the reactions were propagated up to 48 serial passages, where 1:50 serial dilutions were used in each step. This corresponds, including the initial brain derived seed dilution, to a total dilution of native prions of 2.25×10^{-85}. Thus, rec. PrP^{res} could readily be generated that is devoid of any brain derived PrP^{C} or potential brain derived co-factors.

Using solid state NMR spectroscopy, we characterized conformationally selected rec. PrP^{res} and identified three distinct prion conformation present in Sc237, but only one conformation present in 263K. Notably the 263K prion strain conformation is also present in the Sc237 prion conformational mixture. Experimentally, this indicated that overall seed conformations are not altered or influenced by shearing mechanisms, but rather conformation can be selected even from mixed aggregates. We were also able to record the high quality solid state NMR spectra for all identified rec. PrP^{res} conformations. Thus, form this work it is evident that a structure determination of prions will be possible.

In experimental transmissions, both native hamster strains did not show any significant differences in incubation time, glycosylation pattern or brain lesion profile. In order to check the infectivity of rec. PrP^{res} we also carried out *in vivo* inoculations into wild type male syrian hamsters. This experiment is still on-

going at the time of writing this thesis. It might allow for the first time to correlate prion infectively to single conformations.

Zusammenfassung

Der Begriff Prion wurde von Stanley Prusiner geprägt, um eine neuartiges biologischen Agenz zu beschreiben, dass nur aus selbst replizierenden infektiösen Proteinen besteht. Prionen verursachen tödliche neurodegenerative Erkrankungen, zu denen Scrapie bei Schafen, BSE bei Rindern, und die Creutzfeldt-Jakob Erkrankung (CJD) des Menschen gehören. Sie entstehen durch die Konversion des normalen, hauptsächlich alpha-helikalen, zellulären prion proteins (PrP^{C}), in ein infektiöses, beta-sheet reiches Konformer (PrP^{Sc}). Dieser mechanistische Vorschlag wird auch als die „Protein-Only Hpothese" bezeichnet, die davon ausgeht, dass ein einziges Protein für die Eigenschaften der Prionen, inklusive der diversen Phänotypen der Erkrankung, verantwortlich ist. Für Jahrzehnte hat diese Hypothese die wissenschaftliche Gemeinschaft motiviert die genauen Eigenschaften diese neuartigen Agens zu entschlüsseln. Trotzdem gibt es immer noch eine vielzahl unverstandener Eigenschaften der Prionen, und ihrer molekularen Struktur.

Die Entwicklung des *in vitro* "protein misfolding cyclic amplification" (PMCA) Assay's erlaubt die Analyse der PrP^{C} to PrP^{Sc} Konversion. Ein Überschuss an PrP^{C} und wiederholte Zyklen von Ultraschallbehandlung und Inkubation werden dabei benutzt, um PrP^{Sc} zu amplifizieren. Jedoch hat sich herausgestellt, dass vielen Laboratorien, einschliesslich unseres, die Standard PMCA nur sehr schwer zu kontrollieren ist. Obendrein, würden für eine Strukturbestimmung von Prionen mittels NMR-Spektroskopie sehr gross Mengen an Isotopenmarkierten recombinanten (rec.) Prionen benötigt. Um dies potentiell zu erreichen, wurde in unsere Gruppe eine neuartige Methode entwickelt, genannt "Selective Shearing Amplification" (SSA), die gleichförmige Scherkräfte nutzt, um Prionen Wachstum und Fragmentierung optimal zu balancieren. Zusätzlich erlaubt es SSA, grosse Reaktionsvolumina einzusetzen, was mit keiner publizierten Methode bisher möglich war. Das Hauptziel in dieser Arbeit war es, SSA für die Selektion und homogene Amplifikation von Prion Konformatioen zu etablieren. Dabei sollten die Hamster Prionstämme (263K and Sc237) aus Hamstergehirnen als 'Seed' und natives recombinantes Prion Protein also Substrat verwendet werden.

Zu Beginn der Arbeit wurden experiementelle Bedingungen etabliert, um das zentrale Ziel zu erreichen. Dazu wurden Bedingungen gesucht, die zur Bildung von rekombinantem, partiell proteinase K resistentem PrP (rec. PrP^{res}) führen. PrP^{res} Bildung wurde als Indikator verwendet, um die Reaktionseffizienz zu verbessern. Insgesamt wurden ca. 800 mg unmarkiertes und isotopenmarkiertes (^{15}N and $^{13}C/^{15}N$) rekombinantes Hamster Sc237 and 263K PrP^{res} mit SSA hergestellt. Diese Produkte wurden dann weiter mit SSA, 'negative staining' Electronenmikroscopie, Massenspektrometrie und Festkörper NMR Spektroskopie characterisiert.

Mittels SSA, wurde ein weiter Scherbereicht getestet, der es erlaubte, rekombinate Prion Konformationen zu erhalten. In den Sc237 und 263K induzierten Rekationen wurden erhebliche Mengen an rec. PrP^{res} generiert, während die nicht induzierten Reaktionen keine vergleichbaren Aggregate ergaben. Das rec. PrP^{res} konnte unlimitiert seriell *in vitro* propagiert werden, ohne dass die 'seeding' Aktivität sich änderte. Einige Reaktionen wurden bis zu 48 Mal seriell propagiert, wobei jeweils 1:50 Verdünnungen verwendet wurden. Dies entspricht, einschliesslich der Anfangsverdünnung, einer Gesamtverdünnung der nativen Prionen von 2.25×10^{-85}. Damit ist es folglich möglich, rec. PrP^{res} zu generieren, das frei von PrP^{C} und potentiellen andren Co-Faktoren aus Hirngewebe ist.

Mittels Festkörper NMR spectroscopy, haben wir das Konformationell selektierten rec. PrP^{res} charakterisiert. Dabei wurden drei spezifische Prion Konformation in Sc237 entdeckt, aber nur eine in 263K. Es ist herauszustellen dass diese Konformation auch als Teil der konformationellen Mischung in Sc237 vorhanden ist. Experimentell, wurden die Konformationen also nicht durch die Scherkräfte induziert, sondern sie können sogar aus Mischungen selektiert werden. Wir waren in der Lage hochwertige Festkörper NMR Spektren für alle identifizierten rec. PrP^{res} Konformationen zu erhalten. Damit wird es aufgrund dieser Arbeit möglich sein, die 3D-Strukturen von Prionen zu bestimmen.

In experimentellen Transmissionen der nativen Hamster Prion Stämme, sind diese aufgrund Ihrer Inkubationszeiten, Glykosylierungsmuster oder Hirnpathologie nicht unterscheidbar. Um die Infektiosität des rec. PrP^{res} zu prüfen, wurden Inoculationen in männlichen Goldhamstern durchgeführt. Dieses Experiment ist noch nicht abgeschlossen. Potentiell könnten aber zu ersten Mal Prion Phänotypen mit einzelnen PrP^{res} Konformationen korreliert werden.

1 Introduction

1.1 Transmissible Spongiform Encephalopathies

The vast majority of infectious diseases of humans and animals are caused either by parasites, fungi, bacteria, or viruses. A common component to all these classes of disease-causing agents is the presence of the molecule such as DNA or RNA which is capable of encoding structural or enzymatic constituents of the agent. Although components of the host's cellular machinery may be required for replication of the agent (as is the case with certain viruses), maintenance of the nucleic acid genome is essential for the persistence and spread of the infectious agent.

An emerging class of diseases is the transmissible spongiform encephalopathies (TSEs) or prion diseases that are caused by a yet unknown agent. Some of the distinctive features are neuronal vacuolation (spongiosis), neuronal death, and explicit glial reactions. In addition, a defining characteristic is the deposition, mainly in the brain and lymphoreticular tissues, of an abnormal form of host-encoded prion protein (PrP). Also, no adaptive immune responses are stimulated upon infection, most likely because the mammalian immune system is largely tolerant to PrP of the same species. These diseases are atypical in that (i) there can be a long latency period between infection and progression to clinical disease (Collinge et al., 2003) and (ii) the diseases can manifest with sporadic, genetic, or infectious etiologies (Prusiner, 1998). The infectious agents in these diseases exhibit numerous properties which are inconsistent with the existence of a nucleic acid genome. Firstly, the TSE agent is largely resistant to treatments which destroy nucleic acids such as ionizing radiation and nucleases but are sensitive to reagents which destroy proteins (Alper et al., 1966). Secondly, no nucleic acid of substantial length has ever been found in purified fractions of the infectious agent implying the absence of a nucleic acid genome (Kellings et al., 1993; Safar et al., 2005). Thirdly, unlike viruses, TSEs do not elicit an immune response (Clarke and Haig, 1966). Finally, although certain viral diseases are compatible with a

genetic etiology (i.e. the integration of retroviruses into the host genome or the modulation of virus receptors by heritable mutations) spontaneous viral diseases cannot be easily rationalized. These results led to the idea that TSEs are caused by infectious self-replicating proteins (Griffith, 1967).

Table 1: Main TSE's of human and animals

Disease	Host	Notes
Sporadic Creutzfeldt-Jacob disease (sCJD)	Human	The most prevalent human prion disease, affecting, on average, <3 people per million
Variant Creutzfeldt-Jacob disease (vCJD)	Human	Form of CJD probably contracted by the consumption of BSE infected beef products
Kuru	Human	A prion disease propagated by ritual cannibalism by the Fore tribe of Papua New Guinea
Familial CJD/ Fatal familial insomnia/ Gerstmann-Sträussler Scheinker syndrome	Human	Prion diseases associated with germline mutations in the PRNP gene, encoding the prion protein
Scrapie	Sheep and goats	The archetypal prion disease of animals, endemic in several countries and passed both horizontally and vertically
Atypical scrapie	Sheep and goats	A recently discovered prion disease of older sheep and goats, of unknown origin
Bovine Spongiform Encephalopathy (BSE)	Cattle	Prion disease that was endemic in UK cattle in the 1980s and 1990s. BSE is believed to have arisen as a result of changes to rendering practices
Atypical BSE	Cattle	Two recently discovered (spontaneous ?) prion diseases of cattle that can be L-or H-type depending on the size of the PK resistant core of PrP^{Sc}
Chronic Wasting Disease (CWD)	Cervids such as deer and elk	A prion disease of farmed and wild cervids, currently in epidemic proportions in North America as a result of apparently high transmissibilty

Table 1: Summary of TSEs that have been described in humans, and mammalian species that are relevant for human food safety, i.e. cattle, sheep, goat and elk, and the most commonly used experimental animals, i.e. mouse and hamster.

1.1.1 Neuropathology and Pathogenesis of Prion Diseases

There are four principle neuropathological findings for prion disease.(1) spongiform change (vacuolar degeneration of brain parenchyma)(Glatzel and Aguzzi, 2001), (2) death of neurons (Cronier et al., 2004), (3) astrocytic gliosis (DeArmond et al.,2004) (in itself a non-specific reactive response to CNS damage but of unusual intensity in prion disease), and (4) the presence of extracellular amyloid plaques in some but not all varieties of prion disease (Will et al., 1996).

The majority of prion diseases (including scrapie, mouse-adapted scrapie, BSE, and CJD) are characterized by large amounts of spongiform degeneration. Spongiform changes can vary in size and density and range from microvacuolation to the fusion of vacuoles to produce status spongiosis. The degree of spongiform change does not appear to correlate with neuronal loss. Amyloid plaques are also present in the brain in some of the human prion diseases, most notably kuru, vCJD and GSS. These amyloid plaques exhibit birefringence when stained with Congo red and viewed under polarized light. However, regions of pathology within the brain are usually specific to and diagnostic of a given prion disease or prion strain (Figure 1).

PrP^{Sc} deposition in the central nervous system is also a hallmark feature of prion disease (Prusiner, 1991). The type of PrP^{Sc} deposit and its location varies among the human prion diseases. PrP^{Sc} is also a component of amyloid plaques. A characteristic of vCJD and kuru is florid amyloid plaques. They are often described as ‘florid plaques’ due to decoration of the perimeter of the plaque with regions of spongiform change. PrP^{Sc} deposition is also present in peripheral tissues of patients with vCJD, primarily in secondary lymphoid tissues.

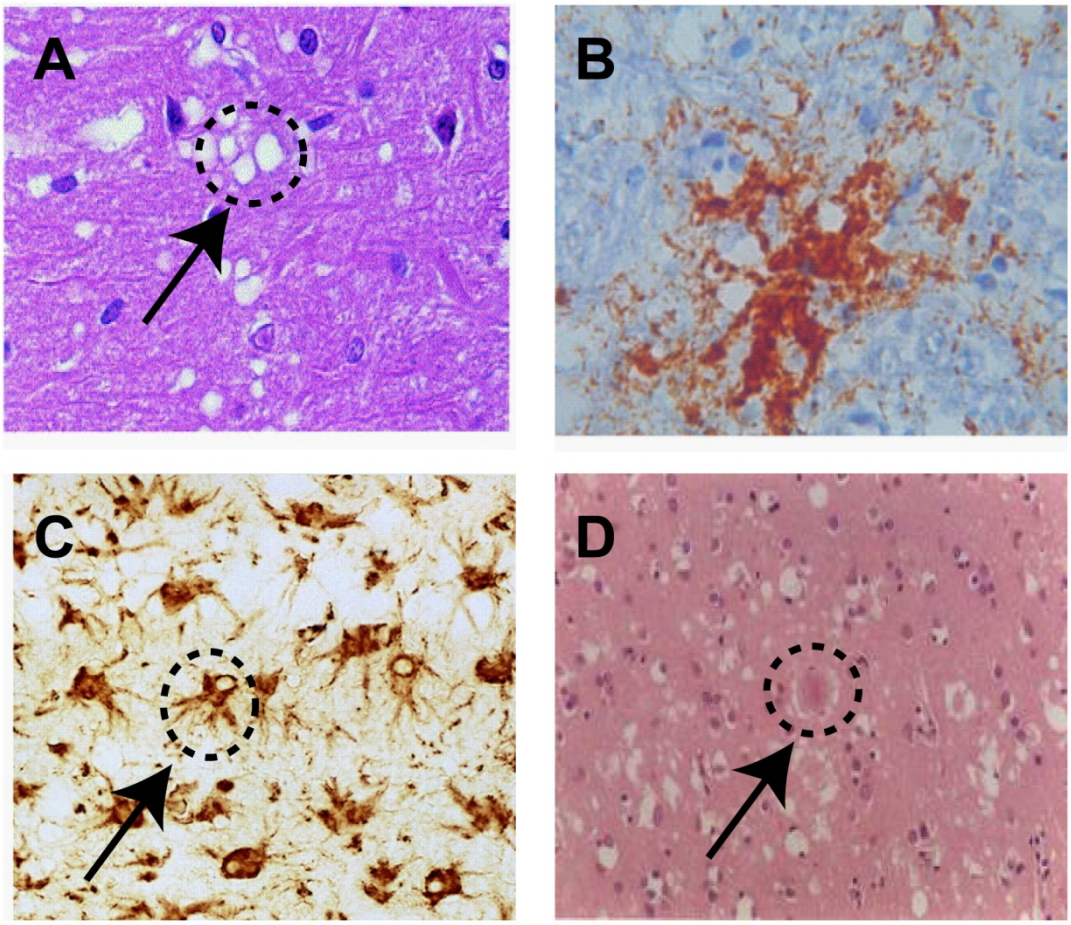

Figure 1: The neuropathological feature of transmissible spongiform encephalopathies. A: Spongiform (vacuolar) degeneration in the grey matter of the brain of a CJD patient stained with hematoxylin–eosin (HE). Image taken from Aguzzi, 2001. Vacuolation of the brain (black arrows) is observed in most prion diseases and causes the degeneration of neuronal processes and eventually results in the death of neurons. **B:** Deposits of PrP amyloid as observed by immunohistochemistry in the brain of an elk infected with CWD. Image taken from Watts et al. 2006. **C:** Activation of astrocytes in the brain of a patient with CJD as observed by immunostaining for glial fibrillary acidic protein (GFAP). Image taken from DeArmond et al. 2004. **D:** 'Florid' plaque (black arrow) consisting of a central PrP amyloid deposit surrounded by a halo of spongiform change in the brain of patient with vCJD. Image taken from

To confirm a protein-like agent, the protein had to be purified and characterised. Purification of the infectious agent revealed that a single protein required for transmission of the disease was present in the brain of infected animals (in this case, hamsters infected with an isolate originally obtained from a sheep TSE) but absent in brains of healthy animals (Bolton et al., 1982). This protein which corresponds to ~ 142 amino acids had a molecular weight of 27-30 kDa. The accumulation of evidence linking a protein to the TSE agent led

Stanley Prusiner to introduce the concept of a prion (proteinaceous infectious particles) and the protein-only hypothesis to explain TSEs in 1982 for which he was later awarded the 1997 Nobel Prize in Medicine (Prusiner 1998).

1.2 The 'Protein-Only' Hypothesis

According to the prion, or 'protein-only', hypothesis, the central pathogenic event of prion disease is the conformational conversion of PrP^{C} into the PrP^{Sc} isoform (Prusiner, 1998). Strictly interpreted, this hypothesis claims that PrP^{Sc} is composed solely of misfolded PrP protein and that this misfolded protein alone is the infectious agent of prion disease. The generation of PrP^{Sc} through this misfolding event leads to neurodegeneration by an as yet unidentified mechanism.

Several lines of evidence support the idea that the conformational conversion of PrP^{C} can be induced by physical interaction with PrP^{Sc}. That PrP knockout mice whose PrP gene, *PRNP*, is ablated are resistant to prion infection indicates that PrP^{C} is required for PrP^{Sc} formation (Bueler et al., 1993; Sailer et al., 1994). Additionally, the development of the first *in vitro* PrP^{C} conversion assay by Caughey provided more data supporting a direct interaction between PrP^{C} and PrP^{Sc}. In Caughey's cell-free assay, radiolabeled PrP^{C} purified from mammalian cells was combined with a stoichiometric excess of unlabeled PrP^{Sc} and incubated under non-physiological conditions. This reaction resulted in the amplification of protease-resistant, radiolabeled PrP^{Sc} which could only have been derived from the substrate PrP^{C} (Kocisko et al., 1994). More recently, researchers using a novel *in vitro* prion conversion assay called protein misfolding cyclic amplification (PMCA) have improved upon Caughey's initial results. Using PCMA, native PrP^{C} can be converted under physiological conditions into PrP^{Sc} in reactions containing sub-stoichiometric amounts of PrP^{Sc} (Deleault et al., 2007; Saborio et al., 2001). Together these findings, among others, support the hypothesis that PrP^{Sc} is formed through an autocatalytic process whereby PrP^{Sc} interaction with PrP^{C} induces its

conformational conversion to form nascent PrP^{Sc}. However, definitive proof of the 'protein-only' hypothesis is still lacking.

Attempts have been made to generate infectious prions *in vitro* solely from misfolded recombinant PrP protein, but to date none of these preparations have been infectious to wild-type animals when inoculated intracerebrally (Legname et al., 2004). Until an infectious prion can be generated with only PrP protein, the 'protein-only' hypothesis of prion disease will remain unproven.

While it is accepted that PrP^{C} undergoes a conformational change to form PrP^{Sc}, the precise molecular mechanism of this misfolding event is unknown. Several models exist which describe how this process could occur. According to the **template-assisted model**, PrP^{Sc} contains the information which is required to induce refolding of PrP^{C} upon physical interaction. The misfolding event in this model is possibly catalyzed by a cofactor and involves the formation of a PrP intermediate during refolding (Abid and Soto, 2006; Cohen and Prusiner, 1998). The conversion of PrP^{C} results in the formation of homodimeric PrP^{Sc} which can interact with other PrP^{Sc} dimers to form larger aggregates. According to the **nucleation-polymerization model**, the PrP^{C} and PrP^{Sc} conformational states exist in equilibrium, but due to instability of PrP^{Sc} monomers, the PrP^{C} state is favored. However, the formation of multimeric PrP^{Sc} could stabilize and interact with monomers of spontaneously formed PrP^{Sc}, leading to the formation of PrP^{Sc} polymers (Abid and Soto, 2006).

A variation of this model, called the **nucleated-assisted model**, was recently proposed (Abid and Soto, 2006). In this model, a PrP^{C} conformational intermediate forms by interaction with a conversion co-factor. The association of these intermediate PrP^{C} molecules induces a second structural conversion in PrP^{C} resulting in the formation of stable PrP^{Sc} oligomers. It is known that molecules of PrP^{Sc} readily aggregate both in vitro and in vivo. In vivo, PrP^{Sc} can form extracellular deposits of amyloid filaments (DeArmond et al., 1985). In vitro, protease treatment and detergent extraction of PrP^{Sc} induces the

formation of rod-like structures (Atarashi et al., 2008). While these observations indicate that PrP^{Sc} can oligomerize, isolation of a PrP folding intermediate during conversion would provide valuable insight into the mechanism of prion formation. Recombinant PrP folding intermediates have been studied in vitro but it is unknown whether these species are relevant to the formation of PrP^{Sc} (Apetri and Surewicz, 2003).

1.2.1 Prion Strains

One aspect of prion biology that is not fully explained by current conversion models is the existence of prion strains. Prion strains are distinct isolates which display unique biological properties and result in characteristic phenotypes when propagated in a given species. Strains can be identified and differentiated on the basis of clinical manifestation (such as the “scratching” and “drowsy” strains of scrapie when given to goats) (Pattison and Millson, 1961), differential incubation times (Dickinson et al., 1968), pathological lesion profiles (i.e. different strains target different neuroanatomic areas of the brain) (DeArmond et al., 1993), the ratio of glycoforms (unglycosylated, monoglycosylated and di-glycosylated) within protease-digested preparations of PrP (Collinge et al., 1996), the size of the PK-resistant PrP fragment (Bessen and Marsh, 1994; Telling et al., 1996), differential reactivity to luminescent conjugated polymers (Sigurdson et al., 2007), and other biochemical properties such as conformational stability (Legname et al., 2005) (Figure 2). The existence of prion strains comprises one of the main challenges to the protein -only hypothesis and opponents argue that such diversity cannot be encoded in the absence of a nucleic acid (Bruce and Dickinson, 1987). Indeed, multiple prion strains can exist for a given PrP amino acid sequence suggesting that strain variety is encoded by a different mechanism.

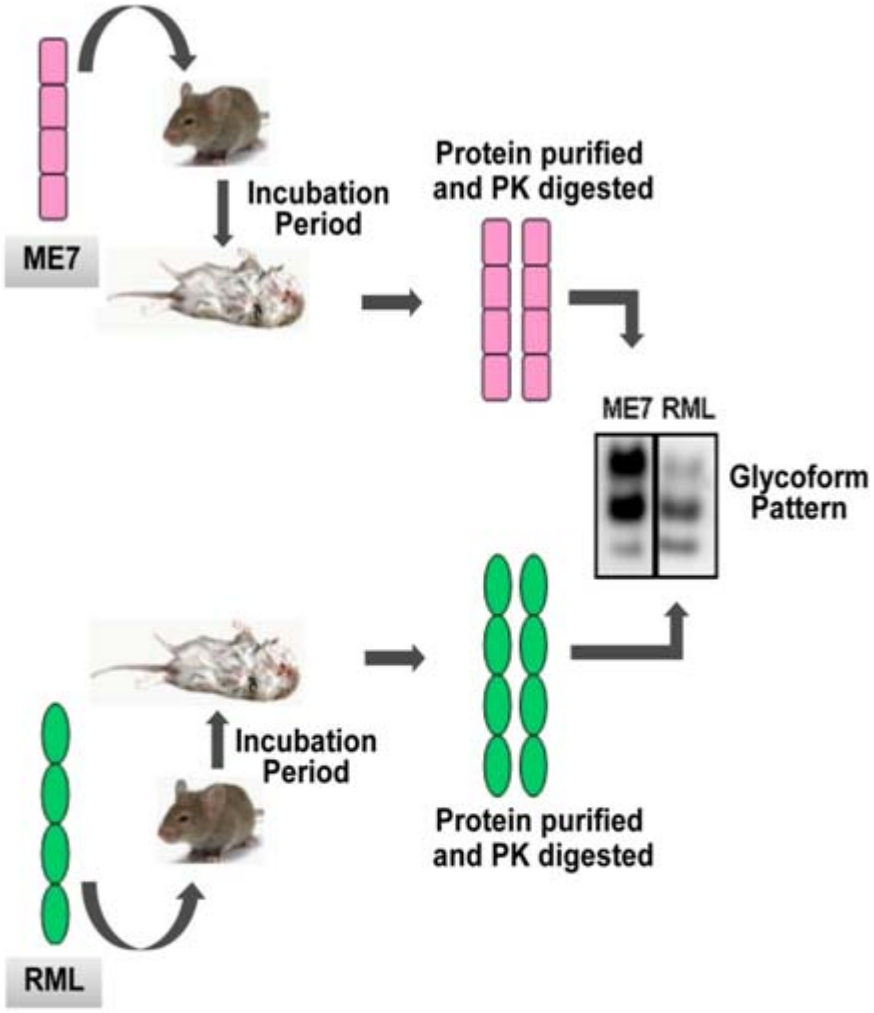

Figure 2: Molecular Analysis of Prion Strains. Two mouse Prion strains (ME7 and RML) are shown as an example of prion strain variability. Transmission of different prion isolates to an identical host results in distinct disease phenotypes like incubation period, neuro-pathological damage and the glycosylation pattern (shown in the western blot insert). Typically, these phenotypic traits persists upon serial transmission.

Mammalian PrP genes are highly conserved, and this hypothesis suggests that only a restricted number of different PrP^{Sc} conformations are thermodynamically permissible and constitute the range of observed prion strains (Collinge and Clarke, 2007). Although a significant number of different PrP^{Sc} conformations might be possible across the range of mammalian PrPs, only a subset of these would be allowed within a given mammalian species. Substantial overlap between the favoured conformations for PrP^{Sc} derived from species A and species B might therefore result in relatively easy transmission

of prion diseases between these two species, whereas two species with no preferred PrP^{Sc} conformations in common would have a large barrier to transmission (Figure 3).

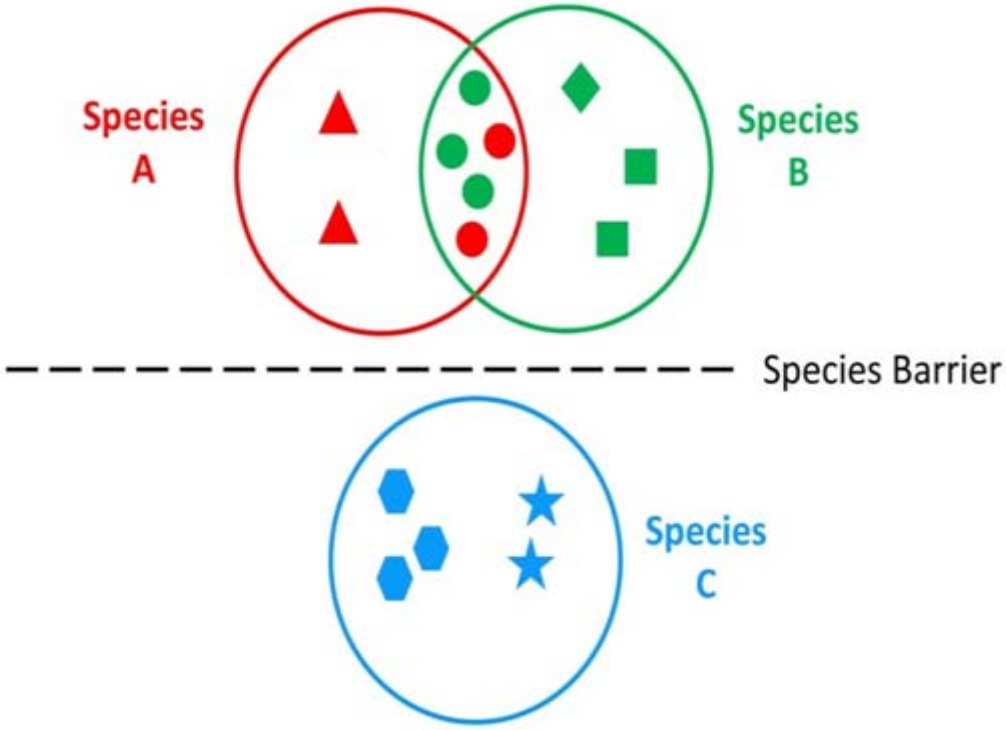

Figure 3: Conformation selection model of prion transmission barriers. Within a given species, PrP^{Sc} might exist in multiple conformations. Quite possibly, some of these may be compatible with the amino acid sequence of another species and some which are not. Thus interspecies transmission will occur only to the extent that the PrPSc conformation is compatible with both amino acid sequences. Since there is an overlap of the conformation between species A and species B, there would be an easy transmission of infection between them. On the contrary, species C does not exhibit any conformation which is in common with species A or species B, so there would be a large barrier to transmission.

According to this model of a prion transmission barrier, BSE would represent a thermodynamically highly favoured PrP^{Sc} conformation that is permissive for PrP expressed in a wide range of different species, accounting for the remarkable promiscuity of this strain in mammals. In this Figure, there is overlap between the allowable PrP^{Sc} conformers between species A and species B. This overlap facilitates transmission between these species involving the 'green' and 'red' strains. There is no overlap or allowed

conformers between species A or B with species C resulting in a substantial transmission barrier between species C and A, or C and B. Passage of strains through an intermediate host might allow the adaptation of a particular strain to a new host.

1.2.2 Transmission Barrier

When prions from one species are introduced into a second species, there is often a significant species barrier effect which limits the transmission of prions. Species barrier effects include prolonged incubation time and inefficient transmission (i.e. only a small proportion of inoculated animals get the disease). The species barrier has important implications for human health as it appears that there is a significant species barrier between humans and CWD or scrapie prions. In contrast, BSE prions appear to be rather promiscuous and can enter a number of diverse species including humans in the form of vCJD (Will et al., 1996). At the molecular level, the species barrier is likely dictated by the amino acid sequence of PrP. Between different mammalian species the primary transmission of prions is generally inefficient and this effect is conventionally called a 'species barrier'. The amino acid sequence of PrP is highly conserved between mammalian species (Schatzl et al. 1995; Wopfner et al. 1999), and within the proteinase K resistant core of PrP^{Sc}, there are only eight amino acid substitutions between mice and hamsters (Figure 4 A). Still, mice do not develop prion disease after challenge with hamster prions. Transgenic mice that express both hamster PrP and mouse PrP can be infected with hamster prions, and then selectively incorporate hamster PrP into prion particles (Prusiner et al. 1990). The exclusive expression of a mouse/hamster chimeric PrP, termed MH2M, makes mice susceptible to both hamster and mouse prions (Scott et al. 1993), and the resulting prions transmit disease to both wild-type hamsters and wild-type mice. Thus, the species barrier is determined by the primary amino acid sequence of the prion protein, and the substitution of only a few amino acid residues can completely alter prion transmission patterns. (Prusiner et al., 1990) (Figure 4 B). This is remarkable, as there are only few amino acids difference between the two

PrPs. Interestingly, the bank vole appears to be susceptible to prions from a variety of human prion diseases despite a low degree of sequence homology between human and vole PrP (Nonno et al., 2006). This suggests that factors other than the PrP amino acid sequence may influence the species barrier.

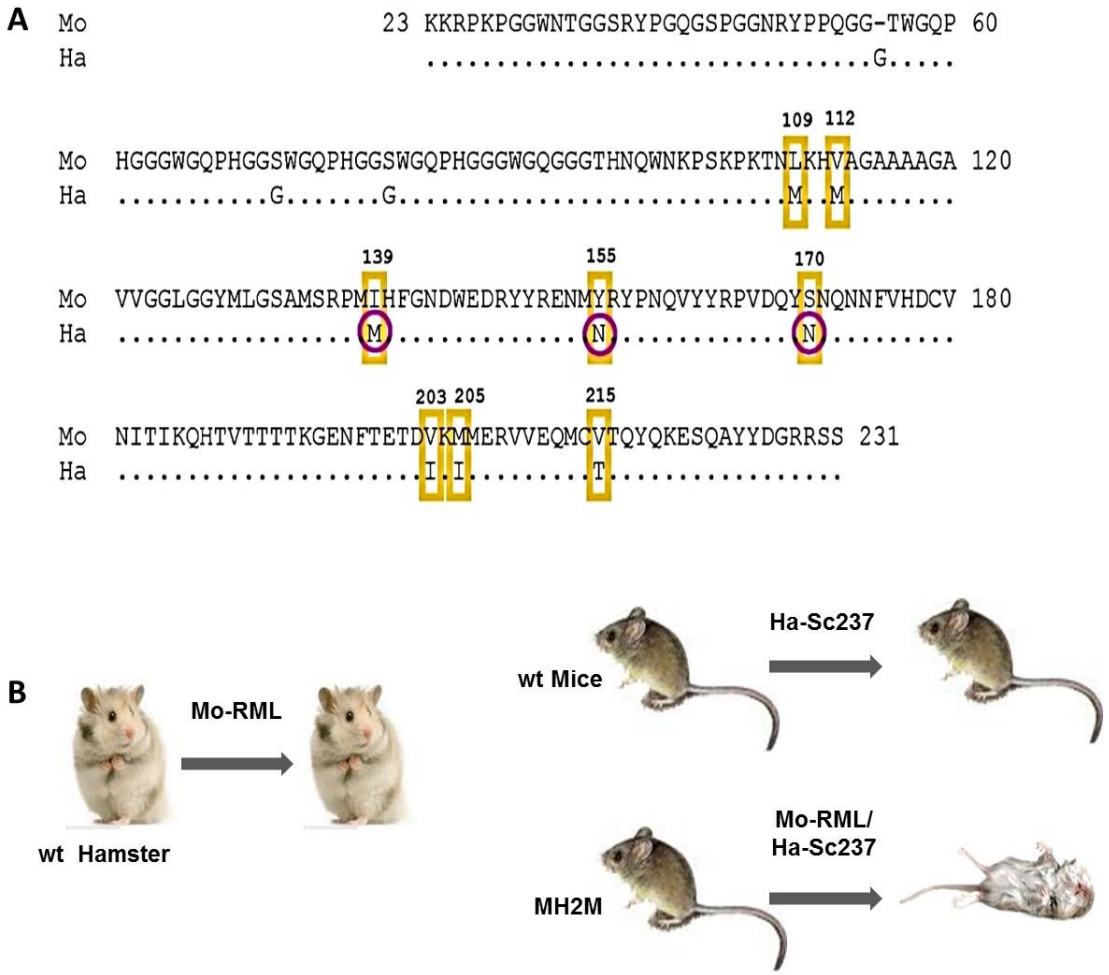

Figure 4: Amino acid sequence alignment of Mouse (Mo) and Hamster (Ha) prion protein **(A)**. The difference between acids between two species are indicated by sequence numbers and yellow rectangles. **(B)** Species barrier between Hamster and Mice. wt Hamsters when challenged with mouse prions, do not develop a prion disease and the same is true for wt mice which remains healthy after inoculation with hamster prions. However, chimeric mice, termed MH2M, which expresses mouse/hamster PrP makes mice susceptible to both hamster and mouse prions (Scott *et al.* 1993), and the resulting prions transmit disease to both wild-type hamsters and wild-type mice.

Within a given species, the amino acid of PrP can also profoundly influence prion disease susceptibility and incubation times. For example, two polymorphisms in the mouse PRNP gene (encoding the L108F and T189V polymorphisms in mouse PrP) control prion incubation time (Barron et al.,

2005;Moore et al.,1998; Westaway et al., 1987). A second example is the sheep gene in which polymorphisms at ovine PrP residues 136, 154, and 171 have a strong effect on susceptibility to scrapie with the VRQ allele being associated with increased susceptibility (Westaway et al., 1994). Thirdly, no cases of sporadic CJD have been found in individuals with the lysine variant of the codon 219 E/K polymorphism in human PrP (Shibuya et al., 1998). Finally, the codon 129 M/V polymorphism in the human PRNP gene controls both prion disease phenotype (i.e. determining FFI versus gCJD phenotypes when in cis to a D178N mutation) and susceptibility to disease (no cases of vCJD have been observed in nonmethionine homozygotes (Smith et al., 2004).

1.3 The Prion Protein – Agent responsible for TSE's

Following the purification of PrP, the encoding gene (PRNP) was identified. Amino acid sequencing of the N-terminus of PrP^{27-30} was used to derive a cDNA clone encoding a host protein, which subsequently demonstrated that PrP^{27-30} was encoded by a single-copy chromosomal gene (Oesch et al., 1985). The presence of PrP mRNA in the brains of both infected and unaffected animals (Barry et al., 1986) provided evidence that PrP could exist in two different forms: the normal cellular isoform termed PrP^{C} and the disease-associated form, PrP^{Sc} (Sc stands for scrapie). In general, PrP^{Sc} is described as an abnormal isoform of PrP which stimulates conversion of PrP^{C} into PrP^{Sc} and causes disease. Limited proteolysis of PrP^{Sc} (~33-35 kDa) produces a smaller protease resistant molecule of ~ 142 residues designated as PrP^{27-30}; under the same conditions PrP^{C} is completely hydrolysed (Basler et al., 1986; Oesch et al., 1985; Prusiner, 1984). PrP^{C} can be solubilised by low concentration of detergents whereas PrP^{Sc} or PrP^{27-30} remains insoluble and polymerises into highly ordered amyloid structures known as prion rods or Scrapie associated fibrils (SAF) (Prusiner, 1983; Merz et al., 1983).

Although insolubility as well as protease resistance can differentiate PrP^{Sc} from PrP^{C} but studies have shown that these properties act only as surrogate markers, as are high β-structure content and polymerisation into amyloid

(Jansen et al., 2001; Xiong et al., 2001). Absence of these markers does not indicate lack of prion infectivity, therefore selecting an appropriate method of sample preparation from scrapie infected brain can influence the sensitivity of PrP^{Sc} detection because PrP^{Sc} is not uniformly distributed in the brain. Some of the general distinguishing features of PrP^{C} and PrP^{Sc} are listed in Table 2.

Table 2: Differences between PrP^{C} and PrP^{Sc}

PrP^{C}	PrP^{Sc}
Normal Cellular form	Pathological form
Protease sensitive Mr (-PK) 33-35 kDa Mr (+PK) fully degraded	Protease resistant (partly) Mr (-PK) 33-35 kDa Mr (+PK) 27-30 kDa
Soluble	Insoluble (precipitates/aggregates)
Monomer	Polymer (Scrapie Associated Fibrils/ Prion Rods)
Mainly α helical	Predominant β sheet structure
Non Infectious	Infectious (Protein only Hypothesis)

1.3.1 PrP^{Sc} – The Pathological Isoform of Prion Protein

High resolution structural analysis of PrP^{Sc} by NMR spectroscopy or X-ray crystallography has been hindered by the aggregated nature and general insolubility of purified PrP^{Sc} and PrP^{res}. At the secondary structure level it is known that PrPSc and PrPres have an increased β-sheet content compared to PrP^{C} (Cohen et al. 1993). Studies using antibodies have shown that certain epitopes which are exposed in native PrP^{C} are masked in native PrP^{Sc} and this idea forms the basis for the CDI assay for prions (Prusiner et al. 1998). In particular, residues 90 to 120 of hamster PrP are inaccessible in PrP^{Sc} suggesting that regions within the N-terminal unstructured domain of PrP^{C} are conformationally altered in PrP^{Sc} (Peretz et al. 1997). In contrast, a recent study using hydrogen/deuterium backbone amide exchange found that the β-sheet core of amyloid fibrils formed from recombinant human PrP(90-231) is composed of residues from α-helices 2 and 3 (Surewicz et al. 2007). Upon

treatment with proteinase K, PrP^{Sc} spontaneously forms amyloid fibrils termed prion rods (Prusiner, 1983). Electron microscopy on two-dimensional crystals obtained from PrPres has provided low resolution structural data and implies the presence of parallel β-helices (Wille et al. 2002). Further studies on these crystals has led to a model for PrP^{Sc} in which individual units are composed of a trimer of PrP^{Sc} containing parallel left-handed β-helices (Wille et al. 2007). A distinct model for the structure of PrP^{Sc} has been obtained by molecular dynamics simulations (DeMarco et. Al. 2004). Simulations of hamster PrP with the D147N mutation at low pH lead to a β-sheet enriched structure which readily forms hexameric protofibrils. Currently there is no consensus as to which model, if either is correct and to date there is no high resolution structural information available for PrP^{Sc}.

PrP^{Sc} Formation

In scrapie infected cells, PrP^{C} molecules destined to become PrP^{Sc} exit to the cell surface prior to conversion into PrP^{Sc} (Borchelt et al., 1990; Stahl et al., 1987). Like other GPI anchored proteins, PrP^{C} appears to re-enter the cell through a subcellular compartment bounded by cholesterol rich, detergent insoluble membranes, which may be caveolae or early endosomes (Gorodinsky and Harris, 1995;Naslavsky et al., 1997;Vey et al., 1996). Within this cholesterol rich, non-acidic compartment, GPI anchored PrP^{C} can be either converted into PrP^{Sc} or partially degraded (Taraboulos et al., 1995). Subsequently, PrP^{Sc} is cropped at the amino terminus in an acidic compartment in scrapie infected culture cells to form $PrP^{27\text{-}30}$ (Xiong et al., 2001).

Cellular Localization of PrP^{Sc}

Investigation of the sub-cellular distribution of PrP^{Sc} remains challenging due to the lack of antibodies specific to PrP^{Sc}. Early studies reported that the majority of PrP^{Sc} is intracellular, mostly co-localized with Golgi markers and

sequestered within lysosomes of scrapie-infected N2a (ScN2a) cells (Borchelt et al., 1992; Xiong et al., 2001). Vey et al., demonstrated accumulation of PrP^{Sc} in CLDs derived from the plasma membrane in ScN2a cells (Vey et al., 1996). In prion-infected brains, PrP^{Sc} accumulates at the plasma membrane (Sim and Caughey, 2009) and occasionally in structures which contain the cation-independent mannose 6-phosphate receptor, ubiquitin-protein conjugates, a-glucuronidase, and cathepsin B, termed late endosomal/lysosomal compartments (Arnold et al., 1995). More recent reports have described the accumulation of PrP^{Sc} in various cellular compartments: the perinuclear Golgi region of neurons in scrapie-infected transgenic mice (Barmada and Harris, 2005); the late endosomal compartments in infected GT1-7 and N2a cells (Pimpinelli et al., 2005) and the cell surface and early endocytic/ recycling vesicles in hippocampal neurons (Godsave et al., 2008). In SN56 cells and hamster cortical neurons, exogenous Alexa-labelled PrP^{Sc} internalized into vesicles which stain positive for late endosomal/lysosomal markers (Magalhaes et al., 2002) .Mange et al. showed accumulation of PrP^{Sc} in the nuclei of prion-infected N2a cells (Mange et al., 2004) by demonstrating that nuclear PrP interacts with chromatin in vivo. Several in vitro studies have shown accumulation of PrP^{Sc} -like conformers (prion protein conformers that are not necessarily infective) in the ER (Ivanova et al., 2001; Lehmann and Harris, 1997) Golgi and plasma membrane of infected cells (Ivanova et al., 2001). Under certain conditions, PrP^{Sc} -like conformers have been reported to accumulate in the cytosol (Ma and Lindquist, 2002) and there is also evidence for cytosolic PrP^{Sc}-containing aggresomes in prion-infected cells following proteasome inhibition (Kristiansen et al., 2005). The tentative conclusion from these studies is that PrP^{Sc} is widely distributed within infected cells, although improved methods for in-situ detection of PrP^{Sc} are clearly needed to establish the relative proportion of the protein in these cellular sites.

1.3.2 PrP^{C} – The Normal Cellular form of Prion Protein

Human PrP is initially expressed as a 253 amino acid polypeptide (Figure 5). The N-terminus of PrP^{C} contains a signal sequence directing it to the endoplasmic reticulum (ER) (Caughey et al., 1989). Once in the ER, this signal

sequence is removed and PrP^C undergoes several stages of post-translational modification. An approximately 18 amino acid hydrophobic C-terminal sequence directs the addition of a GPI anchor while in the ER, and this GPI sequence is simultaneously cleaved from PrP^C resulting in the mature form PrP^C which is approximately 209 amino acids in length, depending on the species (Stahl et al., 1987). PrP^C can undergo N-linked glycosylation at two sites, initially via the addition of high mannose glycans in the ER which is followed by carbohydrate modification in the Golgi (Haraguchi et al., 1989). Thus, PrP^C can exist in three glyoforms: unglycosylated, monoglycosylated, and diglycosylated. The structures of PrP^C from various species have been determined and are remarkably similar: the N-terminus is unstructured in solution whereas the C-terminal domain consists of a three α-helix bundle with two short β-strands. Additionally, a single disulfide bond is introduced between cysteine residues located within the C-terminal domain (Turk et al., 1988). To date, no differences in post-translational modification between PrP^C and PrP^{Sc} have been identified.

Another feature of the cellular prion protein is an N-terminal octarepeat region consisting of five repeats of the sequence PHGGGWGQ in the case of human PrP. The octarepeat region is notable for several reasons. Firstly, the histidine residues are capable of binding copper with four copper-binding sites located within the octarepeat region (Brown et al., 1997) and copper is known to induce endocytosis of PrP^C (Pauly and Harris, 1998). Secondly, expansions of the octarepeat domain (with up to fourteen total repeats) are known to cause genetic prion disease classified as either gCJD or GSS (Krasemann et al., 1995) and expression of this mutant protein in transgenic mice causes a non-transmissible neurological syndrome (Chiesa et al., 1998). The second notable region is the hydrophobic tract prior to the beginning of the structured domain. This sequence is well conserved amongst PrP^C sequences from a variety of species. Mutations within this sequence can increase the formation of Ctm PrP (a transmembrane topological variant of PrP in which the C-terminus is luminal and the N-terminus is cytoplasmic) which has been linked to neurodegeneration (Hegde et al., 1999). Furthermore, as N terminal deletions in PrP^C invade this domain, the truncated proteins become increasingly toxic to

transgenic mice (Shmerling et al., 1998). The extreme N-terminus of PrP (the basically-charged region beginning at residue 23 of mouse PrP) is important for its proper trafficking in the cell (Sunyach et al., 2003). Upon suramin-induced misfolding of PrP^C, constructs lacking this region remain on the cell surface, indicating a defect in the trafficking and recycling of misfolded proteins (Gilch et al., 2004).

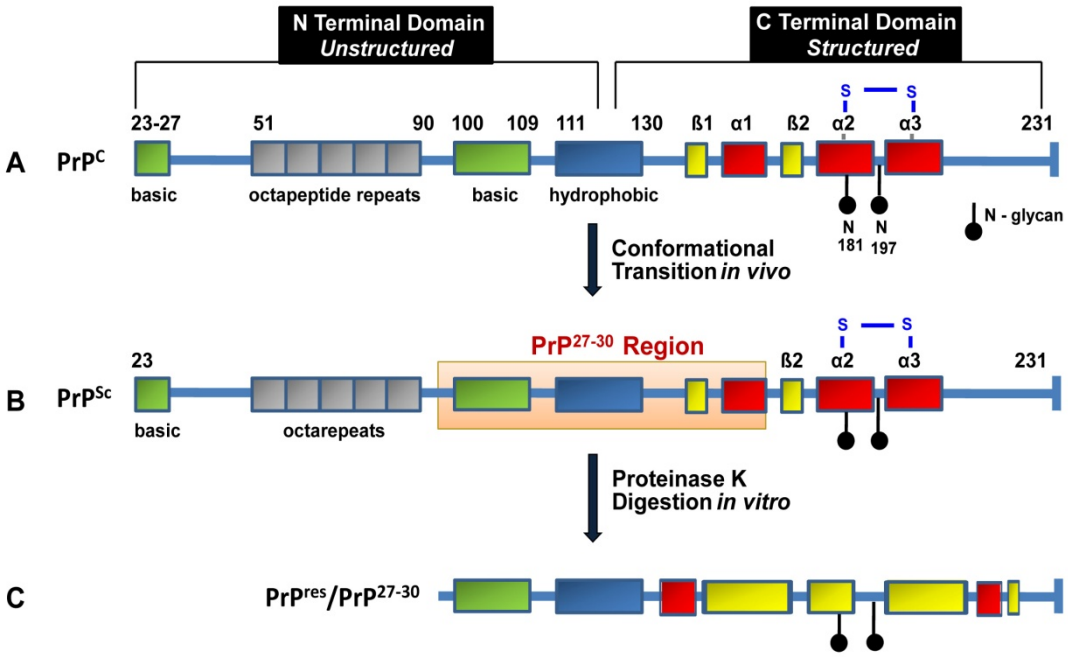

Figure 5: Schematic representation of murine PrP sequence illustrating post-translational modifications of PrP^C and PrP^{Sc}. (A) Sequence of mPrP (23-231) is represented as a blue line and the sequence motifs are depicted by colored boxes. Two basic stretches are shown in green, a hydrophobic stretch is shown in blue and the five octapeptide repeats are shown in grey. Colored boxes illustrate secondary structure elements with α helices shown in red and β strands in yellow. PrP^C is rich in α helices. The two potential N-glycosylation sites surrounded by a disulfide bridge are close to α helical regions. **(B)** In prion disease, the host-encoded cellular prion protein (PrP^C) undergoes a conformational transition to a disease-associated conformer termed PrP^{Sc}. The approximate region of PrP^C known to be conformationally altered in PrP^{Sc} is shown in orange color rectangular box, although the exact boundaries are unknown. **(C)** Detection of prion disease is commonly achieved in vitro by treatment with proteinase K which cleaves PrP^{Sc} near residue 90 to generate the protease-resistant fragment termed PrP^{res} or PrP^{27-30}. Note, the structure for PrP^{res} is a hypothetical representation. The higher beta sheet content and the fact that most of the predicted beta sheet structures are downstream of β1 and β2 strand regions of PrP^C is also noteworthy. These strands have been hypothesized to form a potential "nucleation site" that triggers the formation of PrP^{res}.

Cellular Biology of PrP^C

Investigating the biosynthesis, posttranslational processing, cellular localization, and trafficking of PrP^C and PrP^{Sc} allows examination of the properties of PrP in the setting of native cellular structures. The function of

PrP^C and co-factors that are likely to be critical in mediating the efficient conversion of PrP^C into PrP^{Sc} can only be elucidated in detail in a cell culture model system. PrP^C is a glycoprotein, normally attached to the surface of neurons, especially synaptic membranes, and glia cells of the brain and spinal cord in all mammals via a glycophosphatidylinositol (GPI) anchor (Moser et al., 1995; Stahl et al., 1987). The expression pattern of PrP^C is diverse and developmentally regulated in skeletal muscle, kidney, heart, secondary lymphoid organs and the CNS, suggesting a wide-ranging and conserved function of the protein (Aguzzi and Polymenidou, 2004; Bendheim et al., 1992; Caughey et al., 1988; Dodelet and Cashman, 1998; Moser et al., 1995).

Cellular Localization of PrP^C

To date, the precise cellular localization of PrP^C in neurons remains elusive. Most studies have shown that PrP^C is predominantly present in detergent-resistant microdomains (DRM or lipid rafts) on the plasma membrane, in particular in the axon or synaptic membrane (Mironov et al., 2003). Other putative sites of PrP^C localization are: the ER (Sarnataro et al., 2004), the Golgi, endolysosomes (Magalhaes et al., 2002), exsosomes (Fevrier et al., 2004), the plasma membrane (Sarnataro et al., 2002), clathrin coated pits (Sunyach et al., 2003), caveolae (Zahn et al., 1997), lipid rafts (Vey et al., 1996), and the cytosol. Although PrP^C is known as a cell-surface GPI-anchored protein, it does not remain on the cell surface; it constitutively cycles between the plasma membrane and an endocytic compartment from which most of the PrP^C is recycled back to the cell surface (Shyng et al., 1993). More than 90 % of surface PrP^C is internalised within two minutes and returned to the cell surface within six minutes (Sunyach et al., 2003). During this process, PrP^C is cleaved near residue 110, probably in an acidic cellular compartment (Merz et al., 1981). The biological role of PrP^C internalization is unknown, but studies have demonstrated that internalization is induced by copper and zinc ions and thus could have a physiological function in chelating extracellular copper ions or in modulating the signal activity of the protein (Pauly and Harris, 1998; Watt and Hooper, 2003). Understanding the endocytic itinerary of PrP^C

is fundamental, since both general inhibition of endocytosis (Godsave et al., 2008; Gohel et al., 1999) and/or a direct modification of the internalization route of PrP^C by replacing the GPI anchor with a transmembrane sequence containing a coated pits localization motif (Fournier et al., 2000) affect the infection and the conversion processes(Beranger et al., 2002; Borchelt et al., 1992; Xiong et al., 2001).

The mechanism of PrP^C uptake is currently debated. Dynamin, clathrin-coated pits, rafts and caveolae appear to play an important role. Immunogold localization of PrP^C in clathrin coated pits and vesicles suggest that PrP^C internalizes via clathrin-mediated endocytosis (Sarnataro et al., 2009; Sunyach et al., 2003). Magalhaes and co-workers also demonstrated that cells transfected with a dominant negative mutant of dynamin I (K44A), which blocks fission of invaginated coated pits from the plasma membrane, inhibit PrP^C endocytosis suggesting that PrP^C is internalized via a dynamin dependent pathway (Magalhaes et al., 2002). A basic amino acid motif in the N-terminal half of PrP^C polypeptide chain was shown to be essential for efficient clathrin-mediated endocytosis as deletion within this region diminishes internalization of PrP^C (Sunyach et al., 2003). This finding led to the proposal that PrP^C binds through this N-terminal region to a 'PrP^C receptor', a transmembrane protein, that has a coated-pit localization signal causing it to enter the clathrin-dependent internalization pathway. In Chinese hamster ovary cells, which express caveolin-1, PrP^C is absent in clathrin-coated pits and vesicles, instead being localized in caveolae at the trans-Golgi network, the plasma membrane and in interconnecting chains of endocytic caveolae (Zahn et al., 1997). To date, however, no caveolae have been identified in adult mammalian neuronal cells, suggesting this pathway is unlikely to be relevant to prion trafficking in neurons (Morris et al., 2006). An alternative hypothesis regarding PrP^C internalization involves lipid rafts, also called caveolae-like domains (CLDs), which have similar lipid composition to caveolae but lack cavealin-1 (Sabharanjak et al., 2002). Studies have suggested that PrP^C internalization can be raft-dependent and/or raft-mediated depending on the cell type. Sarnataro and colleagues demonstrated that PrP^C is internalized in Fischer rat thyroid (FRT) cells via raft-mediated endocytosis. Cholesterol

depletion and inactivation of cell division cycle 42 (Cdc-42) in FRT cells impaired uptake of PrP^C, suggesting a role for lipid rafts in PrP^C endocytosis (Sarnataro et al., 2009).

Physiological Function of PrP^C

PrP^C is a highly conserved protein that is found in all tetrapods and in birds (Wopfner et al., 1999). Moreover, the structure of PrP^C from different species is highly similar (Calzolai et al., 2005), suggesting that the function of PrP^C is evolutionary conserved. Lately a homologue to prion-protein was identified in the pufferfish (Fugu rubripes), showing high homology with mammalian PrP sequences (Oidtmann et al., 2003; Suzuki et al., 2002) and Gibbs et al. described for the first time, the presence of normal isoform of amyloid protein (PrP) in brains of spawning salmon (Gibbs and Bolis, 1997). Subsequently, further cDNA sequences were identified in other fish species (zebra fish, common carp, stickleback, and rainbow trout) (Maddison et al., 2005; Rivera-Milla et al., 2006).

The most prominent phenotype of PrP^C - deficient mice is their resistance to prion infection, but no other striking phenotype was initially observed (Bueler et al., 1992; Manson et al., 1994). Therefore, it has been suggested that the loss of PrP^C function may be compensated by other proteins. A closer analysis of $PrP^{0/0}$ mice revealed several subtle phenotypic alterations, such as altered circadian activity rhythms and patterns (Tobler et al., 1996), modified responses to oxidative stress due to reduced activity of Cu/Zn superoxide dismutase, functional changes in the glutamatergic system (Coitinho et al., 2002; Khosravani et al., 2008), peripheral chronic demyelinating polyneuropathy (Bremer et al., 2010), reduced levels of anxiety (Nico et al., 2005), age-related motor behavioral and neuropathological deficits (Nazor et al., 2007; Rial et al., 2009), retarded regeneration of adult muscle (Stella et al., 2010), and alterations in synaptic function (Collinge et al., 1994). Based on these findings, several physiological roles have been attributed to PrP^C, such as modulation of synaptic transmission and neuronal excitability, protection

against oxidative stress, and a role in cell differentiation and neuronal adhesion (Linden et al., 2008). These findings strongly support the notion that physiologically active PrP^{C} is part of signaling cascades implicated in various cellular processes.

Structure of PrP^{C}

It has been indicated that PrP^{C} and PrP^{Sc} are chemically identical; however, the biophysical features of PrP^{Sc} are significantly different from PrP^{C} in respect to solubility, structure, fibril formation, proteinase K resistance and other features. These differences could be either a consequence of ligands bound to one isoform but not to the other or a consequence of a different secondary and tertiary structure of PrP^{C} and PrP^{Sc}, respectively (Riesner, 2003). At the secondary structure level it is known that PrP^{Sc} and PrP^{res} have an increased β-sheet content compared to PrP^{C} (Pan et al., 1993). Fourier-transform infra-red (FTIR) spectroscopy and circular dichroism (CD) were employed to investigate the secondary structure of PrP^{C} and PrP^{Sc}. PrP^{C} contains ~40% α-helix and ~3% β-sheet (Pan et al., 1993; Pergami et al., 1996). Remarkably, PrP^{Sc} contains ~30% α-helix and ~45% β-sheet. This finding supported the unorthodox conclusion that the same PrP polypeptide could adopt two distinct conformations.

Brain derived PrP^{C} poses several disadvantages for three-dimensional structural determination by X-ray or NMR spectroscopic methods. Firstly, the amount of material available was too small, the samples were not sufficiently pure, and the concentration was also less. These problems prompted the need for expression and purification of recombinant PrP labeled with either ^{15}N or ^{13}C.

Using recombinant PrP, Riek et al. (Riek et al., 1996) solved the structure of the C-terminal part of PrP, *i.e*. amino acids (121–231) which consists of three α-helices (amino acids 144–154, 175–193 and 200–219) and a small

antiparallel β-sheet (amino acids 128–131 and 161–164) (Figure 6). Later, structure of 'full-length' PrP (*i.e*. amino acids 23–231) was also analyzed which showed that the C-terminal part (*i.e*. amino acids 126–231) contained the complete globular part of the structure, whereas the N-terminus (*i.e*. amino acids 23–125) was more or less flexible (Donne et al., 1997; Riek et al., 1997; Zahn et al., 2000). In the globular domain, a disulphide bridge connects helix 2 and helix 3 (Lopez Garcia et al., 2000).The region between the β-sheet and helix 2 (amino acids 166–171) could be determined with less accuracy possibly because of some structural flexibility. This region, however, is of particular functional interest. Different lines of evidence such as antibody binding, transgenic animals with mutations in that region, binding of the hypothetical factor X, *etc*. argue that the species barrier might be localized in that region. Furthermore, the minor differences in the structure of mouse and hamster PrP on the one hand and of bovine (Lopez Garcia et al., 2000) and human PrP on the other are restricted to that part of the molecule.

The NMR-structure of PrP is a monomeric structure. Several reports in the literature indicate that PrP in its α-helical structure can form dimers under physiological or close to physiological conditions (Jansen et al., 2001; Meyer et al., 2000). Dimers in solution show the intact intramolecular disulphide bridge. Consequently, dimerization is not induced by oxidizing the disulphide bridge and reforming it in an intermolecular structure. The latter situation was, however, found in a recent crystal structure of a dimer of PrP (120–231)(Knaus et al., 2001); dimers were formed by domain swapping and intermolecular disulphide bridging. Whether this structure is a consequence of the long-time crystallization, or might indicate a physiological state, cannot be stated at present.

As mentioned above, PrP^{Sc} or $PrP^{27–30}$ are not accessible to structural analysis by NMR or X-ray analysis because of their insolubility. Attempts were made (Pan et al., 1993) to use the structure described above as a starting model, where α-helices were changed into β-sheets to develop a model for PrP^{Sc}. These models assume that helix 2 and helix 3 are unchanged in accordance with antibody binding data, but they are incomplete in the sense that they are

models for isolated molecules whereas PrP^{Sc} as well as $PrP^{27–30}$ were found only in aggregated forms. Thus, one has to assume that the PrP^{Sc} structure is stabilized by intermolecular interactions.

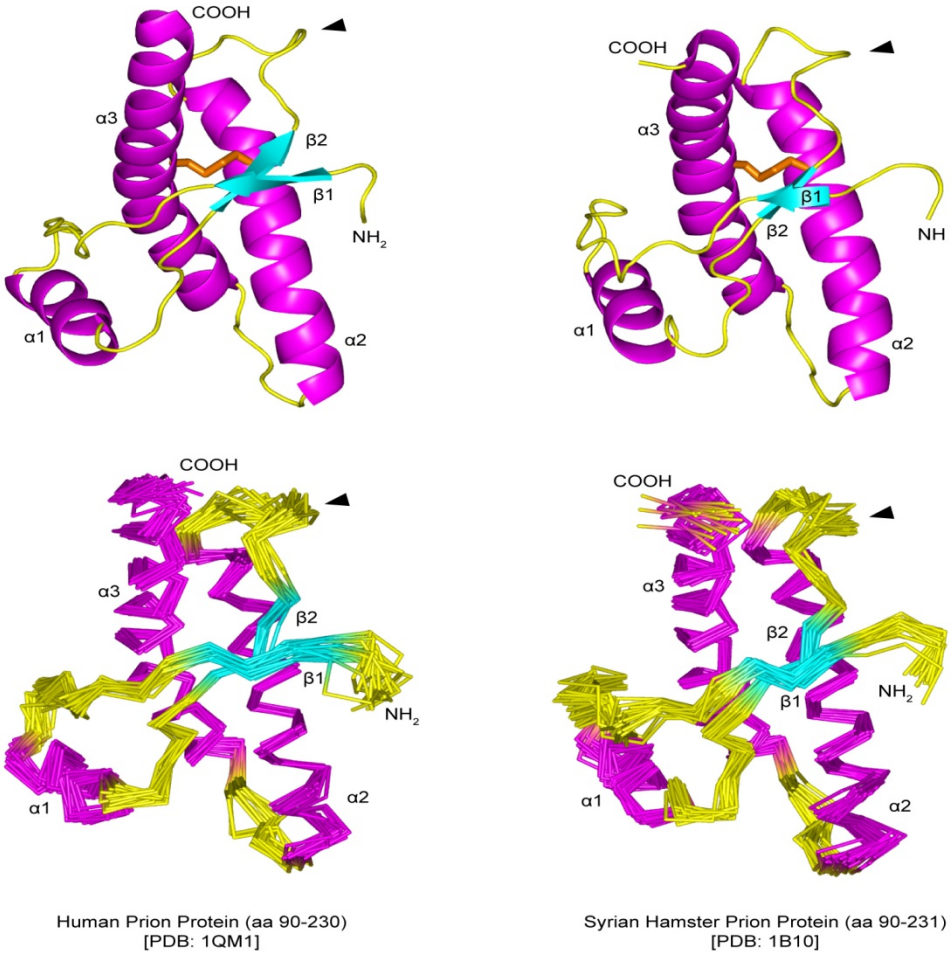

Figure 6: (Left) Three dimentional structure representation of the human prion protein domain, hPrP (90-230), and (right) syrian hamster prion protein sh (90-230). Top panel shows the ribbon diagram with alpha helices in magenta and beta strands in cyan. The disulfide bond between helices alpha2 and alpha3 is shown in orange. The beta2-alpha2 loop is indicated by an arrowhead. Bottom panel shows the polypeptide backbone as a superposition of the 20 conformers used to represent the NMR structure.

A new approach was followed by Wille and coworkers to prepare two-dimensional crystalline-like arrays of PrP^{Sc} - or PrP^{Sc} -like molecules (Wille et al., 2002). Those samples were studied by electron microscopy and, because of the crystalline-like arrangement; images could be reconstructed from the repetitive unit with fairly high resolution. A hexagonal symmetry was visible, but it could not be decided whether one unit is built from 3 or 6 molecules. The electron density map could be fitted best if, instead of β-sheets, a β-helix was

assumed. The structure of the β-helix type is known from other fibrillar proteins; spectroscopically, β-sheets and β-helices cannot be differentiated, so that the new model would not contradict earlier spectroscopic studies. In summary, the β-helical N-terminus is located in the inner part of the hexagonal unit, with the helices 2 and 3 at the outer side and the glycosyl-groups pointing into the space between the hexagonal units.

Recent experimental studies using mass spectrometry analysis coupled with hydrogen-deuterium exchange indicate a PrP^{Sc} conformation completely different from PrP^{C} (Smirnovas et al., 2011), which is in disagreement with the "β-helical" and "spiral" models, in which PrP^{Sc} retains substantial amounts of native α-helices (DeMarco and Daggett, 2004; Govaerts et al., 2004).

1.4 Methods for the in vitro conversion of Prions

A major issue in coping with any infectious disease is the ability to detect the responsible pathogen. In case of TSEs, it is evident that the pathogen is a misfolded multimeric form of the host's prion protein (PrP). This infectious protein, PrP^{Sc}, can instigate its own propagation by binding to its normal counterpart, PrP^{C}, and inducing its conversion to a form that tends to be higher in beta sheet content, polymeric, and protease resistant (Figure 7). The lack of the nucleic acid genome negates the possibility of prions by nucleic acid amplification methods such as PCR. The fact that the infectious agent is composed mainly of a host protein also restricts the use of antibody based detection methods. However, the seeded/templated conformational conversion can be exploited for detection of prion *in vitro.*

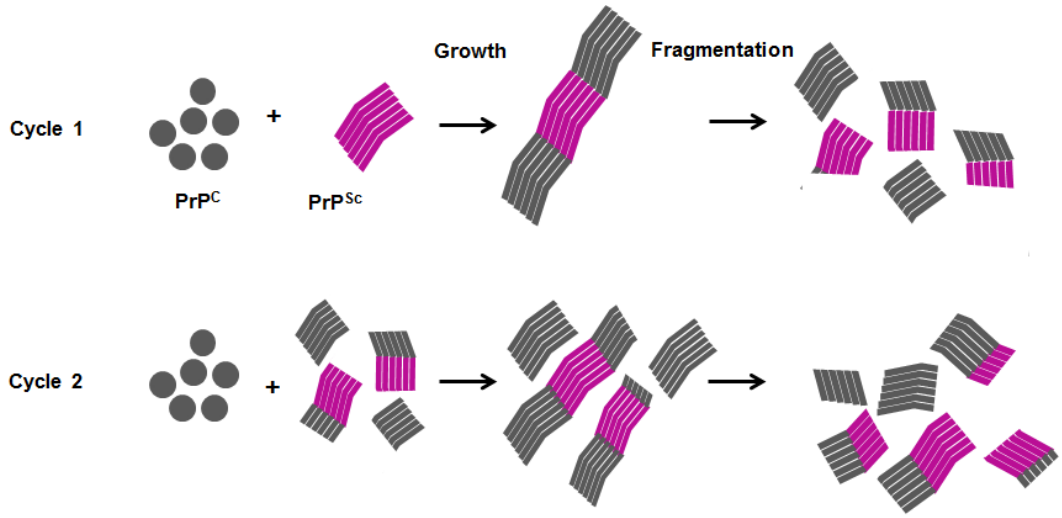

Figure 7: PrP^{Sc} and PrP^{C} are mixed and incubated, allowing the misfolding of PrP^{C}, which permits the incorporation and growth of PrP^{Sc} aggregates. After incubation, samples are submitted to fragmentation in order to fragment PrP^{Sc} polymers, thereby generating new free ends suitable for continued prion replication. This process is cyclically repeated in order to produce an exponential amplification of PrP^{C} conversion.

Table 3 summarises recent developments in the characterisation and detection of prions using assays based on seeded conversion of PrP^{C}.

Table 3: *In vitro* conversion assays for Prions

Assays	Seed (brain derived)	Substrate	Fragmentation mechanism	Detection	Citation
CFC assay	PrP^{Sc}	PrP^{C} (Radiolabeled)	Incubation upto 72 h with occasional mixing	SDS PAGE	Caughey 1999
saPMCA	PrP^{Sc}	PrP^{C} (brain extract)	Ultrasound	Western blotting	Soto 2006
ASA	PrP^{Sc} (Partially purified)	rec.PrP stored in 6M GdmHCl (E. coli)	Continuous shaking with 3 mm glass bead	ThT based fluorescence detection	Colby 2007
QuIC	PrP^{Sc}	rec.PrP (E. coli)	Recurrent Shaking	Western blotting	Atarashi 2008
RT-QuIC	PrP^{Sc}	rec.PrP (E. coli)	Shaking	ThT based fluorescence detection	Atarashi 2011

1.4.1 Cell Free Conversion assays (CFC assay)

The ability of PrP^{Sc} to induce the conversion of PrP^{C} to PrP^{res} was initially demonstrated in cell free reactions in which brain derived PrP^{Sc} was incubated with radioactively labelled PrP^{C}, which, under suitable conditions, bound to the PrP^{Sc} and became similarly partially protease resistant. These cell free reactions were shown to be highly specific in ways that correlated with prion transmission barriers and strains (Caughey et al., 1999). However, the newly generated PrP^{res} was usually substoichiometric relative to the initial PrP^{Sc} seed, and was not associated with new infectivity. (Shaked et al., 1999). As a result, these cell free conversion reactions were not suitable for sensitive detection of PrP^{res} and prions.

1.4.2 Protein Misfolding Cyclic Amplification (PMCA) and Recombinant Protein Misfolding Cyclic Amplification (rPrP-PMCA)

In 2001 Soto and colleagues described a new cell free prion conversion assay called Protein Misfolding Cyclic Amplification (Castilla et al., 2006) which has greatly improved efficiency, continuity, and sensitivity compared to the CFC reactions. In the typical PMCA reaction, crude brain extracts are used as a source of PrP^{C} which is induced to convert by prions in the test tube sample. Under these conditions, PrP^{res} can be amplified to detectable levels.

In 2007, Atarashi et al. tried to replace the substrate from normal brain homogenate to rec. PrP using the standard PMCA set-up.(Atarashi et al., 2007). This method which they called rPrP-PMCA was able to detect as little as 50 ag of PrP^{Sc} and can also differentiate between scrapie – infected and uninfected hamsters using 2 µl of cerebrospinal fluid.

Recently Chen et al. have reported a “Quantitative PMCA” (qPMCA) method to estimate the concentration of minuscule amounts of prions in biological samples. This approach is based on direct correlation between the extent of PrP^{Sc} in a given sample and the number of rounds necessary for its detection. More recently, Wang and colleagues (Wang et al., 2010) described the generation of a recombinant prion with features typical of in-vivo generated

prions using three components: $rPrP^{C}$, POPG (1-palmitoyl-2-oleoylphosphatidylglycerol), and RNA. Following intracerebral inoculation in wild type mice the clinical stage of disease was reached at ~ 150 days. Biochemical characterisation of PrP^{res} generated, as well as the clinical symptoms, histopathology, and second passage behaviour induced by its inoculation strongly supported the conclusion that they had generated TSE infectivity using these three molecular components.

A related study by Kim and colleagues (Kim et al., 2010) reported that prions able to induce disease in wild type hamsters can be generated from purified bacterial $rPrP^{C}$ in absence of any mammalian cofactors using prion seeded rPMCA. This rPMCA product showed variable attack rates upon inoculation into hamsters and therefore contained low levels of infectivity (incubation time from 119 to 401 days) on the first passage. However, upon second passage all animals became ill with an average incubation period of about 80 days. Lesion profiling indicated that rPMCA had altered the strain characteristics of prions (263K strain) that were initially used to seed the serial rPMCA reactions.

However, various research groups including Nishina et al.(Nishina et al., 2006), have reported that such reactions have resulted in a limited yield of the PrP^{Sc} product.

It has also been stated that it is not possible to use standard PMCA method for conversion of rec. PrP to PrP^{Sc}. The reason for this limitation was believed to be the absence of some brain derived factors which are essential for prion propagation. Additionally, lack of glycosylation and glycosylphosphatidylinositol (GPI) anchor in rec. PrP expressed from E.coli also contribute to the difficulty in amplifying reactions with rec. PrP (Eiden et al., 2006; Iniguez et al., 2000; Kirby et al., 2003).

1.4.3 Amyloid Seeding Assay (ASA) for Prions

Colby et al. developed a new amplification assay for prions that utilises thioflavin T to detect amplification using the fluorescent plate reader. (Colby et al., 2007). Thioflavin T is a dye that displays enhanced fluorescence upon

binding to amyloid fibrils. Through this assay, it was demonstrated that multiple prion strains could seed the polymerization of rec. PrP into an amyloid – the feature which could be beneficially used for the detection of prions in biological samples. This method uses partially purified prions as seeds which is accomplished by phosphotungstate (PTA) precipitation and rec. PrP stored in 6M guanidine hydrochloride as a substrate. The final guanidine hydrochloride concentration in the reaction (0.4 M) is such that the substrate is likely in a partially unfolded/destabilised state. Other reaction parameters include incubation at 37ºC, the presence of a 3 mm glass bead in each well to enhance agitation, and continuous shaking of the plate. This assay gives a totally new dimension to prion amplification by being a sensitive and a speedy way for prion detection.

However, there's also a limitation to this assay. Due to variation in the kinetics of ThT positive fibril formation, a number of replicates per sample have to analyse each time. Additionally, this assay often causes formation of spontaneous (non-seeded) rec. PrP fibrils.

1.4.4 Quaking Induced Conversion Reactions (QuIC)

To overcome the shortcomings of rPrP-PMCA, a new method was devised called "QUIC" for quaking induced conversion where sonication is substituted by recurrent cycles of shaking and incubation.(Atarashi et al., 2008). The initial QuIC reactions abbreviated as standard QuIC or S-QuIC were carried out on a thermoshaker with optimized concentrations of detergents. After systematic standardization of reaction parameters like shaking condition, detergent concentrations, incubation time and reaction temperature, the QuIC method was able to distinguish between spontaneous (non-seeded) and the seed specific reactions. The only limitation with these kinds of assays, which till date has not been resolved, is the time associated to detect the amplified product which is only possible through western blotting.

1.4.5 Real Time Quaking Induced Conversion Reactions (RT-QuIC)

Towards addressing the issues which lag behind ASA and S-QuIC, Atarashi et al. (Atarashi et al., 2011) developed a new assay called Real-Time (RT) QuIC which is an amalgamation of both S-QuIC and ASA where the readout has been made easier by using Thioflavin T (ThT). In RT-QuIC, the progress of the QuIC reaction can be monitored continuously in a shaking, temperature controlled fluorescent plate reader. As with ASA, the multiwell plate format makes the RT-QuIC more amenable to high-throughput testing of samples. Using this "real time" version, 200 cerebrospinal fluid samples from sCJD or Alzheimer's disease patients were tested and the sensitivity was greater than 80%. However, the sensitivity for vCJD may be somewhat lower (Peden et al., 2012).

The latest adaptation incorporates an antibody binding step to concentrate the prions in the sample in the assay known as **Enhanced QuIC (eQuIC).** Within this approach, there is a remarkable increase on sensitivity for detecting vCJD (down to 2 attograms per mL of protein) including detection in blood samples spiked with vCJD prions (Orru et al., 2011).

1.4.6 Questions still remain to be answered

Several questions in prion biology are still unanswered. In particular, the molecular mechanism behind PrP^{C} to PrP^{Sc} conversion is unclear and the structure of PrP^{Sc} is still missing. In order to obtain the structural information of mammalian prions it is necessary to obtain substantial amounts of isotopically labelled recombinant prions. However, none of the methods published so far are capable of producing a prion sample in milligram's amount within a day. Therefore, it is necessary to develop a suitable method which is capable of amplifying prions under *in vitro* conditions in a homogenous and reproducible manner. Furthermore, the method should hold the potential for propagating prions in any desirable volume without affecting the rate of amplification or loss in the yield. Establishing such a method might resolve all the above mentioned

problems and may provide new insights into the role of prion proteins in human health and disease.

2 Aim and Objectives

The $PrP^{C} \rightarrow PrP^{Sc}$ *conformational conversion* in relation to the pathological effects of prions is poorly understood. The structure determination of PrP^{Sc} continues to be a major challenge in prion research. The mechanism of propagation of these infectious agents will not be fully understood until their structure is solved. However, the elucidation of prion structure by NMR spectroscopy requires extensive amounts of isotope labelled recombinant (rec.) prions. Since none of the published methods has thus far accomplished the task, a novel method called “Selective shearing amplification (SSA)” was developed in our lab to overcome this key bottleneck.

The first objective of this work is to develop a standardized approach using SSA for the amplification of hamster brain derived prions, *in vitro*, using exclusively recombinant PrP^{C} as a substrate. Key parameters that might influence this process will be investigated. In particular, these include (i) the PrP^{Sc}, i.e. seed, concentration, (ii) the PrP^{C} concentration, i.e. substrate, (iii) the processing conditions, (iv) the buffer composition, and (v) also the amplification rates. All these parameters might significantly impact the degree of amplification achieved, and most importantly the quality of the obtained product. Once the initial optimization has been achieved, Sc237 and 263K hamster prions will be serially propagated *in vitro* in order to dilute the initial brain derived seed below the detection limit.

The second objective of this work is to characterize *in vitro* propagated rec. PrP aggregates by (i) SSA to confirm PrP^{res} conformational *in vitro* selection, (ii) negative staining electron microscopy to detect morphological diefference, (iii) Mass spectrometry to identify major proteinase K (PK) resistant peptides, and (iv) solid state NMR spectroscopy to identify specific conformational differences at atomic resolution.

3 Materials and Methods

3.1 Materials

3.1.1 Instruments

A list of all instruments used during this thesis can be found in Table 4

Table 4: Instruments

SSA Array	Self-made Patent no. EP2489427(A1) - 2012-08 22
Electrophoresis chamber (SDS-PAGE)	XCell4 SurelockTM Midi-Cell (Invitrogen)
Autoclave	HAST 4-5-6 (Zirbus)
shear-generators for mechanical SSA	Silent crusher S - Generator 7 F (Heidolph)
Incubator	FunctionLine (Heraeus)
pH-Meter	MP 230 (Mettler-Toledo)
Photometer	Ultraspec 3,000 (Pharmacia Biotech)
Thermoshaker	Thermomixer comfort (Eppendorf)
Dry bath	FB15103 (Fisher Scientific)
Microcentrifuge	5417 R (Eppendorf)
Mid bench centrifuge	4K15C (Sigma)
Deionized water supplies	Milli-Q Plus (Millipore)

3.1.2 Chemicals

All laboratory chemicals were of p.a. grade and purchased from Sigma-Aldrich (Taufkirchen, Germany), Merck (Darmstadt, Germany), Carl Roth GmbH (Karlsruhe, Germany), Serva (Heidelberg, Germany), Biozym Diagnostik (Hameln, Germany) or AppliChem (Darmstadt, Germany).

3.1.3 Consumables

All consumables were purchased from Becton Dickinson, Eppendorf, Greiner, Macherey-Nagel, Nunc, Thermo Fisher Scientific, TPP or Roth, unless otherwise stated.

3.1.4 Shear Generators

Generator 7 F – Heidolph

Cat. Number: 596-07010-00

3.1.5 Reaction Tubes

Reagenzröhrchen 7F/20ml – Heidolph

Cat. Number: 596-00007-00-0

3.1.6 100 kDa Filter for Protein

Macrosep Advance Centrifugal Device 100K MWCO − Pall Corporation

Cat. Number: MAP100C37

3.1.7 Kits

Pierce® Silver stain kit − Thermo Fisher Scientific

Cat. Number: 24612

3.1.8 Protein Marker

SeeBlue® Plus2 Pre-Stained Standard – Invitrogen

3.1.9 Enzymes

100X N2 supplement – Invitrogen
Proteinase K (PK) – Merck

3.1.10 SDS Gels

NuPAGE® Novex 4-12% Bis-Tris Midi Gel – Invitrogen

Cat. Number: WG1403BOX

3.1.11 rec. Hamster PrP (23-230)

The protein solution should be filtered through a 100 kDa filter (PALL) immediately before use.

3.1.12 Additional Agents

4 x LDS sample buffer − Invitrogen
20 x MES running buffer − Invitrogen

3.1.13 Prion Strains

Prion strains which have been used to seed *in vitro* SSA reactions are listed below (Table 5).

Table 5: Prion Strains

Sc237	Dr. Eckhard Flechsig and Prof. Dr. Michael Klein (Institute of Virology, University of Würzburg)
263K	Bruce W. Chesebro, M.D. (National Institutes of Allergy and Infectious Diseases, Hamilton)

3.1.14 Buffer Solutions

The buffers used this thesis are listed in table 6.

Table 6: Buffer Solutions

2 x Proteinase K (PK) digestion buffer	2% (w/v) N-Lauroylsarcosin in 1x PBS	
PK solution	0.5 µg/ml PK in 2 x PK Digestion buffer	
10 x PBS for SSA reaction	$Na_2HPO_4.\ 2H_2O$	100 mM
	$NaH_2PO_4.\ H_2O$	100 mM
	NaCl	1300 mM
	pH	6.9
4 X Reaction Buffer	10% SDS stock	40 µl/ml
	10% Triton X-100 stock	40 µl/ml
	10 X PBS stock	400 µl/ml
	Milli-Q H_2O	520 µl/ml
Perfusion Buffer (PB)	EDTA	5.00 mM
	KCl	2.68 mM
	$KH_2PO_4.\ H_2O$	1.76 mM
	$Na_2HPO_4.\ 2H_2O$	8.09 mM
	NaCl	137 mM
	pH	7.4
	Filter with 0.2 µm membrane	

3.2 Methods

3.2.1 Recombinant PrP Expression and purification

Expression

Recombinant Syrian hamster full-length prion protein (23–231) was expressed in Escherichia coli and purified as described previously (Zahn et al., 1997). DNA Sequences coding for hamster (residues 23–231) were amplified and ligated into the pETRO_shPrP(23-231) vector. After transforming the plasmids into BL21 (DE3) cells, we expressed the PrP^c using the auto-induction media. Auto-inducing cultures were incubated overnight 37 °C (250 rpm). Next day, cultures were spun down at 7150 g for 7 min. (4°C). Obtained pellets were either directly processed for purification or frozen at -80°C for later use.

Purification

Recombinant PrP was produced with an N-terminal His-tag to allow for specific binding to Ni-NTA (nitrilotriacetic acid) sepharose through the immobilized Ni^{2+} ion. Pooled pellets from three litre expression cultures were resuspended in approximately 10 ml refolding buffer (100 mM sodium phosphate (pH 8.0), 10 mM tris, 6 M guanidine-HCl, 10 mM imadazole). Afterwards the suspension was subjected to sonication using a sonopuls ultrasound system and a TT13 sonotrode (Bandelin) with an output power of 150 W and a setting of 1 sec (on)/1 sec (off) for approximately 45 min. After sonication, the suspension was spun down at 32,500 x g for 30 min. (RT). The supernatant was immediately used for affinity chromatography. In the meanwhile, Ni-NTA was equilibrated with refolding buffer and then supernatant was mixed and coupled with the equilibrated Ni-NTA suspension. The mixture was slowly agitated for one hour at RT. After coupling the column was packed with Ni-NTA resin. Using an AKTA Prime system (GE Healthcare) the denatured protein was refolded on the column using a linear gradient to refolding buffe . Next the protein was eluted with a linear gradient to elution buffer [100 mM sodium phosphate (pH

5.8), 10 mM tris, and 500 mM imidazole]. The purification protocol is given below in table 7.

Table 7: Purification protocol for recombinant shPrP

Step	Buffer	Time (min)	Flow rate (ml/min)
Wash	G	16	2.5
Equilibrate	G	40	2.5
Gradient	G→B	100	0.5
Wash	B	56	2.5
Elute	C	32	2.5
Wash	B	24	2.5

After purification suitable fractions were pooled and dialyzed against 10 mM Tris (pH 8.0). The His-tag of the protein was removed by thrombin digestion for 20-24 hours at RT. The applied thrombin concentration was 2 U per µmol PrP. The digest was stopped by adding 10 µl of benzamidin sepharose per unit thrombin. After adding the sepharose agitation was continued for two hours at RT. Afterwards the sepharose was filtered out and the protein solution was dialyzed three times against water at 4°C. Then, the protein was concentrated and stored at −80°C.

3.2.2 Proteinase K Digestion

All the samples were spun down at 25,000 x g for 20 minutes on the micro centrifuge at 22°C. The supernatant was discarded and the pellet was resuspended in 6 µl of 1 X PBS. Then 6 µl of ice cold 2X PK solution was added to give the end concentration of 0.5 µg/ml PK. After a brief vortexing step, the samples were placed immediately on the thermoshaker (750 rpm, 37°C) for one hour. To stop the digest after one hour, 4 µl of 4 x LDS sample buffer was added to the digestion mixture. The samples were immediately heated at 96°C for 10 minutes. Later all the samples were spun down at 25,000 x g for 10 seconds and loaded onto SDS gel for silver stain analysis.

3.2.3 SDS-Polyacrylamide-gel electrophoresis (SDS-PAGE)

SDS PAGE was performed using a commercially available gels from Invitrogen (NuPAGE® Novex 4-12% Bis-Tris Midi Gels). 12 µl of sample (6 µl of reaction mix + 6 µl of 2x PK) was mixed with 4 µL of 4 x LDS sample buffer (Invitrogen) and heated at 96°C for ten minutes. 15 µL of the sample was then loaded to the individual wells of the SDS gel placed in a vertical electrophoresis tank (XCell4 SurelockTM Midi-Cell, Invitrogen) with 1X SDS running buffer (20 x running buffer, Invitrogen). 7 µl marker was also loaded to one well. Electrophoresis was carried out at 200 V for 35 minutes.

3.2.4 Silver Staining

Silver staining was carried out with a Pierce Silver Stain Kit from Thermo Fisher Scientific. The SDS gel was removed from the electrophoresis cassette and washed twice for 5 minutes in filtered Milipore water to remove the salts of the running buffer. Then the gel was incubated for 15 minutes in fixing solution made of 30% ethanol, 10% acetic acid and 70 % water. The fixing process was repeated once again for 15 minutes. Then the gel was washed twice for 5 minutes each with 10% ethanol and with Milipore water. In the meanwhile the Sensitizer Working Solution was prepared (50 µL Sensitizer mixed with 25 mL water).The gel was incubated with the Sensitizer Working Solution for 1 minute, followed by 2 washes with water for 1 minute each. The Stain Working Solution (0.5mL Enhancer mixed with 25 mL Stain) was prepared and the gel was incubated for 30 minutes. The Developer Working Solution (0.5 mL Enhancer with 25 mL Developer) was prepared. The gel was washed with ultrapure water twice for 20 seconds at each wash. The gel was then incubated with the Developer Working Solution 2 to 3 minutes until the bands appeared. Immediately after the bands appeared 5% acetic acid was added and incubated for 10 minutes.

3.2.5 Prion Decontamination

Table 8: Prion Decontamination procedures

Type of Object	Decontamination
Surface (e.g. lab furnitures), Plastic ware (e.g. dishes, beakers)	1 M NaOH (≥ 1 h), cleaning with 1 % (v/v) LpHse
Solid waste (e.g. gloves, tissue paper) and animal cages	Autoclaving at 134°C
Body parts of prion inoculated animals	Incubated in 1 M NaOH/0.2% (w/v) SDS (≥ 1 h) and autoclaved at 134°C
Metal-objects and glassware	Incubated in 1 M NaOH/0.2% (w/v) SDS (≥ 1 h) and autoclaved at 134°C
Shear-generators	(1) Incubation in 1 M NaOH/0.2% (w/v) SDS for 1 h (2) Auroclaving at 121°C in 1 M NaOH/0.2% (w/v) SDS (3) Auroclaving at 121°C in 5% milk powder

3.2.6 SSA Assay

Selective Shearing Amplification (SSA) Array

Till date, direct structural measurements of rec. PrP aggregates are prevented by the small quantities. Moreover, to further address the need for homogenous and seed specific rec. PrP^{res} preparations, an instrument was designed and built in our group by Dr. Thorsten Lührs (HZI), which we called as “SSA Array”. The principle is based on the use of mechanical shear stress as a shearing mechanism. When the viscous fluid is confined in the gap between two rotating cylinders, homogenous shear fields can be generated that are proportional to the rotation frequency of the cylinder. Using custom-designed, induction-driven

dispersion tools (Heidolph, Silent Crusher S, tool 7F − Stator diameter (outer): 7 mm, Rotor diameter: 3.9 mm, Slot width: 0.6 mm, Shaft length: 55 mm, Volume: 6.0 - 10.0 ml) as shear- generators, homogeneous and reproducible shear forces could be applied to arbitrary reaction volumes. With mechanical SSA, it was possible to test different parameters (e.g. different shearing conditions, cycle times, different seed and substrate concentrations, buffer compositions etc.) using several geometrical identical shear-generators running in parallel. To accomplish this, the SSA-array was built (Figure 8). (A) It consists of 28 slots for shear-generators which can run simultaneously in a temperature-controlled environment maintained by the attached water bath. Using computer controlled switching relays; every single device can be programmed separately for experiments using rotation frequencies ranging from 40 to 1,201. (B) Detailed view of seven dispersion tools in the SSA array. The reaction tube containing the desired volume was inserted onto the dispersion tool and then the whole assembly was sealed with a parafilm in a laminar-flow hood. Then it is inserted into the SSA array and processed at specified parameters. The rotation frequency of each unit is pre-set using the multimeter shown in (A). Using this array, reactions of different volumes can be processed which turned out to be a great advantage for making substantial amounts of labeled recombinant PrP^{res}. (C) Shows the shear generator which can homogenize a reaction volume of 10 ml. The system comprises of a rotor of radius, r, rotating with a frequency, ν, inside a stator. The gap between the rotor and stator of height, h, is filled with a solvent of viscosity η. With these parameters the shear-rate, G, and the shear-force,τ can be calculated. Since shear force is proportional to the rotational frequency, it can be controlled with great precision and reproducibility. Bold arrows indicate local solvent velocity, and the white arrow indicates the direction of rotation. (D) Evolution of cycle time during the course of the reaction.

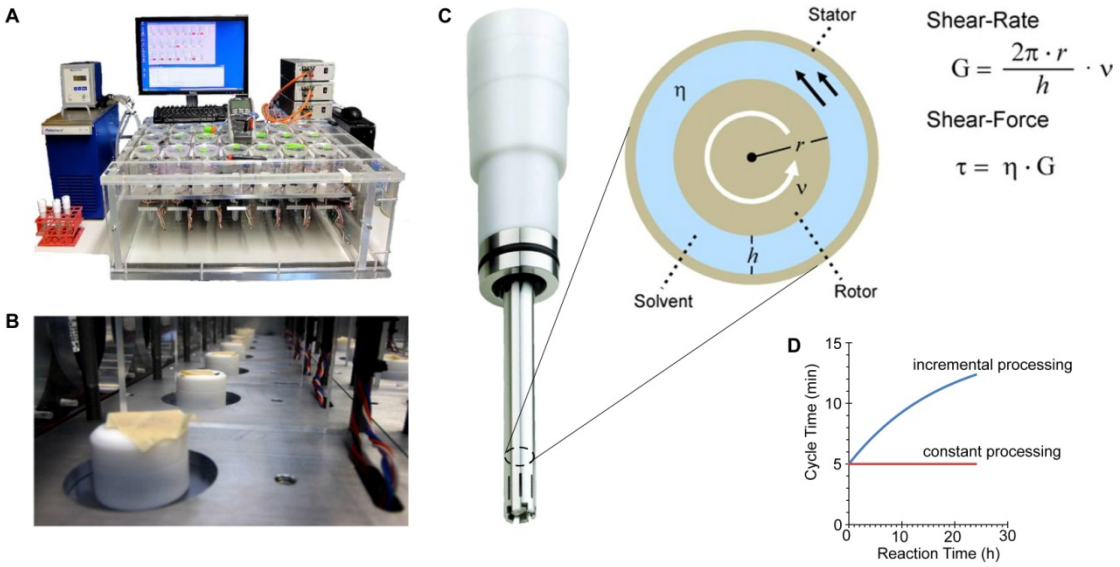

Figure 8: The Selective Shearing Amplification (SSA) array. (A) The SSA array consists of 28 slots for dispersion tools in a temperature controlled environment. Using computer controlled switching relays, every single device can be programmed separately for experiments using a rotational frequency ranging from 30 to 1.300 Hz. **(B)** Detailed view of seven dispersion tools in the aray. Each tool is preasembled in a laminar-flow hood, and sealed aerosol tight. Then it is inserted into the SSA array and processed at specified parameters. **(C)** A dispersion to running with a constant rotational frequency, provides a velocity gradient in the space between rotor and stator. The velocity is zero at the outer wall while the maximum velocity corresponds to the rotor's circumference speed. Apart from the rotor shape, the viscosity and the space between rotor and stator are directly correlated to the applied shear force. Therefore a homogenous and reproducible shear force is achieved. **(D)** Evolution of cycle time during the course of the reaction.

Preparation of Reaction Mixes

Round 0 Reaction

1) Preparation of 4X Reaction Buffer

Composition of 50 ml of 4X Reaction Buffer

10% SDS stock (stored at RT)	2 ml
10% Triton X-100 stock (freshly prepared)	2 ml
10 X PBS stock (stored at -80°C)	20 ml
Milli-Q water	26 ml
Filter through 0.2 µm membrane	

2) Filtration of the Substrate

Recombinant Hamster PrP (23-230) was spun down at 283,807 g for 30 minutes at 4°C. The supernatant was carefully transferred and filtered with a 100 kDa filter (PALL) by spinning at 5000 X g for 45 minutes. Later O.D was measured at 280 nm. In order to achieve the final concentration of 0.3 mg/ml, the protein solution was diluted with ice cold and filter sterilized (0.2 µm membrane) Milli-Q water and stored on ice.

3) Dilution of the Seed

10% (w/v) scrapie brain homogenate (ScBH) was thawed at 22°C under gentle agitation (Eppendorf Thermomixer comfort, 750 rpm). Then it was briefly spinned down at 25,000 x g on the micro-centrifuge and stored on ice. Simultaneously 100X N2 supplement was also thawed and stored on ice. For dilution of the seed, 1X N2 supplement was prepared in 1X reaction buffer. 10% ScBH was diluted 1:50 into 1X N2 and vortexed for one minute and later stored on ice.

4) Preparation of the reaction mix

For 10 ml reaction volume, following components are added in the specified order:

Milli-Q water − Ice cold and filter sterilized (0.2 µm membrane)	3.967 ml
4X reaction buffer − Ice cold and filter sterilized	2.5 ml
sterilized (0.2 µm membrane)	
ScBH seed diluted in 1X N2	0.2 ml
Mix well by pipetting	
0.3 mg/ml of ice cold rec. Hamster PrP (23-230)	3.333 ml
Total volume	10 ml

5) Starting the reaction

Once the reaction mix was prepared, shear generators (Heidolph, Silent Crusher S, tool 7F − Rotor radius: 1.95 mm, Slot width: 0.6 mm, Volume: 6.0 - 10.0 ml, see Fig. 1.6C) were inserted into the reaction mix. The whole assembly was then allowed to warm to 37°C in the water bath for 20 min. Then one by one they were placed on the array and the processing was started: The processing frequency (rotation frequency of the rotor) was pre-set to specific values between 95 Hz and 1200 Hz If not indicated otherwise, the reactions were processed at 37°C for 5 seconds using a cycle time of 5 minutes. In order to trace the buildup of rec. PrP^{Sc} over time, samples of 250 µl each were collected at predefined time-points during the run, and stored at RT for later analysis. All collected kinetic samples were then analyzed at once by PK-digestion and silver staining.

Round 1 Reactions

For serial propagation of rec. prion seeds, 1:50 dilution of the previous round product (round 0 reaction) as a seed was used.

Round 1 reaction mix was prepared in the following order where the components are added in the specified order:

Milli-Q water − Ice cold and filter sterilized (0.2 µm membrane)	3.967 ml
4X reaction buffer − Ice cold and filter sterilized	2.5 ml
sterilized (0.2 µm membrane)	
Sample vol. from previous round	0.2 ml
Mix well by pipetting	
0.3 mg/ml of ice cold rec. Hamster PrP (23-230)	3.333 ml
Total volume	10 ml

Characterization of SSA Products

3.2.7 Mass Spectrometry

To distinguish between Sc237 and 263K Hamster prion strains, samples were analyzed by electrospray ionization mass spectrometry (ESI-MS). The measurements were carried out by Dr. Manfred Nimtz and Andrea Abrahamik (HZI, Braunschweig). A single 10 ml reaction was spun down at 283,807 g for 30 minutes at RT. The pellet was resuspended in 100 µl of 1X reaction buffer. Later it was digested with 0.5 µg/ml proteinase K for one hour at 37°C. The digest was stopped by placing the sample immediately on the dry bath which was already set to 96°C for 10 minutes. Afterwards, sample with inactivated PK was spun down at 25,000 g for 10 minutes at RT. The supernatant was discarded and the pellet was recovered. In order to wash the pellet and to get rid of the detergents, it was resuspended in 200 µl of filter sterilized (0.2 µm membrane) Miili-Q water and again spun down at 25,000 g for 10 minutes. The washing step was repeated 3 times. Finally the pellet was further purified by methanol/chloroform extraction. The resulting pellet was inactivated in 50 µl of hexafluoroisopropanol (HFIP) and analyzed for electrospray ionization mass spectrometry

3.2.8 Electron Microscopy

For analysing rec. PrP^{res} samples through transmission electron microscopy (TEM), aggregates from a 10 ml reaction were collected and digested with 0.5 µg/ml PK for one hour at 37°C. All the brain derived samples (10% Sc237 and 263K infectious brain homogenate along with 10% Syrian hamster normal brain homogenate) were digested with two different PK concentrations – 50 µg/ml and 100 µg/ml. These and PK untreated samples were then settled onto carbon-coated butvar grids for 10 minutes. Excess sample was removed and the grid was air-dried. The fibril-bearing grid was stained with 2% (w/v) uranyl acetate for few seconds. Images from randomly selected areas were captured on a film at 5,000 –25,000× magnification.

3.2.9 Solid state Nuclear Magnetic Resonance (ssNMR) Spectroscopy

For solid-state experiments, pellets of Sc237 at three different frequencies – 189 Hz, 378 Hz and 953 Hz and 263K at 378 Hz and 953 Hz were prepared using $^{13}C/^{15}N$-labeled full length Syrian hamster PrP (23-230). A total of 60 reactions of 10 ml volume corresponding to ~ 30 mg were pooled to make one ssNMR sample at the required frequency. Reactions at 953 Hz were processed for 2 hours at 37°C on the SSA array. Similarly, reactions corresponding to 378 Hz were processed for 6 hours and those running at 189 Hz were completed at 9 hours. Afterwards, when the reaction was over, recombinant PrP aggregates were collected at 283,807 g and analyzed by ssNMR spectroscopy.

4 Results

Prion diseases are associated with the conversion of the α-helix rich prion protein (PrP^{C}) into a β-sheet-rich insoluble conformer (PrP^{Sc}) that is thought to be infectious. The mechanism for the $PrP^{C} \rightarrow PrP^{Sc}$ conversion is still unknown, partly because of the limited knowledge of the structure of PrP^{Sc}. Many efforts have been made over the years to recapitulate PrP^{Sc} formation and prion propagation *in vitro*.

The development of "protein misfolding cyclic amplification" (PMCA) allowed propagation of prion infectivity *in vitro* under cell free conditions. PMCA reactions involved successive rounds of incubation and sonication of either crude brain homogenates (Castilla et al., 2006) or purified brain derived PrP^{C} and, some groups have even tried using bacterially expressed recombinant (rec.) PrP (Atarashi et al., 2007). However, in most of the labs including our own standard PMCA is rather hard to control. The delivery of vibrational energy to samples can vary substantially and unpredictably with tube position, probe age and water bath volume. Later, in the group of Byron Caughey, another method was established called a "Quaking Induced Conversion (QuIC)". In this method, sonication was substituted by recurrent cycles of shaking and incubation (Atarashi et al., 2008). Using a thermoshaker, reactions of 100 µl were processed and converted to proteinase K (PK) resistant forms. This method was much more convenient and reproducible than PMCA. Thus, we adopted "QuIC" as a method of choice in order to generate prions using rec. PrP as a substrate. After thorough screening of all the reaction parameters (such as shaking conditions, detergent concentrations, incubation time and reaction temperature) we could finally amplify prions under *in vitro* conditions. However, we found that the yield of the standard reaction was < 5% and thus the quantity and the quality were insufficient for carrying out structural studies. The QuIC reactions on the thermoshaker worked only in small volumes (≤100 µl). We tried to scale-up the reaction volume to 500 -1000 µl, but were unable to observe any detectable amplification of prions. Thus, in summary, the amplification of prion

protein using agitation by ultrasound or by shaking is volume dependent and the yields of protease resistant prion protein are hardly reproducible. Moreover, the drawback of all these methods is that the quantities of PrP^{Sc} generated are very small, precluding most structural studies.

In this context, an initiative was taken in our group by developing a novel method called “Selective shearing amplification (SSA)”. Using a custom-designed device (See Methods, 3.2.6) we can apply homogeneous and reproducible shear forces to arbitrary reaction volumes. With the help of SSA, we tried to mimic the $PrP^{C} \rightarrow PrP^{Sc}$ conversion *in vitro*. PrP^{Sc} seed from crude brain extracts of scrapie-infected animals was used to induce conversion of rec. PrP^{C} into a PK resistant isoform, PrP^{res}. Newly formed PrP^{res} can then be routinely identified by PK digestion followed by silver stained SDS gel electrophoresis. The fragments generated by PK-digestion were ~ 10-12 kDa along with the 17 kDa product (6-7 kDa smaller than the rec. PrP^{C}) which is characteristic of the PK resistant core of PrP^{Sc}, PrP^{27-30} (Oesch et al., 1985; Hope et al., 1986).

In the current study, an attempt was made to develop a standardized method for rec. prion amplification under *in vitro* conditions using SSA (Figure 9). All the key parameters that could influence the rec. PrP^{res} amplification were tested systematically. The optimization of the main conditions was essential in order to establish a reliable method with optimal settings that support specific PrP^{Sc}-seeded *in vitro* conversion of rec. PrP^{C}. The optimized conditions were then adapted to produce the homogenous and reproducible rec. PrP^{res} sample from two different hamster prion strains, Sc237 and 263K. These rec. PrP^{res} preparations were further characterized by (i) SSA, (ii) Negative staining electron microscopy, (iii) Mass spectrometry and (iv) NMR spectroscopy. Figure 9 demonstrates the experimental scheme designed for this project.

Figure 9: Experimental Layout

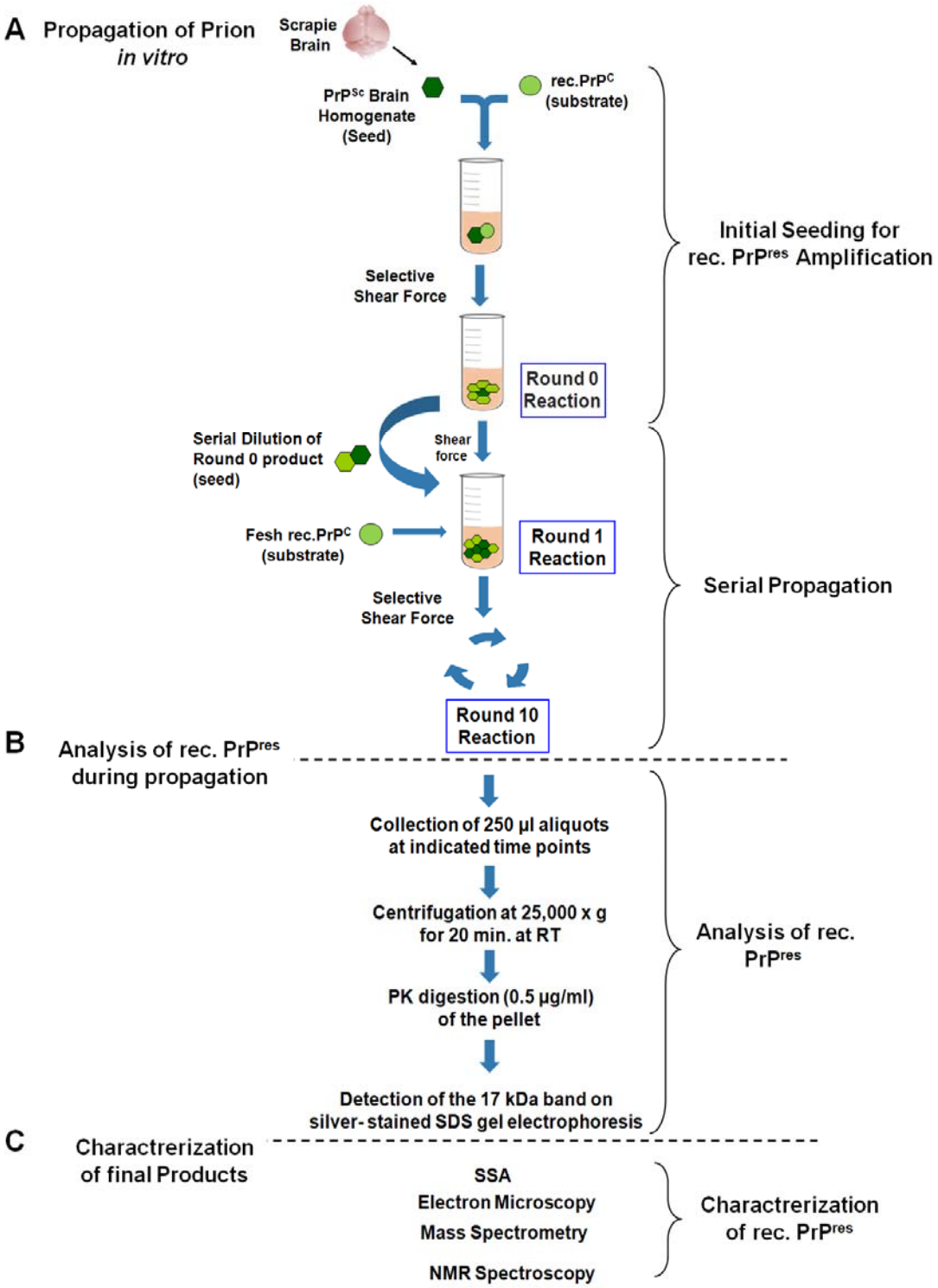

4.1 Conditions for Strain Selective rec. PrP^{res} Amplification

Development of SSA for conversion of rec. PrP^{C} to PrP^{res} requires detailed study and optimization of all the essential parameters that could influence the overall amplification rate. These include (i) the rec. PrP^{C} concentration (substrate), (ii) the PrP^{Sc} concentration (seed), (iii) Protease treatment of the infectious prion seed (for purification of PrP^{27-30}, the protease-resistant core of PrP^{Sc}), (iv) the concentration of detergents in the reaction buffer, (v) the processing conditions and (vi) the minimum 'seed' requirement for amplification upon serial dilution. Initially it was necessary to determine to what extent these individual parameters influenced the degree of amplification achieved. This section focused on the development and optimization of SSA, through systematically testing all the above mentioned conditions which perceived to affect PrP^{Sc} seeded *in vitro* conversion of rec. PrP^{C}.

We started our investigation by following the conditions mentioned in the "QuIC" protocol published by the group of Byron Caughey (Atarashi et al., 2008). However, instead of thermoshaker as a means of agitation, we applied homogenous shear forces by using 10 ml shear generators, for rec. prion protein conversion and amplification. Making "QuIC" method as the basis of our work, we started optimizing conditions by SSA.

As a starting experiment, we tried to generate PK resistant forms using hamster Sc237 brain homogenate as a seed and rec. syrian hamster prion protein, shPrP (23-231), as a substrate. We scanned the entire accessible rotation frequency range (75 Hz – 1200 Hz) using a logarithmic scale with increments of 26%. The reactions were carried out in a volume of 10 ml using a shear generator. A total of 14 shear generators each running at a specified frequency or shear force (7F-Heidolph) were used. The seed and the substrate concentration along with the reaction buffer constituents were initially the same as used in the QuIC protocol (Atarashi et al., 2008). Each 10 ml reaction of 100 µg/ml bacterially expressed hamster rec. PrP^{C} (residues 23-231) was seeded with 1/2500 dilution of a 10% Sc237 brain extract. The reaction buffer contained a combination of 0.1% of an anionic detergent such

as SDS and 0.1% of a non-ionic detergent such as Trion X-100. All the reactions were processed in parallel for 5 seconds every 5 minutes using the SSA-array (See Methods, Fig. 8) for 22 hours at 37°C. Afterwards, the PrP aggregates were collected by centrifugation, digested by PK and analysed by silver-stained SDS-gel electrophoresis. Silver staining offers the advantage to observe all peptides that are generated, whereas western blotting detects only the specific epitopes of the monoclonal antibody. We observed a strong band at 17 kDa (characteristic of the PK resistant core of PrP^{Sc}, PrP^{27-30}) in all the processed reactions other than 75 Hz and 1200 Hz (Fig.10). We assumed that at 75 Hz because of less efficient shearing, we were not able to generate any detectable PK resistant form. However, at 1200 Hz the shear force might be too strong for the prion protein conversion and amplification. We also observed a strong 12 kDa band in all of the processed reactions which was also reported in the "QuIC" assay (Atarashi et al., 2008). Moreover, in the non-processed control (lane 1), we did not observed any amplification at all. This provided the evidence that shear force can successfully substitute sonication and shaking as a means of agitation. Using the shear generators we can scale-up the reaction volume upto 200 mL which cannot be fulfilled by any of the published method so far. Notably, at frequencies of 150 Hz, 378 Hz, and 756 Hz, the 17 kDa band was more intense than other frequencies. These observations provide some initial evidence for the co-existence of multiple PrP^{Sc} conformations within a single prion strain. Thus, we concluded that Sc237 might possibly contain multiple PrP^{Sc} conformations, which can individually be selected by SSA based on their characteristic molecular resistance against seed fragmentation. Overall, with this experiment we demonstrated the applicability of SSA for strain selective conformational conversion and amplification of recombinant PrP.

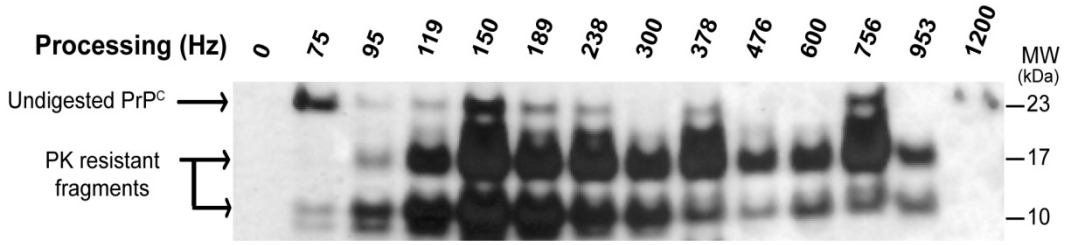

Figure 10: Amplification of Hamster Sc237 prion as a function of rotation frequency after 22 hours. Each 10 ml reaction corresponding to the designated processing frequency is seeded with 1/2500 dilution of a 10% Sc237 brain homogenate using 100 µg/ml rec. shPrP (23-230). The reactions were performed in 0.1% SDS and 0.1% Triton X-100, in PBS at 37°C for 22 hours. All the reactions were processed for 5 seconds every 5 minutes in SSA array. After 22 hours, aggregates were collected at 5000g for 1 hour at RT. The resulting pellets were resuspended in 125 µl of PBS and digested with 0.5 µg/ml Proteinase K for 1 hout at 37°C and analysed by Silver Staining using Thermo Scientific "Pierce Silver Stain Kit". The positions of molecular weight markers are designated in kDa on the right.

4.1.1 Influence of rec. PrP^C (Substrate) Concentration on the Conversion Behavior

With the initial success in achieving conversion and amplification of rec. prion protein using SSA, we then focussed on optimizing and validating individual parameter that could influence the degree of amplification. We used Sc237 hamster prion strain as a seed and 756 Hz processing frequency for carrying out the optimization study. The first parameter that we checked was the rec. PrP^C (substrate) concentration.

We tested three different concentrations (12.5, 25 and 50 µg/ml) of rec. PrP^C along with the standard concentration of 100 µg/ml which was used in the initial experiment in Fig. 10. Other parameters which include (i) the concentration of PrP^{Sc} as a seed (1/2500 dilution of a 10% Sc237), (ii) the processing conditions (5 sec. in every 5 min.), and (iii) the reaction buffer constituents (0.1% of both SDS and Triton X-100) were kept constant as in Fig 10. All the reactions were processed at 756 Hz in the SSA array using a 10 ml volume shear generators where each generator was running with a specified PrP^C concentration. In order to trace the kinetic build-up of the rec. PrP^{res} formed, we collected 250 µl of sample from individual reaction mixes at the indicated time points and stored at RT. After 22 hours when the reaction

was over, all the aliquots were spun down at 25,000 x g for 20 minutes. The resulting pellets were resuspended in 6 µl of PBS containing 0.1% of both SDS and Triton X-100. The samples were digested by 0.5 µg/ml PK for 1 hr. at 37ºC and later analyzed by silver stained gel electrophoresis. Fig. 11 shows the effect of modifying substrate concentration on the rate of rec. PrP^{res} amplification. We obtained the most intense rec. PrP^{res} bands (17 kDa) at the substrate concentration of 50 – 100 µg/ml. We traced the amplification rate of all the reactions and observed that at half the substrate concentration i.e. 50 µg/ml than the "QuIC" assay (100 µg/ml), the same intensity of the 17 kDa (reminiscent to PK resistant core of PrP^{Sc}) band was achieved in just 6 hours. At 22 hr. the reaction was already over-processed as can be seen by the decline in the intensity of the 17 kDa product. Consistent with the previous findings with "QuIC" reactions, we also observed the smaller 10 kDa bands which were also most intense at 50 and 100 µg/ml of substrate concentration. At lower substrate concentrations (12.5 and 25 µg/ml), there was virtually no amplification at all as indicated by the absence of 17 kDa product. We only observed the undigested 23 kDa rec. PrP^{C} band which was subsequently lost over the time. Thus, for the further study we selected 50 µg/ml of substrate concentration as the optimal condition.

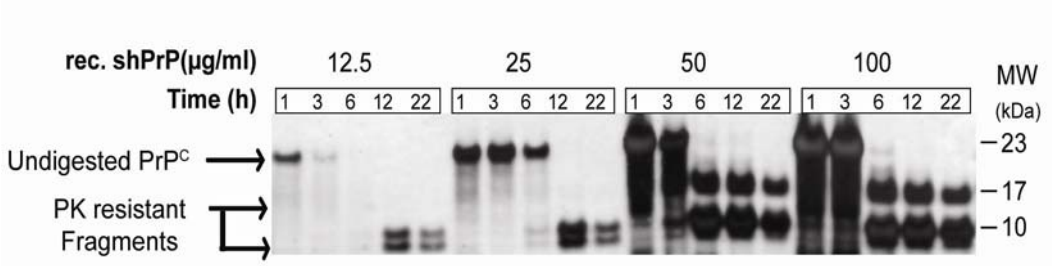

Figure 11: Influence of the substrate concentration. PrP^{res} amplification at varying concentrations of the substrates was determined. 50 µg/ml of shPrP (23-230) as a substrate. Buffer conditions and processing parameters were same as in figure 4.1. At indicated time points, 250 µl samples were collected and spun down at 25,000g for 20 minutes at RT. The resulting pellets were resuspended in 6 µl of PBS and digested with 0.5 µg/ml PK at 37°C for 1 hour. Later all the samples were analysed by silver staining.The positions of molecular weight markers are designated in kDa on the right.

4.1.2 PrP^{Sc} (Seed) Concentration and the Effect of Protease Digestion of Seeds on the Conversion Behavior

After optimizing the substrate concentration, the next parameter tested was the minimum concentration of PrP^{Sc} (seed) required for amplifying rec. PrP^{res}. With the same experiment, we further tried to investigate the impact of protease treatment of seeds on the amplification rate. This was an attempt made towards purifying the seed for structural studies.

For conducting the experiment, 10% Sc237 brain homogenate as a seed was tested at five different dilutions (1/10, 1/25, 1/50, 1/100 and 1/200) using a substrate concentration of 50 µg/ml. After dilution, the seed was digested with 5 µg/ml proteinase K (PK) for 1 hr. The PK was inactivated by heating of the seed at 95ºC for 10 minutes. Later, using the seeds that were either treated (Fig. 12 B) or not treated with PK (Fig. 12 A), the optimal concentration of PrP^{Sc} was determined. The processing conditions (5 seconds every 5 minutes) and the reaction buffer constituents (0.1% of SDS and Triton X-100) were kept constant. All the reactions were processed at 756 Hz frequency in the SSA array using the 10 ml shear generators. In order to trace the amplification rate of the reactions, 250 µl of samples were collected at indicated time points and stored at RT for later analysis by silver stained SDS gel electrophoresis.

Fig. 12 demonstrates the optimal PrP^{Sc} concentration required for rec. PrP^{C} conversion and amplification along with the effect of protease treatment of PrP^{Sc}. On comparing Fig. 12 A (undigested seed) with Fig. 12 B (seed with PK digestion), overall we observed higher seeding potency of the samples that were not treated with PK (Fig. 12 A), if focused on the 17 kDa band formation. From 1/50 dilution onwards, the effect of proteases can be seen prominently as there was a drastic decline in the rate of amplification if the seed was pre-treated with PK (Fig. 12 B). At 1/50 dilution, undigested seeds could easily amplify rec. PrP^{res} in 6 hours as indicated by the presence of a strong 17 kDa band (Fig. 12 A). Moreover, the reaction product once formed is quiet stable until 22 hour. To the contrary, at the same dilution, PK digested seeds showed a very faint band only after 9 hours which vanishes completely over 22 hours.

Overall, if we compare the 17 kDa band formation under both the conditions, it becomes clear that (i) undigested PrP^{Sc} is more efficient seed than PK digested PrP^{Sc} and (ii) 1/50 is the optimal seed concentration required for efficient conversion of rec. PrP^{C}. Thus, the quantity and the quality of the seed substantially influence the conversion behavior.

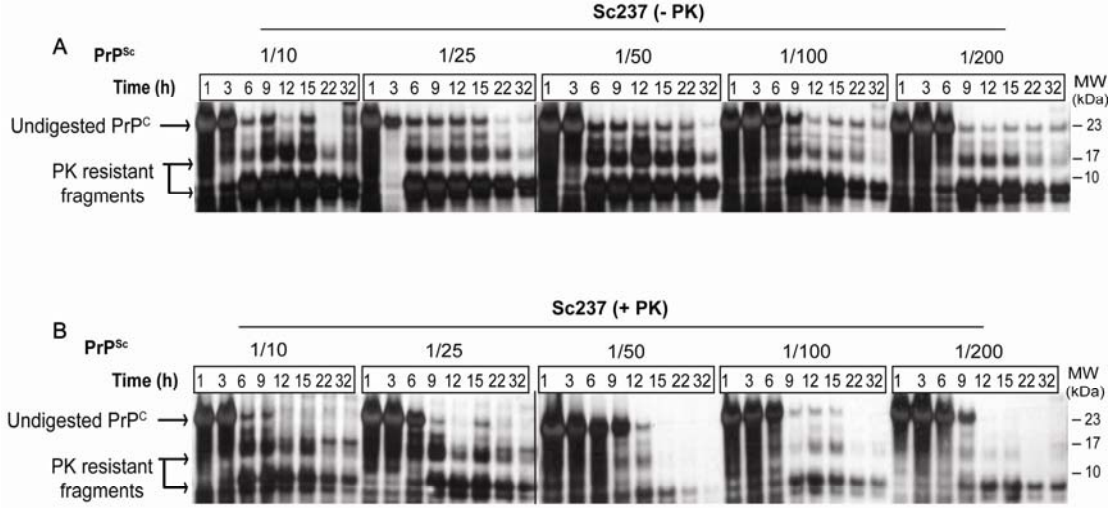

Figure 12: Influence of the seed concentrations and Protease treatment of seeds. 10% Sc237 brain homogenate was either untreated **(A)** or **(B)** treated with 5 µg/ml of PK for 1 hour at 37°C. The activity of PK was terminated by heating the brain homogenate at 95°C for 10 minutes. The impact of protease treatment along with optimal seed concentration for amplification was monitored. The buffer conditions and processing parametes were same as in figure 4.1. All the tools were running at a rotational frequency of 756 Hz at 37°C in the SSA array. Sample collection for kinetics, PK digestion and silver stain analysis was done as described in Methods Section. The black solid line between gels indicated that the particular gel panel is a composite of two gels. The positions of molecular weight markers are designated in kDa on the right.

4.1.3 Concentration of Detergents in the Reaction Buffer

After optimizing the concentration of seed (Fig. 12) and the substrate (Fig 11), the next condition tested was the concentration of both anionic detergent such as SDS and non-ionic detergent such as Trion X-100 in the reaction buffer. Since SDS has been found to induce structural conversion of α-helices to β-sheets and aggregation of hamster rec. PrP (residues 23–231) (Xiong et al., 2001), it was necessary to determine the optimum concentration of detergents in the reaction buffer.

Fig. 13 summarises the effect of varying concentrations of both SDS and Triton X-100 on rec. PrP^{res} amplification. The standard concentration of both the detergents used in "QuIC" assay was 0.1%. We tested different concentrations of SDS and Triton X-100 (0.09, 0.1 – standard, 0.11, 0.12, 0.13 and 0.14%) using the optimal concentration of seed (1/50 of 10% Sc237 brain homogenate) and the rec. PrP^{C} as a substrate (50 µg/ml). The processing conditions were kept constant like previously (5 sec. in every 5 min). All the reactions were running at the rotational frequency of 756 Hz Amplification rates of the reactions were traced by collecting 250 µl of samples at indicated time points. All the samples were stored at RT and later digested with 0.5 µg/ml PK and analysed by silver staining. Fig. 13 A showed the effect of different concentrations of SDS using the standard concentration (0.1%) of Triton X-100. We obtained the most intense 17 kDa band (corresponding to the PK resistant core of PrP^{Sc}, PrP^{27-30}) at the concentration of 0.1%. Notably, the presence of SDS had such a major effect on the PrP^{res} amplification, that if we increase the concentration just by 0.01%, the amplification rate dropped drastically. Fig. 13 B showed the effect of different concentrations of Triton X-100 using the standard concentration (0.1%) of SDS. We again observed the maximum amplification at 0.1% Triton X-100 concentration as indicated by the 17 kDa band. However, on decreasing the concentration by just 0.01%, the amplification was hindered completely. Overall, these findings were consistent with the "QuIC" assay where the optimal concentration of both detergents was 0.1% . In both the cases, we also observed the 23 kDa undigested rec. PrP^{C} band along with the smaller 10 kDa C-terminal fragment of the prion protein. Another important observation was the fact that at 0.1% SDS and 0.1% Triton X-100, reaction was completed after 6 hours using SSA. This is consistent with all the previous observations made during the optimization of seed and substrate concentration (Fig.11 and Fig 12). Thus, there was a high degree of reproducibility in PrP^{res} amplification with SSA.

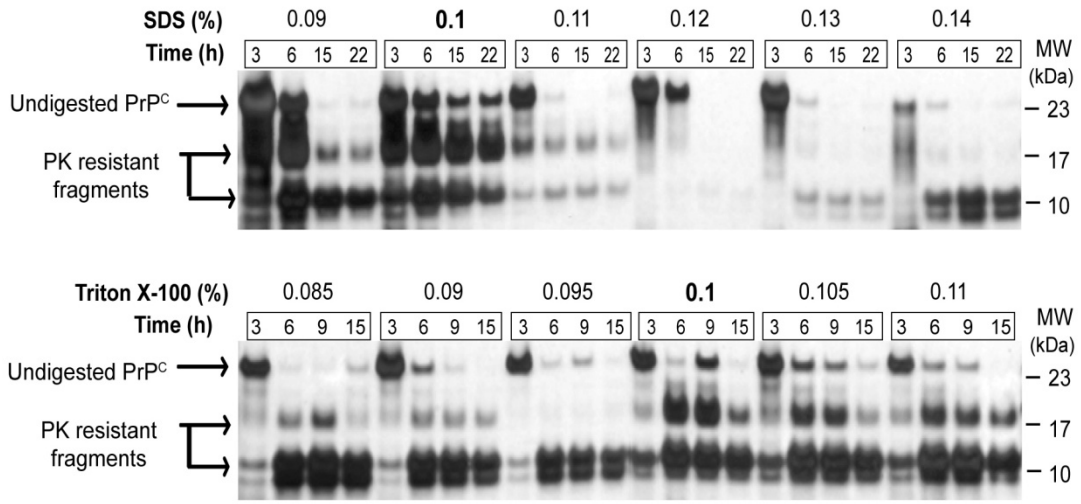

Figure 13: Influence of Detergents on Recombinant Sc237 Hamster Prion Amplification at a rotational frequency of 756 Hz. The standard concentration for SDS and triton X-100 found in the literature is 0.1%. Using the standard concentration of one detergent, the optimal concentration for the other was determined. The reaction buffer with indicated concentrations of the detergents was prepared in PBS. All the reactions were running at 756Hz. frequency with a processing of 5 seconds every 5 minutes. Sample collection for kinetics and silver stain analysis was done as decribed in Methods Section. The positions of molecular weight markers are designated in kDa on the right.

4.1.4 The Effect of Processing Conditions on Strain Selective Amplification of Hamster Prions

We further investigated the influence of processing conditions on detecting strain specific differences between Sc237 and 263K hamster prions using rec. PrP^C as a substrate. We used all the optimized conditions, i.e. 50 µg/ml substrate concentration, 1/50 dilution of 10% Sc237 or 263K hamster prion as a seed and the reaction buffer containing 0.1% of SDS and Triton X-100, for the current investigation. The constant processing of 5 sec. in every 5 min was substituted with incremental processing where 5 seconds processing time remains constant but the cycle time increases exponentially (See Methods Fig 8D).

Fig. 14 summarises the differences between Sc237 and 263K prions under the influence of incremental processing. For both Sc237 and 263K prion strains, we observed a characteristic pattern of bands at 23, 17 and 10 kDa. As explained previously, most notable was the formation of 17 kDa band on

the gel. The amplification rate of the reactions was monitored up to 12 hours. 250 µl of samples were collected at indicated time points and later digested by 0.5 µg/ml PK and analyzed by silver staining. After 12 hours, multiple amplification optima were observed for Sc237. We assumed at least three optima to be present at processing frequencies of 1200 Hz, 378 Hz and possibly around 189 Hz (Fig. 14 A). At 1200 Hz, we noticed the fastest amplification rate as the reaction was completed in 4 hours. However, the other optima were not as clear since the amplification was observed over the wide range of processing frequencies. Notably, when the same experiment was performed using the 263K strain (Fig. 14 B), only one optimum near the maximal processing frequency (1200 Hz) was observed. Unlike Sc237, the maximum amplification was obtained only at one rotational frequency of 1200 Hz where the reaction was completed in 4 hours. At lower frequencies, there was virtually no amplification at all.

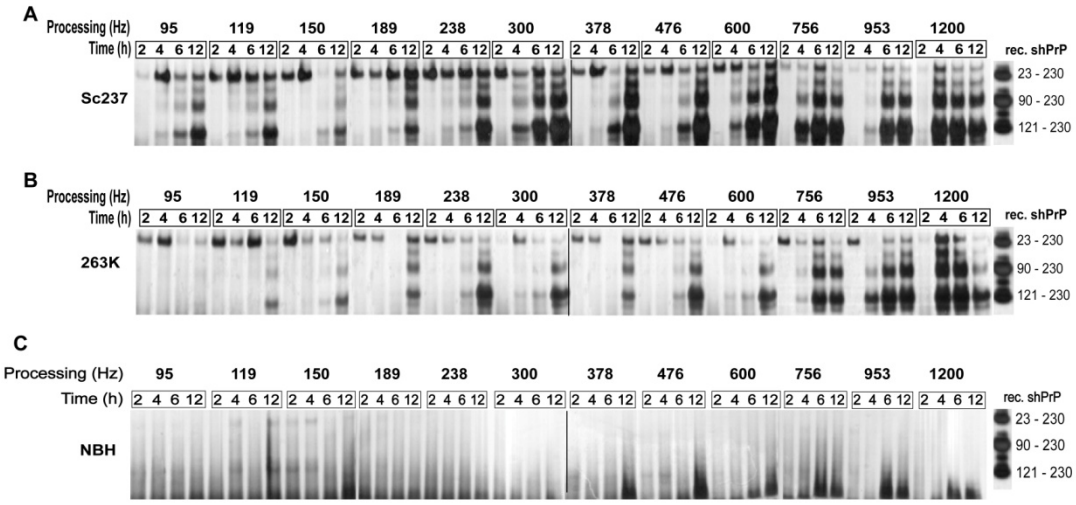

Figure 14: Strain specific amplification of Hamster Prions. Seeding with **(A)** Sc237 and (**B)** 263K and **(C)** NBH as a function of rotation frequency and time. (A and B) Reactions of 10 ml containing 50 µg/ml of rec.shPrP (23 - 230) were seeded with 1/2500 dilution of a 10% brain extract either from a terminally diseased syrian hamster or healthy hamster. All the reactions were performed at 37°C in 0.1% SDS and 0.1% Triton X-100, in PBS following incremental processing. Sample collection for kinetics and silver stain analysis was done as decribed in Methods Section. On the right,the migration pattern of three recombinant shPrP fragments is indicated by the corresponding amino acid numbers. Each panel is a composite of two gels as indicated by black solid line between the lanes

Except for the seed, the two reactions were identical in terms of their composition. For further proof, we then conducted a non-seeded reaction,

using the same processing tools as before, where the seed was replaced with the normal brain homogenate from the healthy hamster (Fig. 14 C). All the other conditions were same as seeded reactions. Evidently, we did not observe any detectable formation of PrP^{res} on the silver stained gel, not even at 1200 Hz. This proved that PrP^{res} formation is not induced shearing mechanisms and that the processing tools can be fully decontaminated for the process. Thus, from the mixed initial seed population, homogenous shearing appears to select the optimally fragmented population and suppresses all others.

4.1.5 The Minimum 'Seed' Requirement for Amplification upon Serial Dilution

All the key parameters that could influence the conversion and the amplification behaviour of rec. PrP^{res} have now been optimized. However, we still needed to figure out the optimal dilution of the initial round product into the subsequent round for efficient serial propagation of prions seeds. Based on our previous observations, we chose to run a single reaction at 756 Hz for 12 hours (Fig.11 and Fig.12). The resulting reaction product was added as a seed into fresh rec. PrP^{C} at four different (1/25, 1/50, 1/100 and 1/250) dilutions and the next round of propagation was initiated.

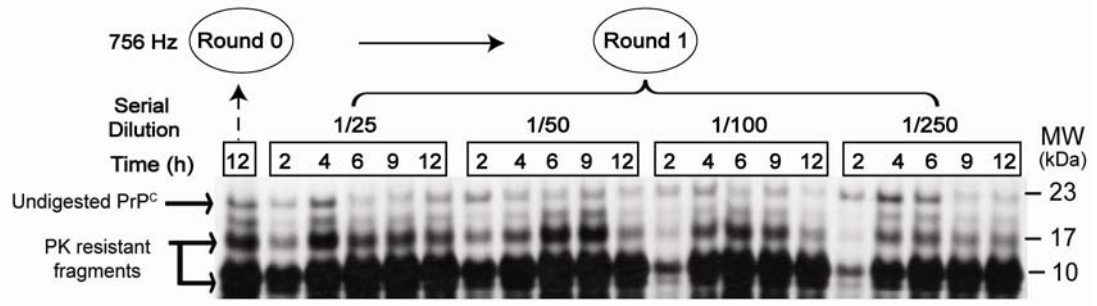

Figure 15: The influence of serial rec. PrP^{res} seed dilutions for Sc237 propagation. Optimal dilution of the round 0 product for serial amplification was determined at a rotational frequency of 756 Hz. Round 0 reaction was performed under the same conditions as mentioned in Fig. 6 legend. The 12 hour reaction product was subsequently diluted by the indicated factor into fresh rec.shPrP and subjected to another round at 756 Hz. Kinetic samples were collected for round 1 and digested by PK and analysed by silver staining as described Methods Section.

Fig. 15 demonstrated the most intense 17 kDa bands at 1/25 dilution (4 h. product) and at 1/50 dilution (6 h. product). The intensity of 6 h. product at 1/100 is slightly less than 1/50. Thus, between 1/25 and 1/50, we decided to choose for the higher dilution of the seed i.e. 1/50 for serial propagation of hamster prions.

4.2 Serial Propagation of Hamster Sc237 and 263K Prions

We have thus far optimized all the required conditions for amplification of hamster brain derived prions using recombinant PrP^{C} as a substrate. In summary, the optimized conditions are: (i) Substrate concentration – 50 µg/ml (ii) Seed concentration – 1/50 of 10% Sc237 or 263K brain homogenate, (iii) Reaction buffer – 0.1% SDS and 0.1% Triton X-100, (iv) Processing conditions – incremental processing and (v) Dilution of previous round seed for serial propagation – 1/50. We adapted all the above mentioned optimized parameters for *in vitro* serial propagation of Sc237 and 263K hamster prions.

In order to dilute out all of the original $PrP^{27–30}$ associated infectivity, we performed ten serial rounds of reactions over the entire range of rotational frequency (95 – 1200 Hz) using both Sc237 (Fig. 16 A) and 263K (Fig. 16 B) hamster strains. We used all the optimized conditions for serial propagation where the initial round product was diluted 1/50 into the subsequent round. The round 0 reactions for all the rotational frequencies were processed for 9 hours. We selected 9 hours because the reactions at higher frequencies are not overly processed at the same time providing the opportunity for lower frequency reactions to amplify as well. However, for subsequent rounds we traced the amplification rate for all the reactions until it was stabilized. For demonstration, we showed the amplification rate of three frequencies – 189, 378 and 953 Hz for both Sc237 (Fig. 16 C) and 263K (Fig. 16 D) prions.

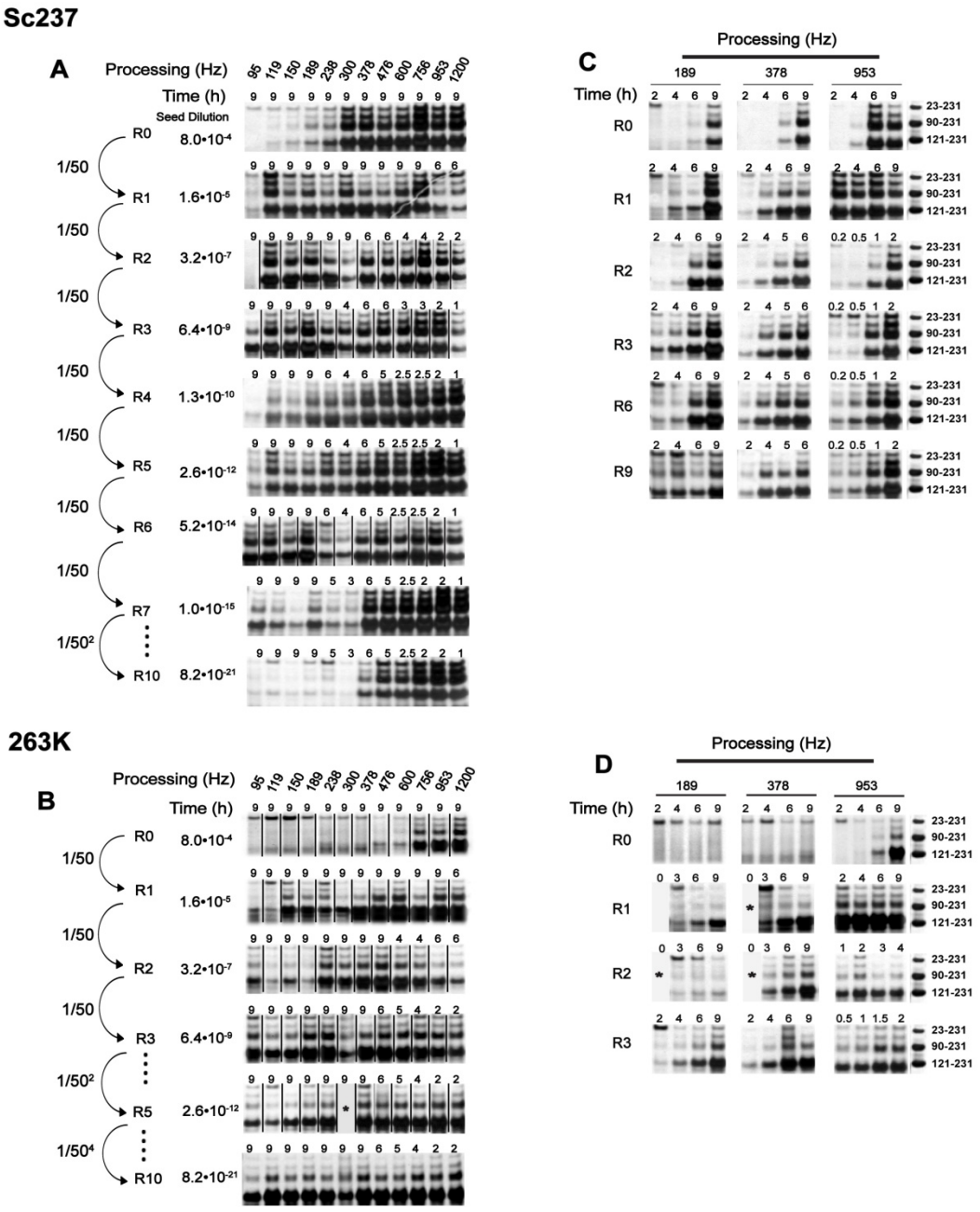

Figure 16: Serial propagation of Sc237 and 263K hamster prions. Both **(A)** Sc237 and **(B)** 263K comprised of 10 serial rounds of amplification over the entire accessible shear force range. At each round, reaction kinetics was traced for all the rotational frequencies as demonstrated in **(C)** for Sc237 and **(D)** for 263K. For representation, kinetics data of only three frequencies – 189 Hz, 378 Hz and 953 Hz is highlighted which were chosen for further structural characterisation. From the kinetics data, time point showing the maximum yield of rec.PrP^{res} was selected to seed the next round at a dilution of 1/50. During each round, a total of 450 µl of sample from individual reaction mixes was collected at pre-defined time points and stored at RT (250 µl for silver stain analysis and 200 µl as a seed). These samples were digested using 0.5 µg/ml PK and analysed by silver staining. For Sc237, the overall reaction kinetics was stable after round 7 and for 263K after round 5. The dotted line represents that further serial rounds were done following the same time points. Round 10 samples with optimized time points were shock frozen at -80°C. The black solid lines between lanes indicate that the particular gel panel is a composite of multiple gels. Asterisk (*) shows that no sample was loaded on the gel.

From each round, at the indicated time points we collected 250 µl of sample for silver stain analysis and an additional 200 µl as a seed. Later on the basis of silver stain result, we used the product which showed the maximum yield as a seed for the next round. This approach was followed till round 7 for Sc237 and round 5 for 263K. Once the amplification rate was stabilized, the reactions of the following rounds were processed for the specific optimized time point. By doing this, we tried to avoid over-processing of the samples which could negatively influence on the overall quality of the reaction product for later structural analysis by NMR. After round 10, all the samples were shock frozen in liquid nitrogen and stored at -80ºC in aliquots of 500 µl for future use.

4.3 Characterization of *in vitro* Propagated rec. PrP Aggregates

Once the serial propagation of both Sc237 and 263K has been successfully achieved, the next objective was to characterize these *in vitro* propagated rec. PrP aggregates by (i) SSA to confirm *in vitro* PrP^{res} conformational selection (ii) negative staining electron microscopy to detect morphological differences, (iii) mass spectrometry to identify major proteinase K (PK) resistant peptides, and (iv) solid state NMR spectroscopy to identify specific conformational differences at atomic resolution. Since Sc237 amplified well over a broad range of processing frequencies and showed multiple optima, we selected three frequencies − 189, 378 and 953 Hz for structural characterization. However, for 263K, we selected only two frequencies − 378 and 953 Hz as we observed only one optima at the maximal processing frequency.

4.3.1 Characterization by SSA

Splitting Experiment – Sc237 (953 Hz)

We next explored the potential of SSA for selecting rec. PrP^{res} conformation *in vitro*. For testing this, we used the serially propagated Sc237 and 263K samples which were frozen at -80ºC after round 10. After thawing the seed,

we typically performed five to six serial rounds at 37ºC in order to activate the seed and then tested for rec. PrP^{res} conformational selection by splitting the resulting reaction mix for processing across the entire shear force range on SSA array.

(Fig. 17 A) demonstrated serial propagation of rec. Sc237 – 953 Hz seed up to round 26 which clearly proves that rec. PrP^{res} generated by SSA can be propagated indefinitely.

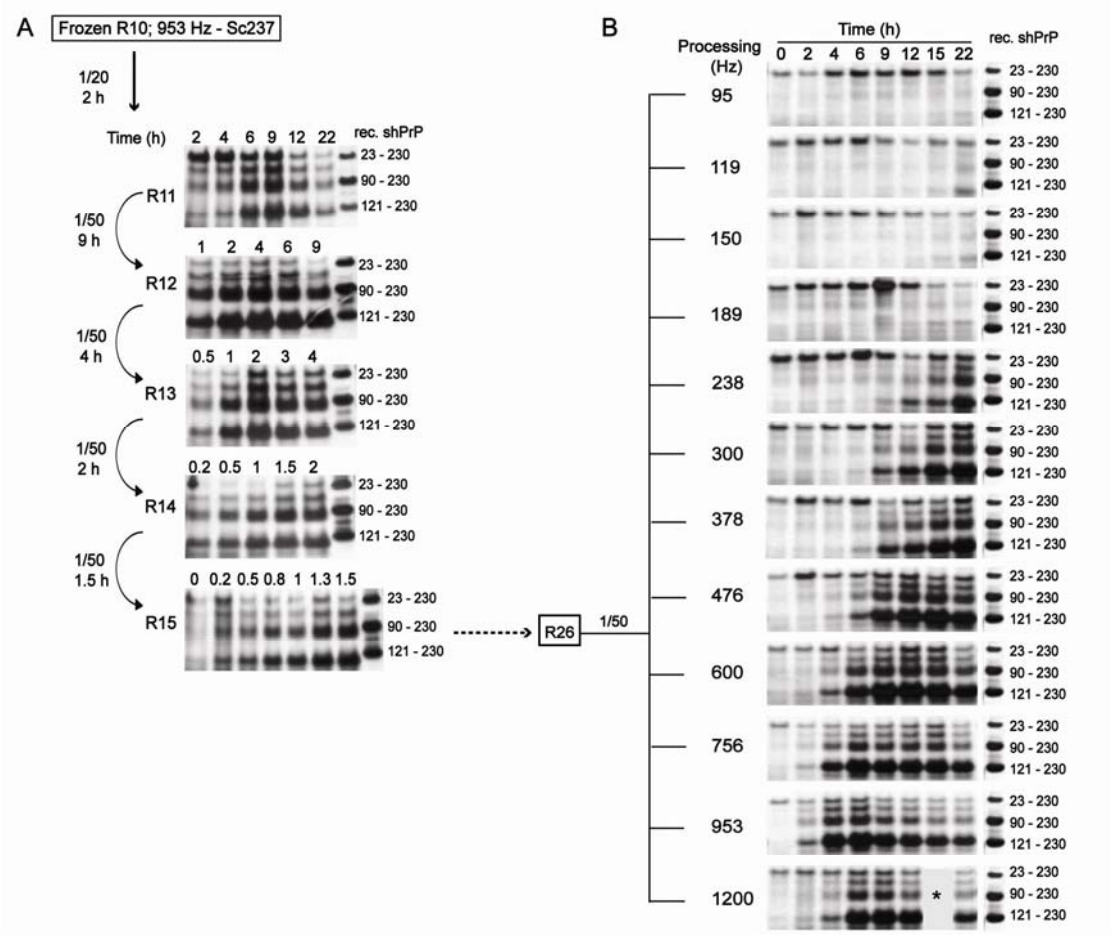

Fig. 17: Selection and purification of 953 Hz optima of Sc237. (A) Serial propagation of round 10 rec. Sc237 - 953 Hz prion seed using an initial dilution of 1/20. For subsequent rounds, 1/50 dilution of kinetically selected previous round's seed was used. Reaction kinetics was traced until the Sc237 - 953Hz seed showed the maximal activity at ≈ 2 hours. (Note: Round 10 Sc237 - 953Hz seed was frozen at 2 h). Further rounds were were carried under the same conditions for 2 hr. processing. **(B)** Splitting Experiment. Round 26 Sc237 - 953Hz prion seed was diluted by the indicated factor and the individual reaction mixes were then processed at the specified frequencies. At indicated time points, samples were collected and stored at RT for later analysis by silver staining (See Methods). Asterisk (*) indicate that no sample is loaded on the gel.

After thawing the round 10 Sc237 seed at 953 Hz, it was serially propagated for additional 26 rounds following the same approach as in Fig 4.2. This was done in order to overcome the effects of freeze-thawing the sample and also to purify the seed for *in vitro* conformational selection. On splitting the round 26 rec. Sc237- 953 Hz product (corresponding to 2.7 x 10^{-46} dilution relative to the initial seed), we clearly observed an amplification optimum at 953 Hz frequency and all other optima were relatively suppressed (Fig. 17 B). At lower frequencies there was no amplification at all. The first detectable 17 kDa band appeared at 238 Hz after 15 hours. As the frequency increases the lag time of prion amplification decreases. Notably at 953 Hz, the reaction was completed in the shortest period of time of four hours (as indicated by the formation of the intense 17 kDa band) which at 1200 Hz was delayed to six hours. Thus we concluded that selective shearing is capable of purifying individual seed populations from PrP^{Sc} conformational mixtures.

Splitting Experiment – 263K (953 Hz)

For the proof of principle, we next repeated the same splitting experiment but with 263K hamster prion strain (Fig. 18). After round 10 we serially propagated the rec. 263K – 953 Hz seed for additional 40 rounds (corresponding to 4.4 x 10^{-70} dilution relative to the initial seed) and then split the resulting reaction mix. We observed the same behavior as with Sc237. PrP^{res} amplification was observed only at ≥953 Hz processing, and all other optima were effectively lost. At 1200 Hz the reaction was completed in the shortest time of 2 hours (as indicated by the formation of the intense 17 kDa band) which was not observed at any other frequency. Thus, we clearly demonstrated that SSA can select PrP^{res} conformations *in vitro*.

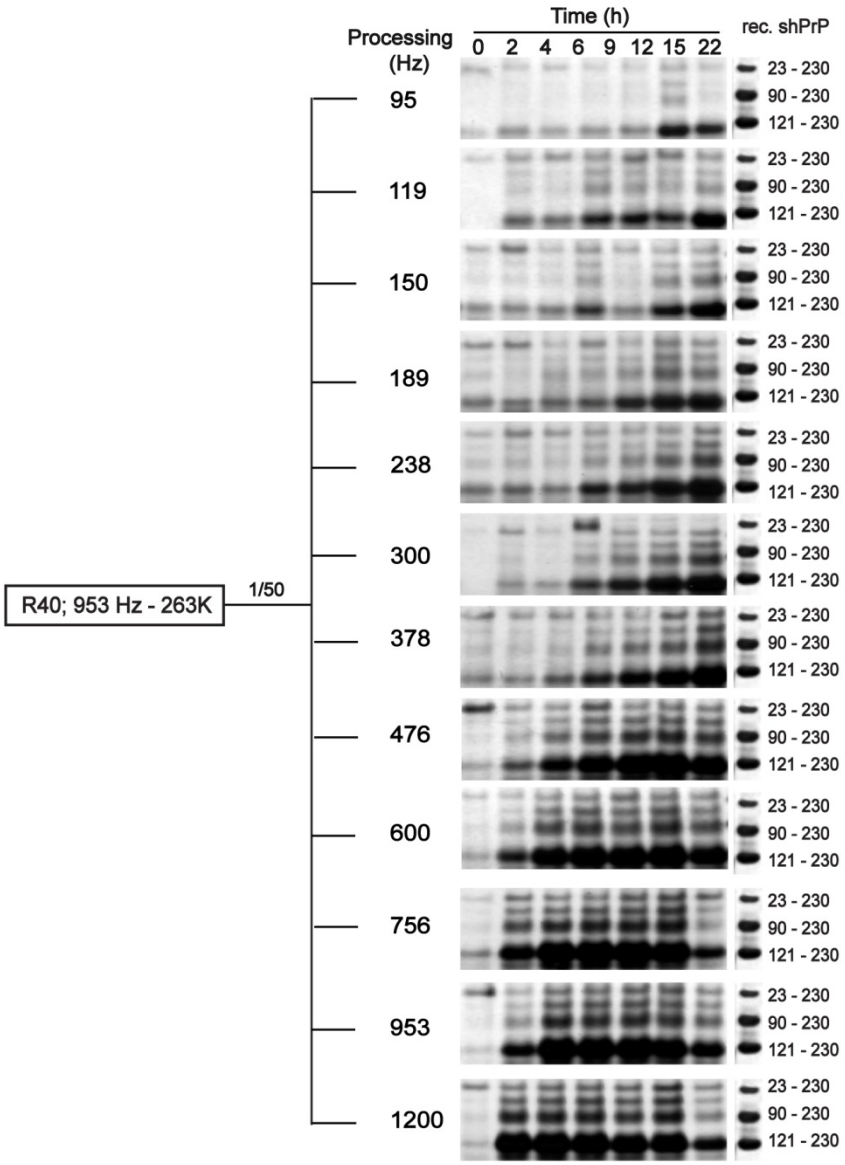

Fig. 18: Splitting Experiment. Round 40 (R40) 263K - 953 Hz. prion seed was diluted by the indicated factor and the individual reaction mixes were then processed at the specified frequencies. At indicated time points, samples were collected and stored at RT for later analysis by silver staining (See Methods).

Splitting Experiment – Sc238 (378 Hz)

We next tried to perform the splitting experiment with rec. Sc237 – 378 Hz seed corresponding to 43rd serial *in vitro* passage (Fig 19). At frequencies ≤150 Hz there was no amplification at all. From 189 Hz onwards, we observed a strong 17 kDa band appearing at 22 hours. This demonstrates that the specific seeding activity of rec. PrP^{res} seeds is dependent on the particle size of the aggregates, which is controlled by the fragmentation processes. In

general, as shown by the electron micrographs (Sim and Caughey, 2009) rec. PrP^{res} are large sized aggregates which on selective shearing will amplify on a broader shear force range on SSA array. Thus we hypothesized that SSA has the potential to select differentially structured rec. seeds based on their specific mechanical fragmentability.

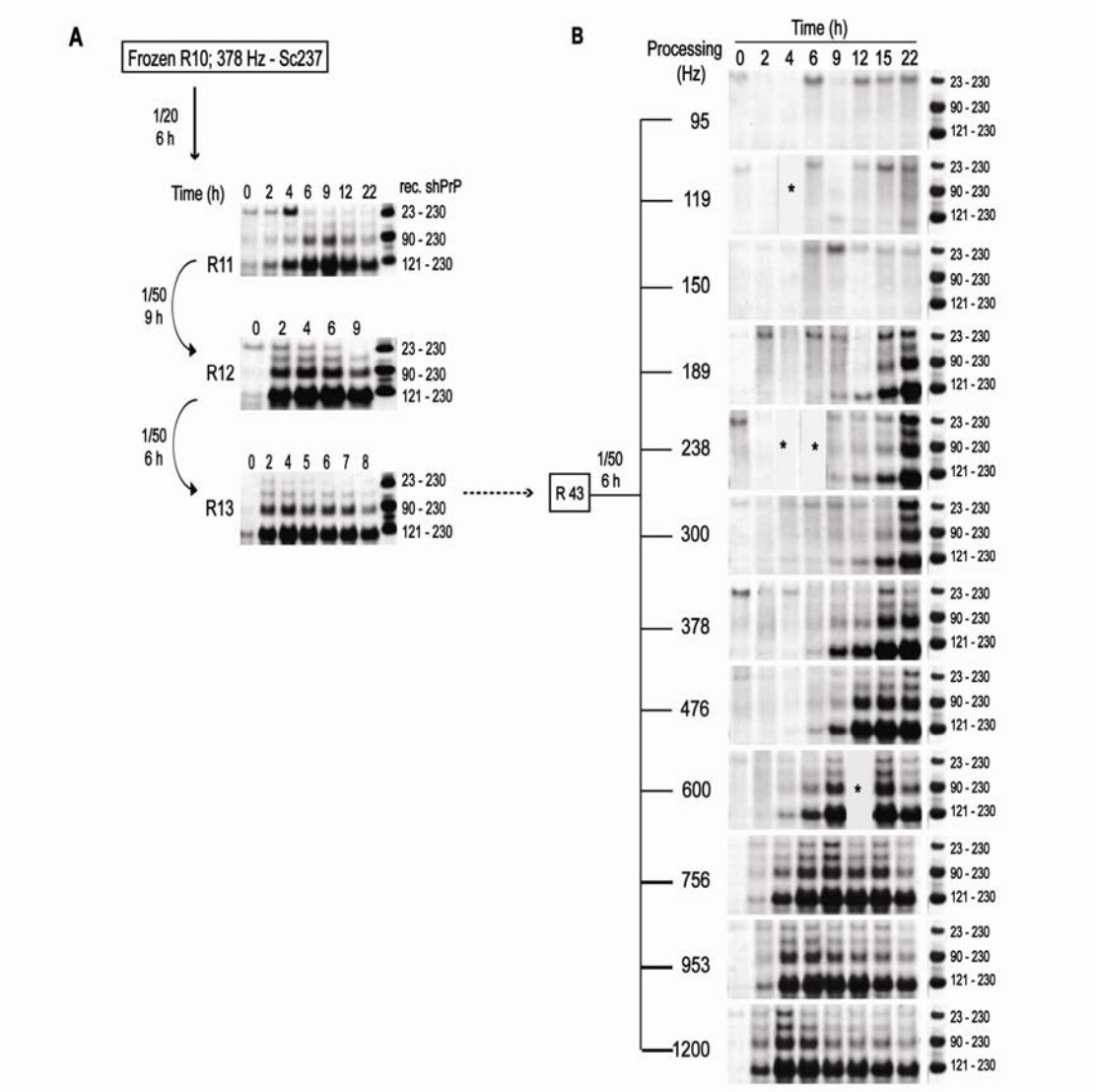

Fig. 19: Selection and purification of 378 Hz optima of Sc237. (A) Serial propagation of round 10 Sc237 - 378 Hz. prion seed using an initial dilution of 1/20. For subsequent rounds, 1/50 dilution of kinetically selected previous round's seed was used. Reaction kinetics was traced until the Sc237 - 378 Hz. seed showed the maximal activity at ≈ 6 hours. (Note: Round 10 Sc237 - 378 Hz. seed was frozen at 6 h). Further rounds were were carried under the same conditions for 6hr. processing. **(B)** Splitting Experiment. Round 43 Sc237- 378 Hz. prion seed was diluted by the indicated factor and the individual reaction mixes were then processed at the specified frequencies. At indicated time points, samples were collected and stored at RT for later analysis by silver staining (See Methods). Asterisk (*) indicate that no sample is loaded on the gel.

4.3.2 Characterization by Negative Staining Transmission Electron Microscopy (TEM)

To study the morphological differences between *in vitro* propagated Sc237 and 263K aggregates, the rec. PrP^{res} samples were examined with transmission electron microscopy (TEM). In the brain of the scrapie infected animal, PrP^{res} is often found as diffuse amorphous deposits which intermittently arranges itself into fibrils and extracellular plaques (Sim and Caughey, 2009). Merz et al. isolated scrapie associated fibrils (SAF) which are consistently found in TSE affected humans and animals and described distinct filaments within these fibrils (Merz et al., 1981). In 1983, Prusiner et al. described another form of scrapie fibrils, termed as prion rods, where the clear substructure was somewhat missing and distinct filaments were often hard to characterize (Prusiner et al., 1983).

In this study, we used negative staining TEM to compare rec. PrP^{res} fibrils from both Sc237 and 263K hamster prion strains which are generated by SSA. Additionally, we also tried to obtain the morphological information about the brain derived infectious prion seed from both Sc237 and 263K prions.

Serially propagated rec. PrP^{res} samples from Sc237 (corresponding to − 189, 378 and 953 Hz) and rec. 263K (378 and 953 Hz) were treated with 0.5 µg/ml PK at 37°C for one hour. All the brain derived infectious prion samples (10% Sc237 and 263K brain derived seed and with 10% Syrian hamster normal brain homogenate) were digested with two different PK concentrations – 50 µg/ml and 100 µg/ml. All the samples were then settled onto carbon-coated butvar grids for 10 minutes, stained with Uranyl acetate for few seconds and then analysed by TEM.

Fig. 20 showed electron micrographs of rec. Sc237 and 263K aggregates. at At 953 Hz Sc237 contained primarily matted clumps of fibrils and appeared more like prion rods published by Prusiner (Prusiner et al., 1983). They appeared to be different from 263K aggregates at the same frequency. The

263K fibrils (953 Hz) looked well defined with individual proto-filaments being visible and the morphological specificities were distinct. Bars designate 200 nm. This strongly indicated that Sc237 differ substantially from 263K strain.

In general at 378 Hz, 263K fibrils looked much cleaner and defined than Sc237 and the details of fibril morphology were more readily observed. However, on comparing the 263K fibrils at 378 and 953 Hz we could not observe any consistent ultrastructural differences and they looked almost similar. This is consistent with the silver stained results (Fig. 14 B) that 263K consisted of only one detectable PrP^{res} population at frequency ≥ 953 Hz. Notably, on comparing Sc237 at 378 and 953 Hz we observed marked diffrences between the two. In Sc237 at 378 Hz, individual fibrils were visible, though they were without any definition and the edges were completely blurred.

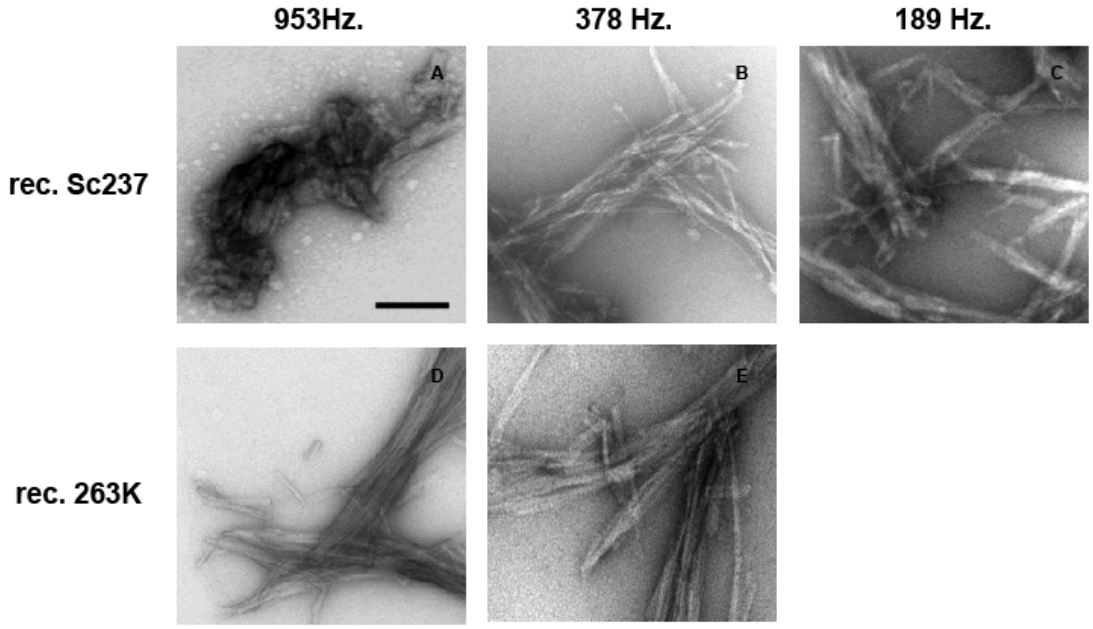

Fig. 20: TEM comparison of rec. Sc237 and 263K fibrils. Serially propgated rec. Sc237 aggregte at 953 Hz **(A)** , 378 Hz. **(B)** and 189 Hz. **(C)**. Serially propgated rec. 263K aggregte at 953 Hz **(D)** and 378 Hz. **(E)**. All the samples were digested with 0.5 µg/ml PK at 37°C for one hour. PK digestion was terminated by heating the samples at 95° C for 10 minutes. All the samples were then settled onto carbon-coated butvar grids for 10 minutes and stained with Uranyl acetate for few seconds. Bar designate 200 nm. TEM images were taken at 25,000x magnification.

At 189 Hz Sc237 revealed thick overlapping fibre bundles and overall the morphology looked different from Sc237 at 378 and 953 Hz. Each fibril consisted of individual proto-filaments that appear to be helically wound around each other. Individual proto-filaments have a diameter of 1.5 –1.9 nm and appear equally spaced by approx. 3.5 nm. Bars designate 200 nm.

On comparing TEM micrographs of the infectious brain derived Sc237 and 263K prion seed, we observed clear morphological differences between the two (Figure 21).

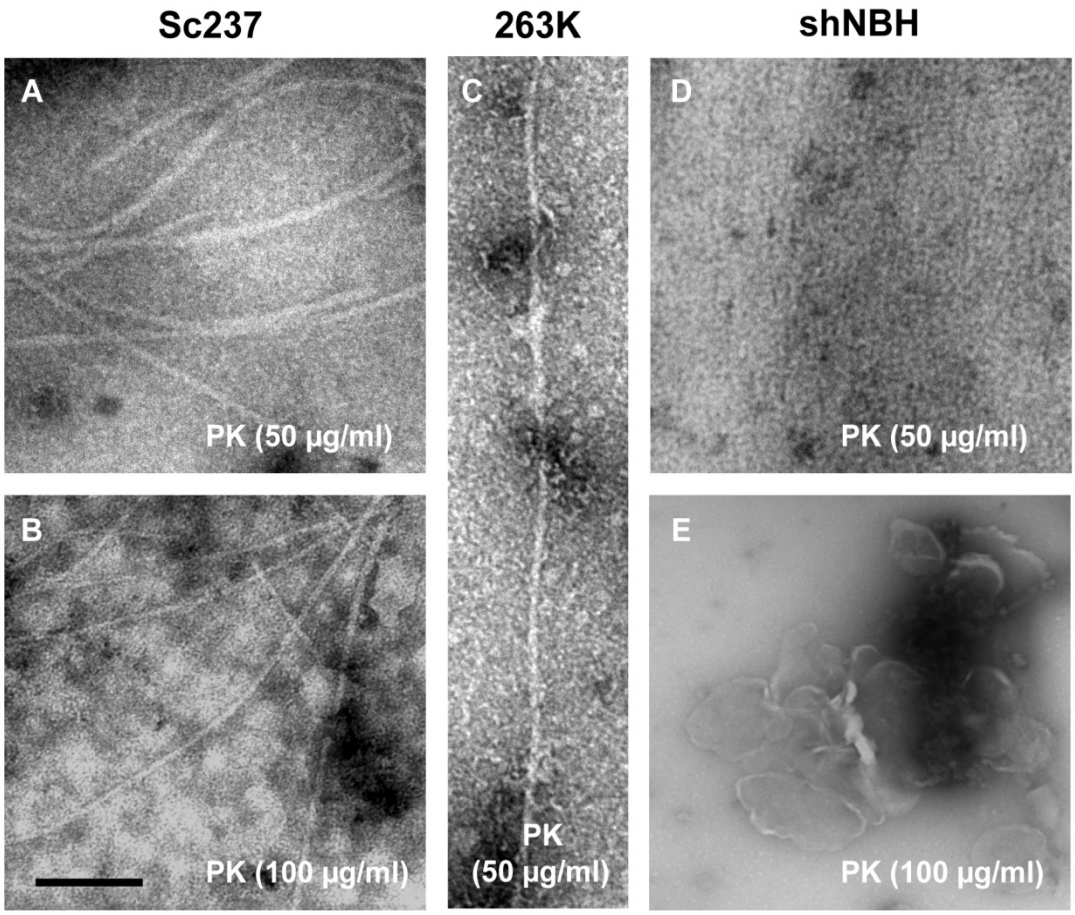

Fig. 21: TEM comparison of Sc237, 263K and shNBH fibrils. 10% Sc237 BH was digested with **(A)** 50 µg/ml PK or **(B)** 100 µg/ml PK for 1 hr. in PBS. PK digestion was terminated by heating the samples at 95° C for 10 minutes. **(C)** 10% 263K BH digested at 50 µg/ml PK for 1 hour without sarkosyl. **(D)** 10% Syrian Hamster normal brain homogenate (shNBH) digested at 50 µg/ml PK for 1 hour without sarkosyl. **(E)** 10% Syrian Hamster normal brain homogenate (shNBH) digested at 100 µg/ml PK for 1 hour without sarkosyl. All the samples were then settled onto carbon-coated butvar grids for 10 minutes and stained with Uranyl acetate for few seconds. TEM images were taken at 25,000x magnification. Bars designate 200 nm.

Sc237 samples showed straight, very long and unbranched fibrils composed of either a single filament, or paired filaments twisted together with irregular periodicity (Fig. 21 A-B). The filaments were typically 7–12 nm in diameter and up to several µm in length. On the contrary, when 263K was examined under the electron microscope, we observed relatively low abundance of fibrils in comparison to Sc237 (Fig. 21 C). However, beaded substructures could be observed along the axis of proto filaments which were absent in Sc237. Similar beads have been described for SAF, and it has been speculated that they might represent subunits of the fibrils (Merz et al. 1981). Notably, in the normal brain homogenate (NBH) from syrian hamster (Fig. 21D), we could not observe any fibrils. We just observed some membranes and vesicles, indicating that fibril formation is the characteristic feature of prions.

4.3.3 Characterization by Electrospray Ionization Mass Spectrometry (ESI-MS)

Detailed mass spectrometric analysis of Sc237 proteinase K (PK) resistant fragments was carried out by electrospray ionization mass spectrometry (ESI-MS). The serially propagated Sc237 samples corresponding to 189, 378 and 953 Hz processing frequencies were digested by 0.5 µg/ml PK for one hour. Following methanol/chloroform precipitation and inactivation of prions by hexafluoroisopropanol, the samples were analyzed by ESI-MS.

The results revealed predominant species at masses of 10967.1, 12016.5, 13448.3, 16094.4 and 19716.2 Da respectively (Fig. 22). Moreover, we observed that in all three frequencies of Sc237 (189, 378 and 953 Hz), the masses were rather same and we could not observe any characteristic changes in terms of their PK resistant mass fragments. However, the sizes of these PK-resistant fragments correlate remarkably well with the structured core region of the prion protein. Thus we concluded that mass spectrometry is not the potential method for observing prion strain specific differences.

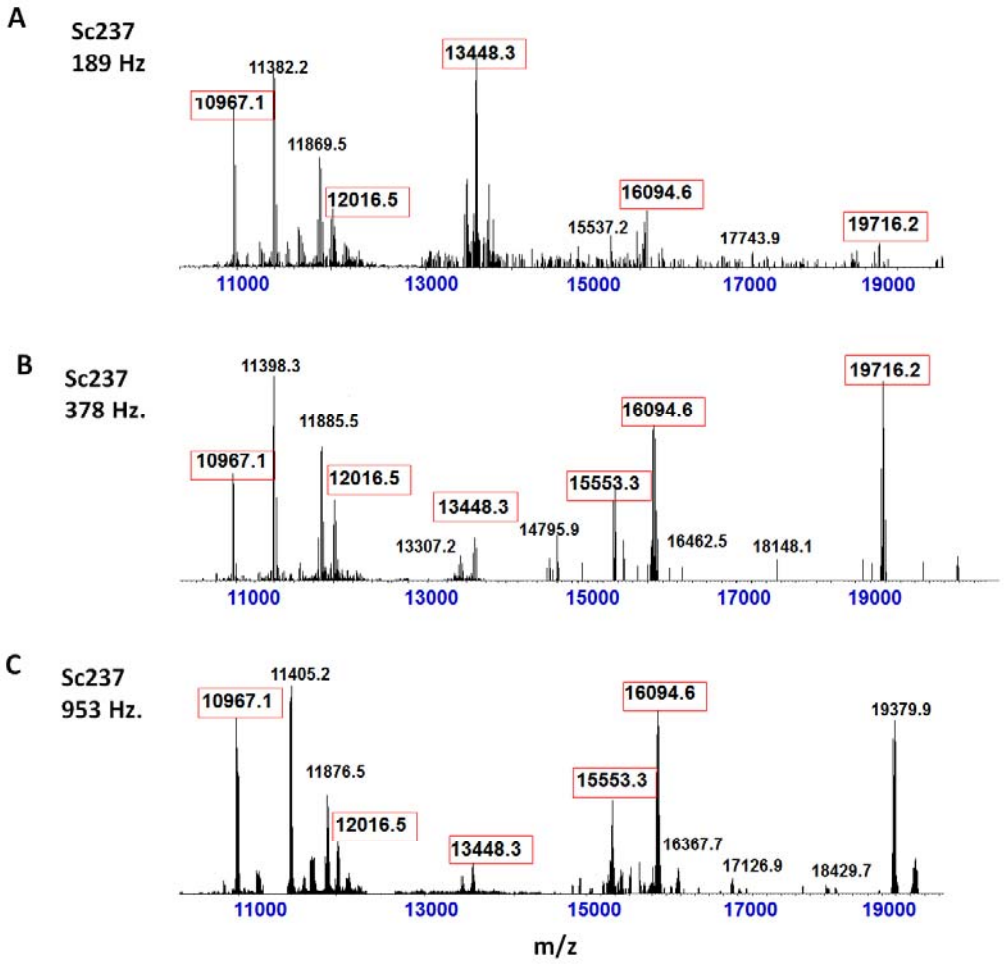

Fig 22: ES-IMS spectrum of the rec. Sc237 Prions. Rec. prions at their corresponding frequencies were digested with 0.5 µg/ml PK for 1 hour at 37ºC. Effect of PK was terminated by heating the samples at 95ºC for 10 minutes. Later all the samples were spun down at 25,000g for 10 minutes. Pellets were collected and rec. PrP^{res} was precipitated with methanol/chloroform. The resulting pellet was inactivated in 50 µl of hexafluoroisopropanol (HFIP) and analysed for electrospray ionization mass spectrometry. **(A)** ES-IMS spectrum of rec. Sc237 – 189 Hz. prions **(B)** ES-IMS spectrum of rec. Sc237 – 378 Hz. prions and **(C)** ES-IMS spectrum of rec. Sc237 – 953 Hz. prions.

4.3.4 Initial Characterization of Selectively Amplified Recombinant PrP^{res} by Solid State NMR

We next prepared uniformly [^{15}N] - labelled and [$^{13}C/^{15}N$] - labelled recombinant prions from Sc237 at three different frequencies – 189 Hz, 378 and 953 Hz and from 263K at 378Hz and 953 Hz rotational frequencies.

In order to obtain a substantial yield of isotopically labelled recombinant Sc237 and 263K prions, we first activated the amplified frozen round 10 seeds

by serial propagation using the unlabelled rec. PrP^C as a substrate. Once activated, we split the resulting reaction mix equally to seed 12 reactions containing the ^{15}N or $^{13}C/^{15}N$ shPrP (23-230), which were then processed under the identical conditions (Fig. 23).

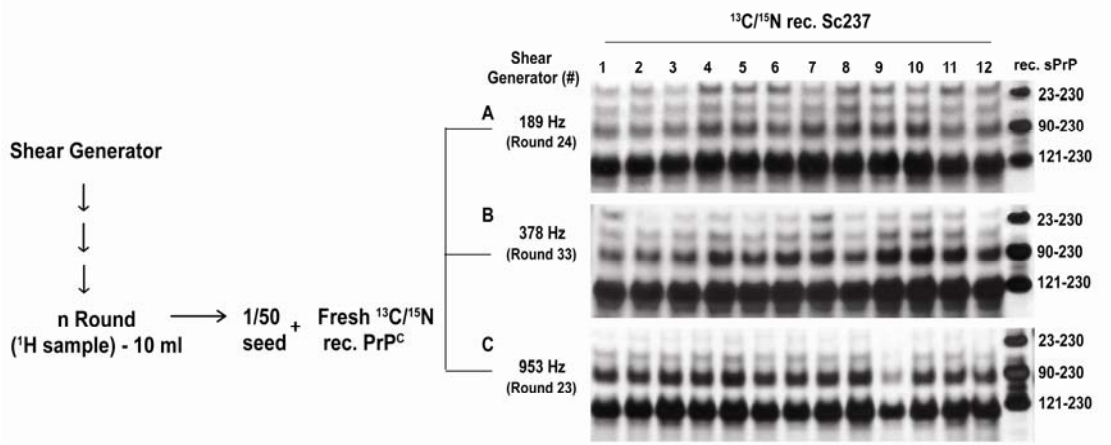

Figure 23: Generation of Isotopically Labelled Sc237 Prions for Solid State NMR. Frozen round 10 seeds were thawed and activated by performing serial propagations *in vitro* using a single shear generator device. Once activated, the resulting reaction mix (n round) was split equally at a dilution of 1/50 to seed 12 reactions containing fresh isotopically labelled shPrP (23-230) as a substrate. All the reactions were then processed under identical conditions. 250 µl aliquots were collected from each reaction which were later digested with 0.5 µg/ml PK and ananlysed by silver staining. **(A)** Preparation of $^{13}C/^{15}$-labelled Sc237 -189 Hz prions at round 24 **(B)** Preparation of $^{13}C/^{15}$-labelled Sc237 -378 Hz prions at round 33 **(C)** Preparation of $^{13}C/^{15}$-labelled Sc237 - 953 Hz prions at round 23. The same processing tools were used for all three frequencies, and the samples were loaded onto the gels in the coresponding order. On the right, migration pattern of three recombinant shPrP fragments is indicated by the corresponding amino acid numbers.

Fig. 23 shows the analytical PK digestion pattern of the obtained products, which is identically propagated over several rounds of serial reactions. Moreover, the yield appears to be rather uniform for all 12 reactions indicating a uniform behaviour of all the utilized processing tools.

With the above mentioned approach (Fig. 23), we performed around 40-50 serial propagation rounds for both Sc237 (189, 378 and 953 Hz) and 263K (378 and 953 Hz) prion strains and generated ~150-170 mg of unlabelled and isotope labelled sample.

Table 9 summarises the total amount of recombinant Sc237 and 263K prions prepared for this project. Overall, approx. 30 mg of $^{13}C/^{15}N$ and 60-70 mg of ^{15}N and unlabelled rec. Sc237 and 263K prions were prepared.

Table 9: Summary of total amount of rec. Sc237 and 263K Prions prepared

Hamster Strain	Frequency (Hz.)	No. of rounds required for seed activation	^{15}N labelled sample	$^{13}C/^{15}N$ labelled sample	^{1}H sample	Total yield
Sc237	189 Hz.	R11 – R19	**69 mg** (R25 – R36)	**30 mg** (R20 – R24)	**72 mg** (R36 – R47)	**171 mg**
	378 Hz.	R11 – R13	**72 mg** (R14 – R2	**31 mg** (R29 – R33)	**60 mg** (R34 – R43)	**163 mg**
	953 Hz.	R11 – R15	**63 mg** (R16 – R24)	**35 mg** (R27 – R31)	**61 mg** (R32– R40)	**159 mg**
263K	378 Hz.	R11 – R14	**59 mg** (R15 – R23)	**31 mg** (R24 – R28)	**61 mg** (R29 – R38)	**151 mg**
	953 Hz.	R11 – R15	**64 mg** (R16 – R24)	**33 mg** (R27 – R31)	**59 mg** (R32– R40)	**156 mg**
						Total 800 mg

In order to investigate the structural properties of the selectively amplified recombinant PrP^{res} (Table 9), we next performed a series of solid state NMR experiments. For the analysis, about 15 mg of the individual reaction products were filled into 3.2 mm zirconium rotors. All NMR experiments were performed on a 14.1 T Bruker Avance III NMR spectrometer equipped with a triple resonance ssNMR probe using spinning frequencies of 10 kHz or of 13 kHz, respectively.

Figure 24 show the 2D [$^{13}C,^{13}C$] DARR spectra of the 953 Hz amplification products derived from 263K prions (Fig. 24A) and Sc237 prions (Fig. 24B). The DARR mixing time was 250 ms, which allows to observe cross-peaks of covalently linked ^{13}C-atoms, and also cross peaks corresponding to pairs of ^{13}C-atoms that are spatially separated by less than 5 Å. Thus, these spectra provide direct evidence of the tertiary structures contained in the individual reaction products. The 263K-953 reaction product displays an overall peak pattern that would be expected for a highly ordered, very well defined proteins

tertiary structure. In contrast, the Sc237-953 sample displays a much less defined peak pattern, which is indicative of an ordered 3D structure that is overall less well defined. When individual parts of the two spectra are compared, several substantial differences in the tertiary structure become immediately evident: (i) in the region marked ‘a’, the spectral range where amino acid side chains of ASP^- and GLU^- are observed. While 263K-953 displays a well-defined pattern that corresponds to at least three ordered negatively charged side chains, the same spectral region of Sc237-953 lacks these peaks, and only weak resonances are observed. This indicates that 263K-953 prions likely contain three salt bridges that form an integral and characteristic part of their 3D structure. (ii) the region marked ‘b’ contains the spectral range that contains the $C^{\beta}/C^{\gamma 2}$ correlations of threonine side chains. For 263K-953, a characteristic peak pattern is observerd indication that numerous threonine amino acids are involved in structure formation. Also in Sc237-953 threonine side-chains are involved in structure formation, however, the overall pattern is distinct from 263k-953, and several cross-peaks are clearly absent from the Sc237-953 spectrum (see arrow-heads). Thus, the 3D-structures of Sc237 and 263K appear to be distinct with respect to threonines. (iii) The spectra region that contains the resonances of isoleucine side chains (marked ‘c’) indicated that all these four contained amino acids of this type in the PrP sequence are ordered in Sc237 and in 263K. However, 263K appears to contain two distinct close contacts between methyl groups of ILE and VAL, and of ILE and THR, respectively (see arrow heads). Thus, there appears to be high structural order around the isoleucines of 263K. (iv) The spectral region that contains medium-range and long-range contacts between the C^{β}-atoms of threonine side chains and side-chain-methylene groups of other amino acids (region ‘d’) are also characteristic and distinct btween the two recombinant prion amplification products.

In summary of these first 2D-ssNMR [^{13}C,^{13}C]-spectra we have to conlude that the reaction products that were obtained from brain derived Sc237 prions, and from 263K prions, respectively, contain readily distinguishable tertiary structures. This suggest that these two prion strains are non-identical.

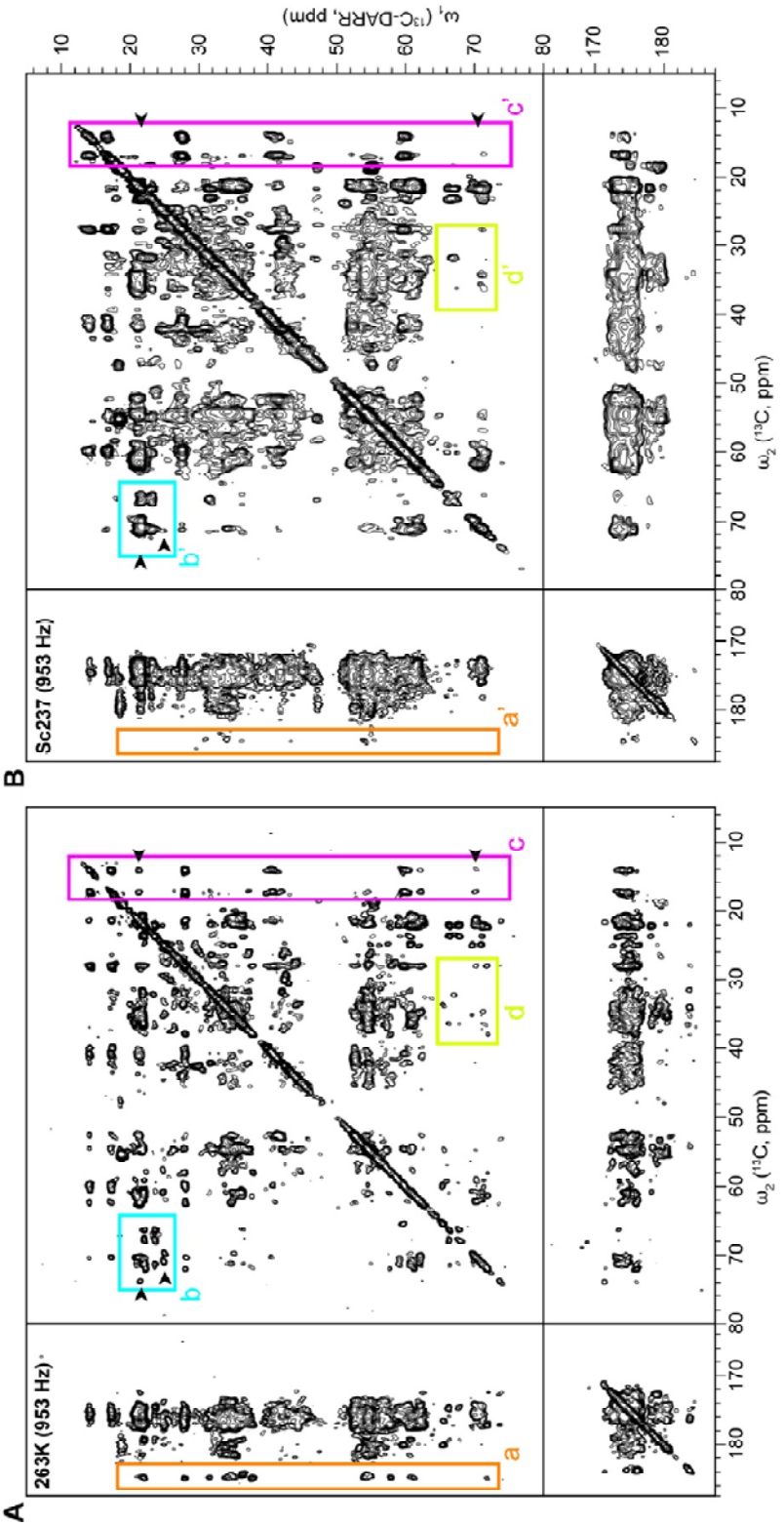

Figure 24: [^{13}C,^{13}C] correlation ssNMR spectrum of recombinant PrP^{res}. (A) The NMR spectrum of the 263K-953 Hz product. **(B)** The NMR-spectum of the Sc237-953-Hz product. (A, B) The spectra region marked 'a' (orange) contains amino acid side chain resonsnces of ASP- and GLU- . The spectra region marked 'b' (cyan) contains C$^{\beta}$/C$^{\gamma 2}$ correlations of threonine amino acid side chains. The spectra region marked 'c' (magenta) contains resonances of isoleucine side chains. The spectra region marked 'd' (light green) contains long-range contacts between the C$^{\beta}$-atoms of threonine side chains and side-chain-methylene groups of other amino acids. Arrow-heads indicate resonances that are present in (A) but not in (B). These spectra were recorded using a DARR-mixing time of 250 ms, and a MAS-spinning frequency of 13.5kHz using a 600 MHz Bruker AVIII NMR-Spektrometer equipped with a custom-made triple resonance CP-MAS probe that contains an air-tight transfer system. Exhaust air was filtered trough a HEP-filter.

residue (Fig. 25).

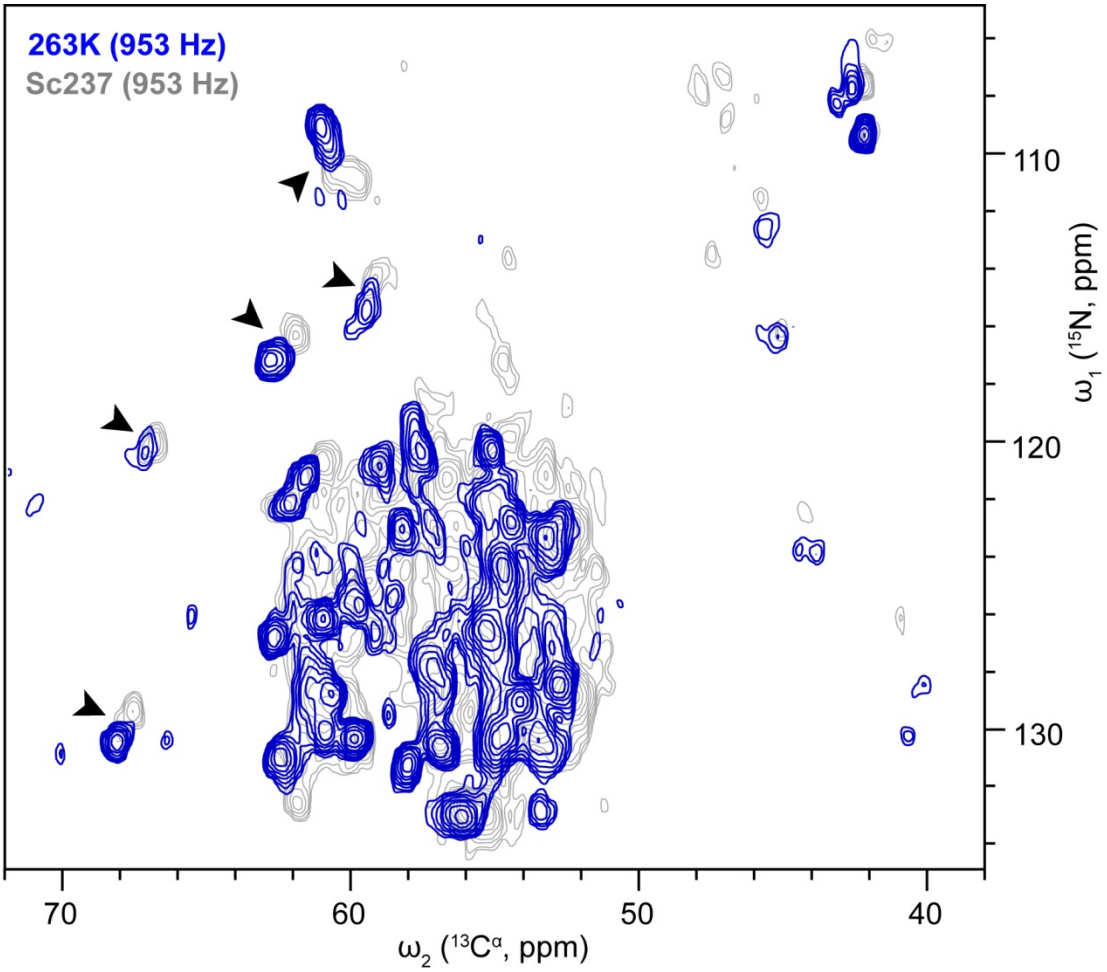

Figure 25: [^{15}N,^{13}C$^{\alpha}$] correlation ssNMR spectrum of recombinant PrP^{res}. The spectra of 263K-953 (blue) and Sc237-953 (grey) are shown as a superposition. The arrow-heads indicate well-separated resonances that are very similar between the two spectra and appear to be only slightly shifted. Both spectra were recorded at a MAS-spinning frequency of 10.0kHz using a 600 MHz Bruker AVIII NMR-Spektrometer as indictaed in Fig. 24.

For 263K-953, we observed a very well-defined set of at least 56 resonances, that showed a good chemical shift dispersion, and narrow line widths of about 0.5–1.0 ppm. However, the same spectrum for Sc237 displayed a different pattern, and the resonances appeared to be broadened when compared to 263K. Still, there appears to be a significant degree of structural similarity between the two strains. A set of five backbone resonances (Fig. 25, see arrow-heads) are shifted between the two spectra, but the overall pattern is very-well preserved. Thus, at least some parts of the 3D structures appear to be almost identically conserved between Sc237 and 263K.

Finally, we compared the structures of all reaction products that were generated from the prions strains Sc237 and 263K (table 9). For this purpose, we recorded [^{13}C,^{13}C] DARR spectra using a DARR mixing time of only 15 ms, where correlation peaks are observed only for neighbouring ^{13}C atoms within individual amino acid side chains. Figure 26A shows the spectral region that contains the $^{13}C^{\gamma}/^{13}C^{\delta}$ correlation peaks of glutamic acid and of glutamine side chains. The reaction products of 263K-953 and of 263K-378 contain the same peak pattern, which provides very strong evidence that the same conformation was selected under both experimental conditions. However, when the three Sc237 amplification products are compared, it becomes immediately evident, that each peak pattern is distinct. Unexpectedly, the product Sc237-189 contains virtually the identical peak pattern as the products 263K-953 and 263K-378. This provides substantial evidence that the 263K conformation is also present in the original Sc237 prion isolate. In addition, while the reaction products Sc237-953 and Sc237-378 look very similar in this spectral region, they can also be distinguished by one shifting resonance (see arrow heads). These structural differences are also readily evident from the two corresponding 1D-traces shown below the 2D spectra regions.

In order to further support the presence of three distinct conformations in the total of five different reaction products, we also compared the corresponding $^{13}C^{\beta}/^{13}C^{\alpha}$ and $^{13}C^{\beta}/^{13}C^{\gamma 2}$ correlations of threonine side-chains (Fig. 26B). Also here the pattern of 263K-953, 263K-378, and Sc237-189 are nearly identical. The distinction of Sc237-953 and Sc237-378 is even more evident in this spectral region, because up to three additional sets of resonances can be identified for Sc237-953 (see arrow heads).

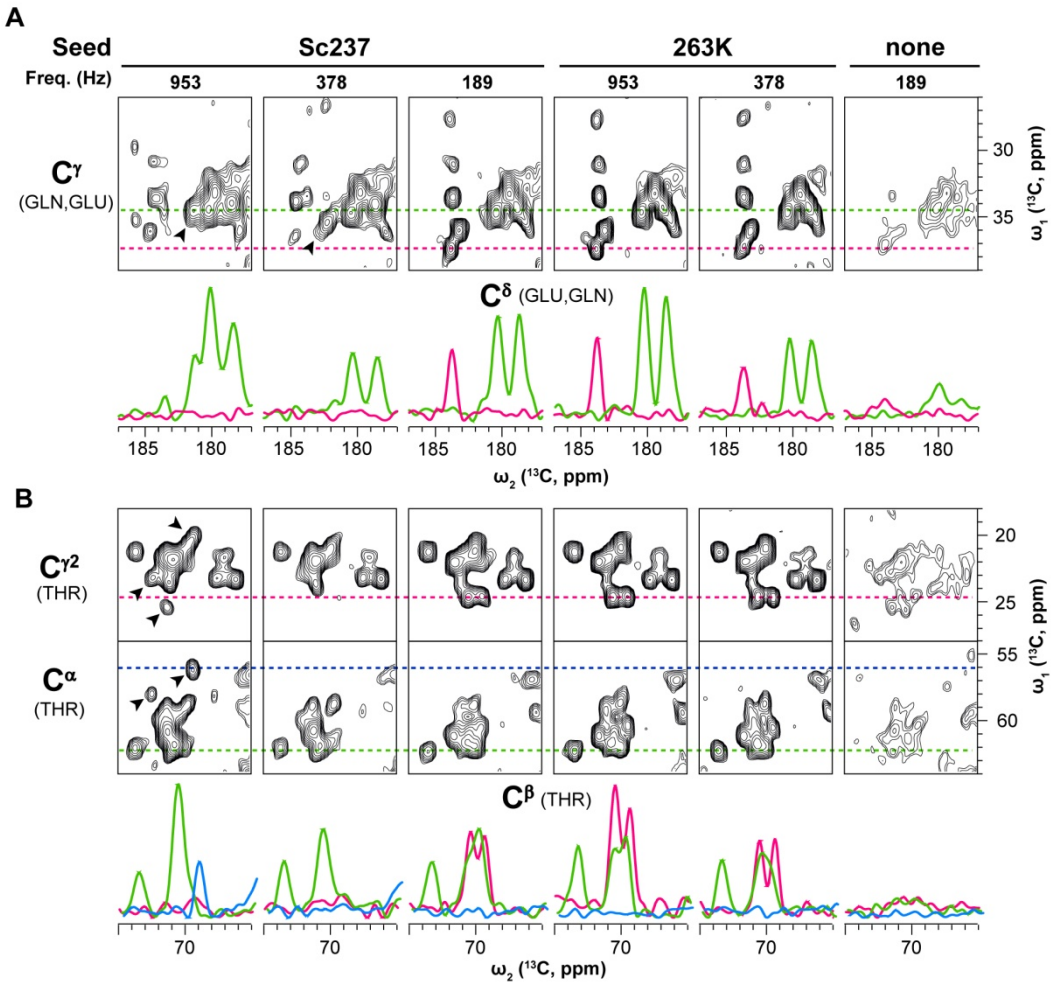

Figure 26: Comparison of [^{13}C,^{13}C] correlation ssNMR spectrum between all recombinant PrP^{res} amplification products. (A) Spectral Region containing ^{13}C$^{\gamma}$/^{13}C$^{\delta}$ correlation peaks of glutamic acid and of glutamine side chains. The arrow head indicated a shifing resonance between Sc237-953 and Sc237-378. **(B)** Spectral Region containing ^{13}C^{ß}/^{13}C$^{\alpha}$ and ^{13}C^{ß}/^{13}C$^{\gamma 2}$ correlations of threonine side-chains. The arrow heads indicate resonaces that are present in Sc237-953, but absent in Sc237-378. (A,B) 1D traces through the individual spectra are shown using the coloring corresponding to the dashed lines in the 2D-spectra. These spectra were recorded using a DARR-mixing time of 15 ms, and a MAS-spinning frequency of 13.5kHz as indicated in Fig. 24

Finally, it has to be noted that the 263K peak pattern has been obtained under three substantially different shearing conditions, and thus shearing per se does not determine the structure that is generated. This is also evident from the spectrum of a spontaneously generated aggregate (spont-189), that is indicative of an inhomogeneous aggregate. Thus these ssNMR-data provide the experimental proof that the amplification products generated by SSA are determined by the utilized initial seed and its conformational composition. In summary, these NMR data provide very strong evidence of the co-existence of three distinct prion conformations in the Sc237 prion isolate. Importantly,

the 263K prion isolate appears to contain only one single conformation, which is also a subset of the Sc237 prion isolate.

5 Discussion

In order to investigate the still obscure attributes related to the structure of prions, it was necessary to obtain sufficiently large amounts of recombinant PrP^{res}. The goal of the project was first to optimize the *in vitro* amplification conditions of rec. PrP^{res} using full length (23-230) hamster prion protein as a substrate. Further these rec. prion aggregates were characterized, primarily by solid state NMR which was followed by electron microscopy and detection by proteinase K resistance on a silver stained gel.

5.1 Recent Advances in Prion Amplification

Till date, several *in vitro* methods for prion protein conversion and amplification have been reported. Soto and colleagues developed the assay called “protein misfolding cyclic amplification (PMCA)” reaction, where in the presence of infectious prions, native PrP^{C} from brain homogenates was converted into an aggregated PrP^{res} using a series of incubation and sonication cycles. The method is sensitive to detect as little as 1 ag of PrP^{sc} (Saa, Castilla et al. 2006). However, the requirement for brain-derived PrP^{C} as the amplification substrate makes the method inapt for generating prions using recombinant PrP^{C} as a substrate. Moreover, there was great degree of variability in the vibrational energy distribution to the samples (Atarashi, Sano et al. 2011). To further add up, (Castilla et al., 2006) stated that for efficient prion propagation using PMCA, co-factors present in brain homogenates were vital. Bacterially expressed recombinant PrP^{C} lacks glycosylation and the glycophosphatidylinositol (GPI) anchor which furthermore raised the problem of using rec. PrP^{C}. Still, in 2007, Atarashi et al. attempted to replace the substrate from normal brain homogenate to rec. PrP using the standard PMCA set-up (Atarashi, Moore et al. 2007). This method called rPrP-PMCA was able to detect as little as 50 ag of PrP^{Sc}. However, the problems associated with sonication as a means of fragmentation still existed. Soon in 2008, Caughey and co-workers developed a method where they substituted sonication with shaking in a thermoshaker and showed prion amplification using rec. PrP^{C} as a substrat. This method was termed as quaking-induced conversion (QuIC)

assay (Atarashi, Wilham et al. 2008). It has the potential to detect sub-femtogram amounts of PrP^{Sc} within a day. The establishment of QuIC assay was found to be a great success as it improved the overall feasibility of the experimental set-up.

However, initial work done in our lab showed that the conversion efficiency both by ultrasound and by shaking is highly volume dependent and yields of the protease resistant prion protein are not consistent (data not shown). Moreover, the typical reaction volume used in these assays was 100 µl which was not sufficient for solid state NMR analysis. So there persists a need for the development of a method by which rec. PrP^{res} samples can be prepared in a homogenous and reproducible manner in sufficient quantities for further structural analysis.

5.2 Development of Selective Shearing Amplification (SSA)

Keeping the needs and perspectives in mind, an instrument was built in our group by Dr. Thorsten Lührs called as “SSA Array” (see Methods). Based on shear induced fragmentation applied by shear generators (7F, Heidolph), we can conformationally select PrP^{Sc} from the brain and amplify the seed specific aggregates using rec. hamster prion protein as a substrate. Most importantly, we can scale-up the volume of the reactions up to 200 ml without affecting the rate of amplification or loss in the yield. With the development of the instrument, we initially focussed on establishing an optimized method for rec. PrP conversion which resulted in consistent and reproducible amplification, while assessing whether all the key parameters (seed and substrate concentration, cycle time, detergent concentration etc.) would lead to a positive or negative effect on overall levels of rec. PrP^{res} amplification.

Using this assay, we could not only amplify specific prion seeds with recombinant PrP but also improved the sensitivity of prion detection by using half the concentration of substrate in comparison to the QuIC assay i.e., 50 µg/ml (Fig. 4.2). This in turn makes the method economically efficient as for

NMR studies we have to isotope label the protein with either ^{15}N or ^{13}C which is very expensive.

Additionally, shear induced fragmentation of seeds for PrP^{res} amplification using rec. PrP^{C} as a substrate allowed clear discrimination between PrP^{Sc}-seeded and non-seeded reaction products (Fig. 4.5). Initial trials revealed that in the presence of 0.1% SDS and 0.1% Triton X-100, 5 seconds processing in every 5 minutes resulted in spontaneous (non-seeded) conversion of bacterially expressed recombinant hamster PrP^{C} to proteinase K (PK) resistant forms. Interestingly, these spontaneously generated forms were totally supressed by finely tuning the processing conditions where the seed fragmentation was precisely controlled.

Furthermore, SSA also showed the potential to differentiate between two closely related prion strains – Sc237 and 263K by the kinetic analysis of *in vitro* selected PrP^{res}. The strain 263K showed only one prominent PrP^{res} population near the maximal processing frequency whereas in Sc237 three distinct optima were identified (Fig. 4.6). This indicated that rec. PrP^{res} amplification for kinetic selection of prion seeds is not influenced by shearing mechanisms and the overall seed conformations are not altered by shearing itself.

Moreover, we observed that rec. PrP^{res} generated by SSA can be perpetuated indefinitely without any loss of seeding activity (Fig. 4.8). Some of the reactions e.g. those running at 189 Hz., 378 Hz. and 953 Hz. were propagated up to round 45 corresponding to a total dilution of 1.4×10^{-78} relative to the initial seed. This provided a very strong proof for the efficiency and robustness of SSA. Thereby we were able to produce virtually unlimited amounts of isotope labelled and conformationally selected rec. PrP^{res} aggregates from both Sc237 and 263K prions (Table 9). With these aggregates we were able to record high quality solid state NMR spectra which indicated that the structural determination of PrP^{res} aggregates is possible (Figures 24-26).

5.3 Conformations of Recombinant PrP^{res}

The protein only hypothesis (see section 1.2) claims that the proteins conformation of PrPSc is necessary and sufficient to transmit prion diseases between susceptible hosts. In particular the work of Prusiner and Co-workers (Legname et al. 2004) provided strong indications that the protein only hypothesis might be true. They used *de novo* generated recombinant PrP fibrils to inoculate transgenic syrian hamster that over expressed PrP(90-230) 16-fold relative to wild-type hamsters. After extended incubation times of >500 days these hamster succumbed to prion disease. However, to date there it is not clear how the type of fibril relates to the prion diseases that they caused. In particular the serial propagation of the de novo induced hamster prion disease was accompanied by a successive shortening in incubation times, and two distinct novel hamster prion strains have been identified from these transmissions and compared to known prion strains (Legname, Nguyen et al. 2006). Moreover, the solid state NMR spectra of the utilized hamster PrP fibrils were analysed and revealed an overall poor spectral quality that was indicative of conformationally mixed aggregates (Tycko, Savtchenko et al. 2010). It is therefore not clear whether any of the conformations that was administered to the hamsters caused the disease, or alternatively, whether these aggregated triggered the spontaneous *de novo* generation of prions in the brain.

In order to see whether our conformationally selected PrP^{res} aggregates contained distinct individual conformations, we analysed all [^{13}C,^{15}N]-labeled samples by solid state NMR spectroscopy (see section 4.3). Upon first inspection of the resulting 2D-NMR spectra (Figure 24), it became immediately clear that SSA had produced homogeneously structured PrP^{res} aggragtes. We compared our data to previously published ssNMR-spectra of recombinant hamster PrP fibrils that had been used to induce prion diseasae in hamsters (Tycko, Savtchenko et al. 2010). It becomes readily evident that the conformation of our strain specifically selected PrP^{res} differs substantially from those other fibrils. In particular in all our samples, resonances corresponding to four isoleucines with narrow line width can readily be identified in the ^{13}C spectral range between 12 and 18 ppm. Corresponding resonances are in

different positions of even absent in the data of Tycko et al. This is particularly noteworthy because all four isoleucine residues of hamster PrP are located in the C-terminal domain, which is alpha-helical (α2 and α3) in PrP (compare Figures 4. And 5.). Thus, significant structural differences exist between our samples and previously investigated PrP fibrils.

When we compared the ssNMR spectra from all [^{13}C, ^{15}N] labelled PrP^{res} reaction products it became clear that in all cases homogeneous samples were obtained. This is particularly noteworthy because a total of sixty individual reactions of 10 ml volume spanning five serial passages were pooled required to generate ~30 mg of [^{13}C, ^{15}N] labelled PrP^{res} for each solid state NMR. If there were any significant variability in the conformation selective amplification between the individual reactions, this would inevitably lead structurally heterogeneous samples and correspondingly poor quality NMR spectra. However, all NMR-spectra were of very good or even excellent quality, which in itself provides very clear evidence of the robustness of the approach established here for the generation of conformationally selected recombinant prion samples.

We were able to identify three different conformations present in the five selected conformational products. From the hamster 263K prion strain, we prepared the solid state NMR sample at two different processing frequencies (378 Hz and 953 Hz), which resulted into the amplification of same PrP^{res} conformation in both cases (Fig. 26). The amplification rate at 953Hz was substantially faster than at 378Hz (Fig. 16D). This clearly indicated that (i) shearing itself does not induce or alter the selected conformations, and (ii) the amplified conformation does also not depend on the amplification rate. Thus, using SSA it appears evident that the obtained product is determined by the prion strain that is used as a seed.

To further investigate the conformation selection, we also amplified rec. PrP^{res} under three different shearing conditions for NMR analysis using the Sc237 strain as a seed. Under all condition, distinguishable PrP^{res} conformations were obtained. While the products obtained with 378 Hz and 953 Hz rotor frequency (see methods), lead to the amplification of conformations that were distinct

from 263K, the reaction product generated at 189Hz rotor frequency generated PrP^{res} aggregates that were essentially undistinguishable from the 263K conformation. From this date we conclude that the 263K strain contain only one single prion conformation, but that the Sc237 prion strain is a mixture of different prion conformation that appear to co-exist *in vivo*. The 263K conformation is thus also a sub-set of the Sc237 conformational mix.

We also compared these rec. PrP aggregates using transmission electron microscopy (TEM) at three different frequencies for Sc237 − 189 Hz., 378 Hz. and 953 Hz. Overall, we observed slightly different morphologies for these aggregates which is due to different lateral association that depends clearly on the shearing conditions. At higher frequencies e.g. 953 Hz. we tend to induce stronger lateral association with prion samples and hence the appearance of these aggregates resemble more like prion rods which was published by Prusiner (Prusiner, McKinley et al. 1983). However, at lower frequencies e.g. 189 Hz. the fibrils don't co-aggregate strongly, rather there is a collection of broken or dissociated smaller fragments. So there is a shear induced fibril - fibril association effect that resulted in morphological variation.

For 263K, we compared the morphologies at two different shearing conditions − 378 Hz. and 953 Hz. In contradiction to the Sc237 strain, 263K showed no difference at both the frequencies. This suggests the evidence for visualising strain differences in prions using shear induced fragmentation. The results of silver staining also supported the above confirmed observation where 263K contained primarily only one PrP^{res} population (Fig. 4.6). Thus overall, the aggregate morphology appear to be closely similar for 263K but there may be a variation in the degree of lateral association which can be readily explained as a shear induced fibrilar-fibrilar aggregation effect.

In summary, our experimental observations on conformationally selected recombinant PrP^{res} are consistent with the history of these two prion isolates. The Sc237 strain has originally been derived from the inter-species transmission of goat scrapie to hamsters. During the same passage history, the 236K strain has been obtained by limiting dilution passages in syrian hamsters (clonal prion selection), while Sc237 has apparently never been

clonally selected (Kimberlin and Marsh 1975; Marsh and Kimberlin 1975; Kimberlin 1976; Kimberlin and Walker 1977). This suggests that the Sc237 prion strain has always contained multiple prion conformations, and that the 263K conformation has coincidentally been selected from that mixture. Thus, it appears possible to investigate prion strain inheritance and strain selection by SSA and solid-state NMR.

5.4 Future Perspectives

The major limitation of the PMCA and QuIC methods was that the detection of protease resistant prion seeded products was done by the time consuming western blotting. By amyloid seeding assay (ASA), an attempt was made to fasten up the whole detection procedure by using fluorescent dye thioflavin T (ThT), that displays enhanced fluorescence upon binding to amyloid fibrils (Colby, Zhang et al. 2007). However, ASA often leads to spontaneous formation of rec. PrP fibrils. Later following the same principle of ASA i.e. detection through fluorescent ThT, another assay was established called real-time (RT)-QuIC which was an amalgamation of QuIC and ASA. RT-QuIC not only provided the faster means for prion detection but also reduced spontaneous rec. PrP fibril formation. Nonetheless, all these methods still pose a problem to scale-up the reaction volume which is distinctly a desideratum for making solid state NMR sample for structural analysis. With our assay, we overcame the problem of increasing reaction volume without affecting the yield of prion amplification. However, the current method involved PrP^{res} detection by silver stained SDS gel electrophoresis. So, there continues to be a need for further technical development of the method that will allow rapid detection of prions. For dealing this issue, in future we will focus our attention towards detection by fluorescent dye ThT, which not only reduce the time for detection but will be more handy and flexible.

Already now we can distinguish the two prion strains Sc237 and 263K based on their conformational composition. At the time of writing this thesis transmissions in hamsters of the conformationally selected aggregates are on-going. The results from these experiments will reveal whether the selected

recombinant conformations are also infectious, and whether the identified conformations are sufficient to induce prion disease.

With this work, a basis has been generated that will allow to investigate the molecular 3D structures of prions in relation to the disease phenotype associated with the initial prion seed. Potentially, it might even be possible to determine how conformations change during interspecies transmissions. Thus, the public health concern about TSE diseases could be readily addressed by the underlying molecular mechanism. Since we can make homogenous conformations from predefined hamster prions as seeds, it would seem also possible to structurally investigate seeds from other neurodegenerative diseases like Alzheimer's and Parkinson's disease using similar approaches as established in this work.

References

Abid, K., and Soto, C. (2006). The intriguing prion disorders. Cellular and molecular life sciences : CMLS *63*, 2342-2351.

Aguzzi, A., and Polymenidou, M. (2004). Mammalian prion biology: one century of evolving concepts. Cell *116*, 313-327.

Alper, T., Haig, D.A., and Clarke, M.C. (1966). The exceptionally small size of the scrapie agent. Biochemical and biophysical research communications *22*, 278-284.

Apetri, A.C., and Surewicz, W.K. (2003). Atypical effect of salts on the thermodynamic stability of human prion protein. The Journal of biological chemistry *278*, 22187-22192.

Arnold, J.E., Tipler, C., Laszlo, L., Hope, J., Landon, M., and Mayer, R.J. (1995). The abnormal isoform of the prion protein accumulates in late-endosome-like organelles in scrapie-infected mouse brain. The Journal of pathology *176*, 403-411.

Atarashi, R., Moore, R.A., Sim, V.L., Hughson, A.G., Dorward, D.W., Onwubiko, H.A., Priola, S.A., and Caughey, B. (2007). Ultrasensitive detection of scrapie prion protein using seeded conversion of recombinant prion protein. Nature methods *4*, 645-650.

Atarashi, R., Sano, K., Satoh, K., and Nishida, N. (2011). Real-time quaking-induced conversion: a highly sensitive assay for prion detection. Prion *5*, 150-153.

Atarashi, R., Wilham, J.M., Christensen, L., Hughson, A.G., Moore, R.A., Johnson, L.M., Onwubiko, H.A., Priola, S.A., and Caughey, B. (2008). Simplified ultrasensitive prion detection by recombinant PrP conversion with shaking. Nature methods *5*, 211-212.

Barmada, S.J., and Harris, D.A. (2005). Visualization of prion infection in transgenic mice expressing green fluorescent protein-tagged prion protein. The Journal of neuroscience : the official journal of the Society for Neuroscience *25*, 5824-5832.

Barron, R.M., Baybutt, H., Tuzi, N.L., McCormack, J., King, D., Moore, R.C., Melton, D.W., and Manson, J.C. (2005). Polymorphisms at codons 108 and 189 in murine PrP play distinct roles in the control of scrapie incubation time. The Journal of general virology *86*, 859-868.

Barry, R.A., Kent, S.B., McKinley, M.P., Meyer, R.K., DeArmond, S.J., Hood, L.E., and Prusiner, S.B. (1986). Scrapie and cellular prion proteins share polypeptide epitopes. The Journal of infectious diseases *153*, 848-854.

Basler, K., Oesch, B., Scott, M., Westaway, D., Walchli, M., Groth, D.F., McKinley, M.P., Prusiner, S.B., and Weissmann, C. (1986). Scrapie and cellular PrP isoforms are encoded by the same chromosomal gene. Cell *46*, 417-428.

Bendheim, P.E., Brown, H.R., Rudelli, R.D., Scala, L.J., Goller, N.L., Wen, G.Y., Kascsak, R.J., Cashman, N.R., and Bolton, D.C. (1992). Nearly ubiquitous tissue distribution of the scrapie agent precursor protein. Neurology *42*, 149-156.

Beranger, F., Mange, A., Goud, B., and Lehmann, S. (2002). Stimulation of PrP(C) retrograde transport toward the endoplasmic reticulum increases accumulation of PrP(Sc) in prion-infected cells. The Journal of biological chemistry *277*, 38972-38977.

Bessen, R.A., and Marsh, R.F. (1994). Distinct PrP properties suggest the molecular basis of strain variation in transmissible mink encephalopathy. Journal of virology *68*, 7859-7868.

Bolton, D.C., McKinley, M.P., and Prusiner, S.B. (1982). Identification of a protein that purifies with the scrapie prion. Science (New York, NY) *218*, 1309-1311.

Borchelt, D.R., Scott, M., Taraboulos, A., Stahl, N., and Prusiner, S.B. (1990). Scrapie and cellular prion proteins differ in their kinetics of synthesis and topology in cultured cells. The Journal of cell biology *110*, 743-752.

Borchelt, D.R., Taraboulos, A., and Prusiner, S.B. (1992). Evidence for synthesis of scrapie prion proteins in the endocytic pathway. The Journal of biological chemistry *267*, 16188-16199.

Bremer, J., Baumann, F., Tiberi, C., Wessig, C., Fischer, H., Schwarz, P., Steele, A.D., Toyka, K.V., Nave, K.A., Weis, J.*, et al.* (2010). Axonal prion protein is required for peripheral myelin maintenance. Nature neuroscience *13*, 310-318.

Brown, D.R., Qin, K., Herms, J.W., Madlung, A., Manson, J., Strome, R., Fraser, P.E., Kruck, T., von Bohlen, A., Schulz-Schaeffer, W.*, et al.* (1997). The cellular prion protein binds copper in vivo. Nature *390*, 684-687.

Bruce, M.E., and Dickinson, A.G. (1987). Biological evidence that scrapie agent has an independent genome. The Journal of general virology *68 (Pt 1)*, 79-89.

Bueler, H., Aguzzi, A., Sailer, A., Greiner, R.A., Autenried, P., Aguet, M., and Weissmann, C. (1993). Mice devoid of PrP are resistant to scrapie. Cell *73*, 1339-1347.

Bueler, H., Fischer, M., Lang, Y., Bluethmann, H., Lipp, H.P., DeArmond, S.J., Prusiner, S.B., Aguet, M., and Weissmann, C. (1992). Normal development and behaviour of mice lacking the neuronal cell-surface PrP protein. Nature *356*, 577-582.

Calzolai, L., Lysek, D.A., Perez, D.R., Guntert, P., and Wuthrich, K. (2005). Prion protein NMR structures of chickens, turtles, and frogs. Proceedings of the National Academy of Sciences of the United States of America *102*, 651-655.

Castilla, J., Saa, P., Morales, R., Abid, K., Maundrell, K., and Soto, C. (2006). Protein misfolding cyclic amplification for diagnosis and prion propagation studies. Methods in enzymology *412*, 3-21.

Caughey, B., Horiuchi, M., Demaimay, R., and Raymond, G.J. (1999). Assays of protease-resistant prion protein and its formation. Methods in enzymology *309*, 122-133.

Caughey, B., Race, R.E., and Chesebro, B. (1988). Detection of prion protein mRNA in normal and scrapie-infected tissues and cell lines. The Journal of general virology *69 (Pt 3)*, 711-716.

Caughey, B., Race, R.E., Ernst, D., Buchmeier, M.J., and Chesebro, B. (1989). Prion protein biosynthesis in scrapie-infected and uninfected neuroblastoma cells. Journal of virology *63*, 175-181.

Chiesa, R., Piccardo, P., Ghetti, B., and Harris, D.A. (1998). Neurological illness in transgenic mice expressing a prion protein with an insertional mutation. Neuron *21*, 1339-1351.

Clarke, M.C., and Haig, D.A. (1966). Attempts to demonstrate neutralising antibodies in the sera of scrapie-affected animals. The Veterinary record *78*, 647-649.

Cohen, F.E., and Prusiner, S.B. (1998). Pathologic conformations of prion proteins. Annual review of biochemistry *67*, 793-819.

Coitinho, A.S., Dietrich, M.O., Hoffmann, A., Dall'Igna, O.P., Souza, D.O., Martins, V.R., Brentani, R.R., Izquierdo, I., and Lara, D.R. (2002). Decreased hyperlocomotion induced by MK-801, but not amphetamine and caffeine in mice lacking cellular prion protein (PrP(C)). Brain research Molecular brain research *107*, 190-194.

Colby, D.W., Zhang, Q., Wang, S., Groth, D., Legname, G., Riesner, D., and Prusiner, S.B. (2007). Prion detection by an amyloid seeding assay. Proceedings of the National Academy of Sciences of the United States of America *104*, 20914-20919.

Collinge, J., and Clarke, A.R. (2007). A general model of prion strains and their pathogenicity. Science (New York, NY) *318*, 930-936.

Collinge, J., Sidle, K.C., Meads, J., Ironside, J., and Hill, A.F. (1996). Molecular analysis of prion strain variation and the aetiology of 'new variant' CJD. Nature *383*, 685-690.

Collinge, J., Whittington, M.A., Sidle, K.C., Smith, C.J., Palmer, M.S., Clarke, A.R., and Jefferys, J.G. (1994). Prion protein is necessary for normal synaptic function. Nature *370*, 295-297.

Cronier S , Laude H , and Jean-Michel Peyrin (2004). Prions can infect primary cultured neurons and astrocytes and promote neuronal cell death. Proceedings of the National Academy of Sciences of the United States of America *101, 12271–1227.*

DeArmond, S.J., McKinley, M.P., Barry, R.A., Braunfeld, M.B., McColloch, J.R., and Prusiner, S.B. (1985). Identification of prion amyloid filaments in scrapie-infected brain. Cell *41*, 221-235.

DeArmond, S.J., Yang, S.L., Lee, A., Bowler, R., Taraboulos, A., Groth, D., and Prusiner, S.B. (1993). Three scrapie prion isolates exhibit different accumulation patterns of the prion protein scrapie isoform. Proceedings of the National Academy of Sciences of the United States of America *90*, 6449-6453.

Deleault, N.R., Harris, B.T., Rees, J.R., and Supattapone, S. (2007). Formation of native prions from minimal components in vitro. Proceedings of the National Academy of Sciences of the United States of America *104*, 9741-9746.

DeMarco, M.L., and Daggett, V. (2004). From conversion to aggregation: protofibril formation of the prion protein. Proceedings of the National Academy of Sciences of the United States of America *101*, 2293-2298.

Dickinson, A.G., Meikle, V.M., and Fraser, H. (1968). Identification of a gene which controls the incubation period of some strains of scrapie agent in mice. Journal of comparative pathology *78*, 293-299.

Dodelet, V.C., and Cashman, N.R. (1998). Prion protein expression in human leukocyte differentiation. Blood *91*, 1556-1561.

Donne, D.G., Viles, J.H., Groth, D., Mehlhorn, I., James, T.L., Cohen, F.E., Prusiner, S.B., Wright, P.E., and Dyson, H.J. (1997). Structure of the recombinant full-length hamster prion protein PrP(29-231): the N terminus is highly flexible. Proceedings of the National Academy of Sciences of the United States of America *94*, 13452-13457.

Eiden, M., Palm, G.J., Hinrichs, W., Matthey, U., Zahn, R., and Groschup, M.H. (2006). Synergistic and strain-specific effects of bovine spongiform encephalopathy and scrapie prions in the cell-free conversion of recombinant prion protein. The Journal of general virology *87*, 3753-3761.

Fevrier, B., Vilette, D., Archer, F., Loew, D., Faigle, W., Vidal, M., Laude, H., and Raposo, G. (2004). Cells release prions in association with exosomes. Proceedings of the National Academy of Sciences of the United States of America *101*, 9683-9688.

Fournier, J.G., Escaig-Haye, F., and Grigoriev, V. (2000). Ultrastructural localization of prion proteins: physiological and pathological implications. Microscopy research and technique *50*, 76-88.

Gibbs, C.J., Jr., and Bolis, C.L. (1997). Normal isoform of amyloid protein (PrP) in brains of spawning salmon. Molecular psychiatry *2*, 146-147.

Gilch, S., Nunziante, M., Ertmer, A., Wopfner, F., Laszlo, L., and Schatzl, H.M. (2004). Recognition of lumenal prion protein aggregates by post-ER quality control mechanisms is mediated by the preoctarepeat region of PrP. Traffic *5*, 300-313.

Glatzel, M., and Aguzzi, A. (2001). The shifting biology of prions. Brain research Brain research reviews *36*, 241-248.

Godsave, S.F., Wille, H., Kujala, P., Latawiec, D., DeArmond, S.J., Serban, A., Prusiner, S.B., and Peters, P.J. (2008). Cryo-immunogold electron microscopy for prions: toward identification of a conversion site. The Journal of

neuroscience : the official journal of the Society for Neuroscience *28*, 12489-12499.

Gohel, C., Grigoriev, V., Escaig-Haye, F., Lasmezas, C.I., Deslys, J.P., Langeveld, J., Akaaboune, M., Hantai, D., and Fournier, J.G. (1999). Ultrastructural localization of cellular prion protein (PrPc) at the neuromuscular junction. Journal of neuroscience research *55*, 261-267.

Gorodinsky, A., and Harris, D.A. (1995). Glycolipid-anchored proteins in neuroblastoma cells form detergent-resistant complexes without caveolin. The Journal of cell biology *129*, 619-627.

Govaerts, C., Wille, H., Prusiner, S.B., and Cohen, F.E. (2004). Evidence for assembly of prions with left-handed beta-helices into trimers. Proceedings of the National Academy of Sciences of the United States of America *101*, 8342-8347.

Griffith, J.S. (1967). Self-replication and scrapie. Nature *215*, 1043-1044.

Haraguchi, T., Fisher, S., Olofsson, S., Endo, T., Groth, D., Tarentino, A., Borchelt, D.R., Teplow, D., Hood, L., Burlingame, A.*, et al.* (1989). Asparagine-linked glycosylation of the scrapie and cellular prion proteins. Archives of biochemistry and biophysics *274*, 1-13.

Hegde, R.S., Tremblay, P., Groth, D., DeArmond, S.J., Prusiner, S.B., and Lingappa, V.R. (1999). Transmissible and genetic prion diseases share a common pathway of neurodegeneration. Nature *402*, 822-826.

Iniguez, V., McKenzie, D., Mirwald, J., and Aiken, J. (2000). Strain-specific propagation of PrP(Sc) properties into baculovirus-expressed hamster PrP(C). The Journal of general virology *81*, 2565-2571.

Ivanova, L., Barmada, S., Kummer, T., and Harris, D.A. (2001). Mutant prion proteins are partially retained in the endoplasmic reticulum. The Journal of biological chemistry *276*, 42409-42421.

Jansen, K., Schafer, O., Birkmann, E., Post, K., Serban, H., Prusiner, S.B., and Riesner, D. (2001). Structural intermediates in the putative pathway from the cellular prion protein to the pathogenic form. Biological chemistry *382*, 683-691.

Kellings, K., Meyer, N., Mirenda, C., Prusiner, S.B., and Riesner, D. (1993). Analysis of nucleic acids in purified scrapie prion preparations. Archives of virology Supplementum *7*, 215-225.

Khosravani, H., Zhang, Y., Tsutsui, S., Hameed, S., Altier, C., Hamid, J., Chen, L., Villemaire, M., Ali, Z., Jirik, F.R.*, et al.* (2008). Prion protein attenuates excitotoxicity by inhibiting NMDA receptors. The Journal of cell biology *181*, 551-565.

Kim, J.I., Cali, I., Surewicz, K., Kong, Q., Raymond, G.J., Atarashi, R., Race, B., Qing, L., Gambetti, P., Caughey, B.*, et al.* (2010). Mammalian prions generated from bacterially expressed prion protein in the absence of any mammalian cofactors. The Journal of biological chemistry *285*, 14083-14087.

Kimberlin, R. H. (1976). "Experimental scrapie in the mouse: a review of an important model disease." Science progress 63(252): 461-481.

Kimberlin, R. H. and R. F. Marsh (1975). "Comparison of scrapie and transmissible mink encephalopathy in hamsters. I. Biochemical studies of brain during development of disease." The Journal of infectious diseases 131(2): 97-103.

Kimberlin, R. H. and C. Walker (1977). "Characteristics of a short incubation model of scrapie in the golden hamster." The Journal of general virology 34(2): 295-304.

Kirby, L., Birkett, C.R., Rudyk, H., Gilbert, I.H., and Hope, J. (2003). In vitro cell-free conversion of bacterial recombinant PrP to PrPres as a model for conversion. The Journal of general virology *84*, 1013-1020.

Knaus, K.J., Morillas, M., Swietnicki, W., Malone, M., Surewicz, W.K., and Yee, V.C. (2001). Crystal structure of the human prion protein reveals a mechanism for oligomerization. Nature structural biology *8*, 770-774.

Kocisko, D.A., Come, J.H., Priola, S.A., Chesebro, B., Raymond, G.J., Lansbury, P.T., and Caughey, B. (1994). Cell-free formation of protease-resistant prion protein. Nature *370*, 471-474.

Krasemann, S., Zerr, I., Weber, T., Poser, S., Kretzschmar, H., Hunsmann, G., and Bodemer, W. (1995). Prion disease associated with a novel nine octapeptide repeat insertion in the PRNP gene. Brain research Molecular brain research *34*, 173-176.

Kristiansen, M., Messenger, M.J., Klohn, P.C., Brandner, S., Wadsworth, J.D., Collinge, J., and Tabrizi, S.J. (2005). Disease-related prion protein forms aggresomes in neuronal cells leading to caspase activation and apoptosis. The Journal of biological chemistry *280*, 38851-38861.

Legname, G., Baskakov, I.V., Nguyen, H.O., Riesner, D., Cohen, F.E., DeArmond, S.J., and Prusiner, S.B. (2004). Synthetic mammalian prions. Science (New York, NY) *305*, 673-676.

Legname, G., Nguyen, H.O., Baskakov, I.V., Cohen, F.E., Dearmond, S.J., and Prusiner, S.B. (2005). Strain-specified characteristics of mouse synthetic prions. Proceedings of the National Academy of Sciences of the United States of America *102*, 2168-2173.

Legname, G., H. O. Nguyen, et al. (2006). "Continuum of prion protein structures enciphers a multitude of prion isolate-specified phenotypes." Proceedings of the National Academy of Sciences of the United States of America **103**(50): 19105-19110.

Lehmann, S., and Harris, D.A. (1997). Blockade of glycosylation promotes acquisition of scrapie-like properties by the prion protein in cultured cells. The Journal of biological chemistry *272*, 21479-21487.

Linden, R., Martins, V.R., Prado, M.A., Cammarota, M., Izquierdo, I., and Brentani, R.R. (2008). Physiology of the prion protein. Physiological reviews *88*, 673-728.

Lopez Garcia, F., Zahn, R., Riek, R., and Wuthrich, K. (2000). NMR structure of the bovine prion protein. Proceedings of the National Academy of Sciences of the United States of America *97*, 8334-8339.

Ma, J., and Lindquist, S. (2002). Conversion of PrP to a self-perpetuating PrPSc-like conformation in the cytosol. Science (New York, NY) *298*, 1785-1788.

Maddison, B.C., Patel, S., James, R.F., Conlon, H.E., Oidtmann, B., Baier, M., Whitelam, G.C., and Gough, K.C. (2005). Generation and characterisation of monoclonal antibodies to Rainbow trout (Oncorhynchus mykiss) prion protein. Journal of immunological methods *306*, 202-210.

Magalhaes, A.C., Silva, J.A., Lee, K.S., Martins, V.R., Prado, V.F., Ferguson, S.S., Gomez, M.V., Brentani, R.R., and Prado, M.A. (2002). Endocytic intermediates involved with the intracellular trafficking of a fluorescent cellular prion protein. The Journal of biological chemistry *277*, 33311-33318.

Mange, A., Crozet, C., Lehmann, S., and Beranger, F. (2004). Scrapie-like prion protein is translocated to the nuclei of infected cells independently of proteasome inhibition and interacts with chromatin. Journal of cell science *117*, 2411-2416.

Manson, J.C., Clarke, A.R., Hooper, M.L., Aitchison, L., McConnell, I., and Hope, J. (1994). 129/Ola mice carrying a null mutation in PrP that abolishes mRNA production are developmentally normal. Molecular neurobiology *8*, 121-127.

Marsh, R. F. and R. H. Kimberlin (1975). "Comparison of scrapie and transmissible mink encephalopathy in hamsters. II. Clinical signs, pathology, and pathogenesis." The Journal of infectious diseases 131(2): 104-110.

Merz, P.A., Somerville, R.A., Wisniewski, H.M., and Iqbal, K. (1981). Abnormal fibrils from scrapie-infected brain. Acta neuropathologica *54*, 63-74.

Meyer, R.K., Lustig, A., Oesch, B., Fatzer, R., Zurbriggen, A., and Vandevelde, M. (2000). A monomer-dimer equilibrium of a cellular prion protein (PrPC) not observed with recombinant PrP. The Journal of biological chemistry *275*, 38081-38087.

Mironov, A., Jr., Latawiec, D., Wille, H., Bouzamondo-Bernstein, E., Legname, G., Williamson, R.A., Burton, D., DeArmond, S.J., Prusiner, S.B., and Peters, P.J. (2003). Cytosolic prion protein in neurons. The Journal of neuroscience : the official journal of the Society for Neuroscience *23*, 7183-7193.

Moore, R.C., Hope, J., McBride, P.A., McConnell, I., Selfridge, J., Melton, D.W., and Manson, J.C. (1998). Mice with gene targetted prion protein alterations show that Prnp, Sinc and Prni are congruent. Nature genetics *18*, 118-125.

Morris, R.J., Parkyn, C.J., and Jen, A. (2006). Traffic of prion protein between different compartments on the neuronal surface, and the propagation of prion disease. FEBS letters *580*, 5565-5571.

Moser, M., Colello, R.J., Pott, U., and Oesch, B. (1995). Developmental expression of the prion protein gene in glial cells. Neuron *14*, 509-517.

Naslavsky, N., Stein, R., Yanai, A., Friedlander, G., and Taraboulos, A. (1997). Characterization of detergent-insoluble complexes containing the cellular prion protein and its scrapie isoform. The Journal of biological chemistry *272*, 6324-6331.

Nazor, K.E., Seward, T., and Telling, G.C. (2007). Motor behavioral and neuropathological deficits in mice deficient for normal prion protein expression. Biochimica et biophysica acta *1772*, 645-653.

Nico, P.B., de-Paris, F., Vinade, E.R., Amaral, O.B., Rockenbach, I., Soares, B.L., Guarnieri, R., Wichert-Ana, L., Calvo, F., Walz, R.*, et al.* (2005). Altered

behavioural response to acute stress in mice lacking cellular prion protein. Behavioural brain research *162*, 173-181.

Nishina, K.A., Deleault, N.R., Mahal, S.P., Baskakov, I., Luhrs, T., Riek, R., and Supattapone, S. (2006). The stoichiometry of host PrPC glycoforms modulates the efficiency of PrPSc formation in vitro. Biochemistry *45*, 14129-14139.

Nonno, R., Di Bari, M.A., Cardone, F., Vaccari, G., Fazzi, P., Dell'Omo, G., Cartoni, C., Ingrosso, L., Boyle, A., Galeno, R.*, et al.* (2006). Efficient transmission and characterization of Creutzfeldt-Jakob disease strains in bank voles. PLoS pathogens *2*, e12.

Oesch, B., Westaway, D., Walchli, M., McKinley, M.P., Kent, S.B., Aebersold, R., Barry, R.A., Tempst, P., Teplow, D.B., Hood, L.E.*, et al.* (1985). A cellular gene encodes scrapie PrP 27-30 protein. Cell *40*, 735-746.

Oidtmann, B., Simon, D., Holtkamp, N., Hoffmann, R., and Baier, M. (2003). Identification of cDNAs from Japanese pufferfish (Fugu rubripes) and Atlantic salmon (Salmo salar) coding for homologues to tetrapod prion proteins. FEBS letters *538*, 96-100.

Orru, C.D., Wilham, J.M., Raymond, L.D., Kuhn, F., Schroeder, B., Raeber, A.J., and Caughey, B. (2011). Prion disease blood test using immunoprecipitation and improved quaking-induced conversion. mBio *2*, e00078-00011.

Pan, K.M., Baldwin, M., Nguyen, J., Gasset, M., Serban, A., Groth, D., Mehlhorn, I., Huang, Z., Fletterick, R.J., Cohen, F.E.*, et al.* (1993). Conversion of alpha-helices into beta-sheets features in the formation of the scrapie prion proteins. Proceedings of the National Academy of Sciences of the United States of America *90*, 10962-10966.

Pattison, I.H., and Millson, G.C. (1961). Scrapie produced experimentally in goats with special reference to the clinical syndrome. Journal of comparative pathology *71*, 101-109.

Pauly, P.C., and Harris, D.A. (1998). Copper stimulates endocytosis of the prion protein. The Journal of biological chemistry *273*, 33107-33110.

Peden, A.H., McGuire, L.I., Appleford, N.E., Mallinson, G., Wilham, J.M., Orru, C.D., Caughey, B., Ironside, J.W., Knight, R.S., Will, R.G.*, et al.* (2012). Sensitive and specific detection of sporadic Creutzfeldt-Jakob disease brain prion protein using real-time quaking-induced conversion. The Journal of general virology *93*, 438-449.

Pergami, P., Jaffe, H., and Safar, J. (1996). Semipreparative chromatographic method to purify the normal cellular isoform of the prion protein in nondenatured form. Analytical biochemistry *236*, 63-73.

Pimpinelli, F., Lehmann, S., and Maridonneau-Parini, I. (2005). The scrapie prion protein is present in flotillin-1-positive vesicles in central- but not peripheral-derived neuronal cell lines. The European journal of neuroscience *21*, 2063-2072.

Prusiner, S.B. (1984). Prions. Scientific American *251*, 50-59.

Prusiner, S.B. (1998). Prions. Proceedings of the National Academy of Sciences of the United States of America *95*, 13363-13383.

Prusiner, S.B., McKinley, M.P., Bowman, K.A., Bolton, D.C., Bendheim, P.E., Groth, D.F., and Glenner, G.G. (1983). Scrapie prions aggregate to form amyloid-like birefringent rods. Cell *35*, 349-358.

Prusiner, S.B., Scott, M., Foster, D., Pan, K.M., Groth, D., Mirenda, C., Torchia, M., Yang, S.L., Serban, D., Carlson, G.A.*, et al.* (1990). Transgenetic studies implicate interactions between homologous PrP isoforms in scrapie prion replication. Cell *63*, 673-686.

Rial, D., Duarte, F.S., Xikota, J.C., Schmitz, A.E., Dafre, A.L., Figueiredo, C.P., Walz, R., and Prediger, R.D. (2009). Cellular prion protein modulates age-related behavioral and neurochemical alterations in mice. Neuroscience *164*, 896-907.

Riek, R., Hornemann, S., Wider, G., Billeter, M., Glockshuber, R., and Wuthrich, K. (1996). NMR structure of the mouse prion protein domain PrP(121-231). Nature *382*, 180-182.

Riek, R., Hornemann, S., Wider, G., Glockshuber, R., and Wuthrich, K. (1997). NMR characterization of the full-length recombinant murine prion protein, mPrP(23-231). FEBS letters *413*, 282-288.

Riesner, D. (2003). Biochemistry and structure of PrP(C) and PrP(Sc). British medical bulletin *66*, 21-33.

Rivera-Milla, E., Oidtmann, B., Panagiotidis, C.H., Baier, M., Sklaviadis, T., Hoffmann, R., Zhou, Y., Solis, G.P., Stuermer, C.A., and Malaga-Trillo, E. (2006). Disparate evolution of prion protein domains and the distinct origin of Doppel- and prion-related loci revealed by fish-to-mammal comparisons. FASEB journal : official publication of the Federation of American Societies for Experimental Biology *20*, 317-319.

Saa, P., Castilla, J., and Soto, C. (2006). Ultra-efficient replication of infectious prions by automated protein misfolding cyclic amplification. The Journal of biological chemistry *281*, 35245-35252.

Sabharanjak, S., Sharma, P., Parton, R.G., and Mayor, S. (2002). GPI-anchored proteins are delivered to recycling endosomes via a distinct cdc42-regulated, clathrin-independent pinocytic pathway. Developmental cell *2*, 411-423.

Saborio, G.P., Permanne, B., and Soto, C. (2001). Sensitive detection of pathological prion protein by cyclic amplification of protein misfolding. Nature *411*, 810-813.

Safar, J.G., Geschwind, M.D., Deering, C., Didorenko, S., Sattavat, M., Sanchez, H., Serban, A., Vey, M., Baron, H., Giles, K.*, et al.* (2005). Diagnosis of human prion disease. Proceedings of the National Academy of Sciences of the United States of America *102*, 3501-3506.

Sailer, A., Bueler, H., Fischer, M., Aguzzi, A., and Weissmann, C. (1994). No propagation of prions in mice devoid of PrP. Cell *77*, 967-968.

Sarnataro, D., Campana, V., Paladino, S., Stornaiuolo, M., Nitsch, L., and Zurzolo, C. (2004). PrP(C) association with lipid rafts in the early secretory pathway stabilizes its cellular conformation. Molecular biology of the cell *15*, 4031-4042.

Sarnataro, D., Caputo, A., Casanova, P., Puri, C., Paladino, S., Tivodar, S.S., Campana, V., Tacchetti, C., and Zurzolo, C. (2009). Lipid rafts and clathrin cooperate in the internalization of PrP in epithelial FRT cells. PloS one *4*, e5829.

Sarnataro, D., Paladino, S., Campana, V., Grassi, J., Nitsch, L., and Zurzolo, C. (2002). PrPC is sorted to the basolateral membrane of epithelial cells independently of its association with rafts. Traffic *3*, 810-821.

Shaked, G.M., Fridlander, G., Meiner, Z., Taraboulos, A., and Gabizon, R. (1999). Protease-resistant and detergent-insoluble prion protein is not necessarily associated with prion infectivity. The Journal of biological chemistry *274*, 17981-17986.

Shibuya, S., Higuchi, J., Shin, R.W., Tateishi, J., and Kitamoto, T. (1998). Codon 219 Lys allele of PRNP is not found in sporadic Creutzfeldt-Jakob disease. Annals of neurology *43*, 826-828.

Shmerling, D., Hegyi, I., Fischer, M., Blattler, T., Brandner, S., Gotz, J., Rulicke, T., Flechsig, E., Cozzio, A., von Mering, C.*, et al.* (1998). Expression of amino-terminally truncated PrP in the mouse leading to ataxia and specific cerebellar lesions. Cell *93*, 203-214.

Shyng, S.L., Huber, M.T., and Harris, D.A. (1993). A prion protein cycles between the cell surface and an endocytic compartment in cultured neuroblastoma cells. The Journal of biological chemistry *268*, 15922-15928.

Sigurdson, C.J., Nilsson, K.P., Hornemann, S., Manco, G., Polymenidou, M., Schwarz, P., Leclerc, M., Hammarstrom, P., Wuthrich, K., and Aguzzi, A.

(2007). Prion strain discrimination using luminescent conjugated polymers. Nature methods *4*, 1023-1030.

Sim, V.L., and Caughey, B. (2009). Ultrastructures and strain comparison of under-glycosylated scrapie prion fibrils. Neurobiology of aging *30*, 2031-2042.

Smirnovas, V., Baron, G.S., Offerdahl, D.K., Raymond, G.J., Caughey, B., and Surewicz, W.K. (2011). Structural organization of brain-derived mammalian prions examined by hydrogen-deuterium exchange. Nature structural & molecular biology *18*, 504-506.

Smith, P.G., Cousens, S.N., d' Huillard Aignaux, J.N., Ward, H.J., and Will, R.G. (2004). The epidemiology of variant Creutzfeldt-Jakob disease. Current topics in microbiology and immunology *284*, 161-191.

Stahl, N., Borchelt, D.R., Hsiao, K., and Prusiner, S.B. (1987). Scrapie prion protein contains a phosphatidylinositol glycolipid. Cell *51*, 229-240.

Stella, R., Massimino, M.L., Sandri, M., Sorgato, M.C., and Bertoli, A. (2010). Cellular prion protein promotes regeneration of adult muscle tissue. Molecular and cellular biology *30*, 4864-4876.

Sunyach, C., Jen, A., Deng, J., Fitzgerald, K.T., Frobert, Y., Grassi, J., McCaffrey, M.W., and Morris, R. (2003). The mechanism of internalization of glycosylphosphatidylinositol-anchored prion protein. The EMBO journal *22*, 3591-3601.

Suzuki, T., Kurokawa, T., Hashimoto, H., and Sugiyama, M. (2002). cDNA sequence and tissue expression of Fugu rubripes prion protein-like: a candidate for the teleost orthologue of tetrapod PrPs. Biochemical and biophysical research communications *294*, 912-917.

Taraboulos, A., Scott, M., Semenov, A., Avrahami, D., Laszlo, L., and Prusiner, S.B. (1995). Cholesterol depletion and modification of COOH-terminal targeting sequence of the prion protein inhibit formation of the scrapie isoform. The Journal of cell biology *129*, 121-132.

Telling, G.C., Parchi, P., DeArmond, S.J., Cortelli, P., Montagna, P., Gabizon, R., Mastrianni, J., Lugaresi, E., Gambetti, P., and Prusiner, S.B. (1996). Evidence for the conformation of the pathologic isoform of the prion protein enciphering and propagating prion diversity. Science (New York, NY) *274*, 2079-2082.

Tobler, I., Gaus, S.E., Deboer, T., Achermann, P., Fischer, M., Rulicke, T., Moser, M., Oesch, B., McBride, P.A., and Manson, J.C. (1996). Altered circadian activity rhythms and sleep in mice devoid of prion protein. Nature *380*, 639-642.

Turk, E., Teplow, D.B., Hood, L.E., and Prusiner, S.B. (1988). Purification and properties of the cellular and scrapie hamster prion proteins. European journal of biochemistry / FEBS *176*, 21-30.

Tycko, R., R. Savtchenko, et al. (2010). "The alpha-helical C-terminal domain of full-length recombinant PrP converts to an in-register parallel beta-sheet structure in PrP fibrils: evidence from solid state nuclear magnetic resonance." Biochemistry 49(44): 9488-9497.

Vey, M., Pilkuhn, S., Wille, H., Nixon, R., DeArmond, S.J., Smart, E.J., Anderson, R.G., Taraboulos, A., and Prusiner, S.B. (1996). Subcellular colocalization of the cellular and scrapie prion proteins in caveolae-like membranous domains. Proceedings of the National Academy of Sciences of the United States of America *93*, 14945-14949.

Wang, F., Wang, X., Yuan, C.G., and Ma, J. (2010). Generating a prion with bacterially expressed recombinant prion protein. Science (New York, NY) *327*, 1132-1135.

Watt, N.T., and Hooper, N.M. (2003). The prion protein and neuronal zinc homeostasis. Trends in biochemical sciences *28*, 406-410.

Westaway, D., Goodman, P.A., Mirenda, C.A., McKinley, M.P., Carlson, G.A., and Prusiner, S.B. (1987). Distinct prion proteins in short and long scrapie incubation period mice. Cell *51*, 651-662.

Westaway, D., Zuliani, V., Cooper, C.M., Da Costa, M., Neuman, S., Jenny, A.L., Detwiler, L., and Prusiner, S.B. (1994). Homozygosity for prion protein alleles encoding glutamine-171 renders sheep susceptible to natural scrapie. Genes & development *8*, 959-969.

Will, R.G., Ironside, J.W., Zeidler, M., Cousens, S.N., Estibeiro, K., Alperovitch, A., Poser, S., Pocchiari, M., Hofman, A., and Smith, P.G. (1996). A new variant of Creutzfeldt-Jakob disease in the UK. Lancet *347*, 921-925.

Wille, H., Michelitsch, M.D., Guenebaut, V., Supattapone, S., Serban, A., Cohen, F.E., Agard, D.A., and Prusiner, S.B. (2002). Structural studies of the scrapie prion protein by electron crystallography. Proceedings of the National Academy of Sciences of the United States of America *99*, 3563-3568.

Wopfner, F., Weidenhofer, G., Schneider, R., von Brunn, A., Gilch, S., Schwarz, T.F., Werner, T., and Schatzl, H.M. (1999). Analysis of 27 mammalian and 9 avian PrPs reveals high conservation of flexible regions of the prion protein. Journal of molecular biology *289*, 1163-1178.

Xiong, L.W., Raymond, L.D., Hayes, S.F., Raymond, G.J., and Caughey, B. (2001). Conformational change, aggregation and fibril formation induced by detergent treatments of cellular prion protein. Journal of neurochemistry *79*, 669-678.

Zahn, R., Liu, A., Luhrs, T., Riek, R., von Schroetter, C., Lopez Garcia, F., Billeter, M., Calzolai, L., Wider, G., and Wuthrich, K. (2000). NMR solution structure of the human prion protein. Proceedings of the National Academy of Sciences of the United States of America *97*, 145-150.

Zahn, R., von Schroetter, C., and Wuthrich, K. (1997). Human prion proteins expressed in Escherichia coli and purified by high-affinity column refolding. FEBS letters *417*, 400-404.

List of Figures

List of Tables